Longevity Genes Revealed by Integrative Analysis of Isoform-Specific *daf-16/FoxO* Mutants of *Caenorhabditis elegans*

Albert Tzong-Yang Chen,* Chunfang Guo,* Omar A. Itani,* Breane G. Budaitis,* Travis W. Williams,* Christopher E. Hopkins,† Richard C. McEachin,‡ Manjusha Pande,‡ Ana R. Grant,‡ Sawako Yoshina,§ Shohei Mitani,§ and Patrick J. Hu*,,††,1**

*Department of Internal Medicine, ‡Department of Computational Medicine and Bioinformatics, **Department of Cell and Developmental Biology, and ††Institute of Gerontology, University of Michigan Medical School, Ann Arbor, Michigan 48109, †Knudra Transgenics, Murray, Utah 84123, and §Department of Physiology, Tokyo Women's Medical University School of Medicine, Tokyo, 162-8666, Japan

ORCID ID: 0000-0002-5611-8062 (P.J.H.)

ABSTRACT FoxO transcription factors promote longevity across taxa. How they do so is poorly understood. In the nematode *Caenorhabditis elegans*, the A- and F-isoforms of the FoxO transcription factor DAF-16 extend life span in the context of reduced DAF-2 insulin-like growth factor receptor (IGFR) signaling. To elucidate the mechanistic basis for DAF-16/FoxO-dependent life span extension, we performed an integrative analysis of isoform-specific *daf-16/FoxO* mutants. In contrast to previous studies suggesting that DAF-16F plays a more prominent role in life span control than DAF-16A, isoform-specific *daf-16/FoxO* mutant phenotypes and whole transcriptome profiling revealed a predominant role for DAF-16A over DAF-16F in life span control, stress resistance, and target gene regulation. Integration of these datasets enabled the prioritization of a subset of 92 DAF-16/FoxO target genes for functional interrogation. Among 29 genes tested, two DAF-16A-specific target genes significantly influenced longevity. A loss-of-function mutation in the conserved gene *gst-20*, which is induced by DAF-16A, reduced life span extension in the context of *daf-2/IGFR* RNAi without influencing longevity in animals subjected to control RNAi. Therefore, *gst-20* promotes DAF-16/FoxO-dependent longevity. Conversely, a loss-of-function mutation in *srr-4*, a gene encoding a seven-transmembrane-domain receptor family member that is repressed by DAF-16A, extended life span in control animals, indicating that DAF-16/FoxO may extend life span at least in part by reducing *srr-4* expression. Our discovery of new longevity genes underscores the efficacy of our integrative strategy while providing a general framework for identifying specific downstream gene regulatory events that contribute substantially to transcription factor functions. As FoxO transcription factors have conserved functions in promoting longevity and may be dysregulated in aging-related diseases, these findings promise to illuminate fundamental principles underlying aging in animals.

KEYWORDS *C. elegans*; aging; longevity; insulin-like growth factor signaling; FoxO transcription factors

FOXO transcription factors control development, metabolism, stress responses, and aging in diverse animal species (Accili and Arden 2004; Barthel *et al.* 2005; van der Horst and Burgering 2007; Kenyon 2010). In invertebrates, FoxO promotes longevity in the context of reduced insulin-like signaling (Kenyon *et al.* 1993; Lin *et al.* 1997; Ogg *et al.* 1997; Slack *et al.* 2011; Yamamoto and Tatar 2011). Phenotypic analysis of knockout mice implicates FoxO transcription factors in the pathogenesis of aging-related diseases such as cancer (Paik *et al.* 2007; Gan *et al.* 2010; Sykes *et al.* 2011), type 2 diabetes (Kitamura *et al.* 2002; Nakae *et al.* 2002; Dong *et al.* 2008; Cheng *et al.* 2009), osteoporosis (Ambrogini *et al.* 2010; Rached *et al.* 2010), and atherosclerosis (Tsuchiya *et al.* 2012, 2013). Furthermore, FoxO3 is required for life span extension in mice subjected to dietary restriction (Shimokawa *et al.* 2015). In humans, FoxO1 and

doi: 10.1534/genetics.115.177998
Manuscript received May 9, 2015; accepted for publication July 24, 2015; published Early Online July 27, 2015.
Available freely online through the author-supported open access option.
Supporting information is available online at www.genetics.org/lookup/suppl/doi:10.1534/genetics.115.177998/-/DC1.
[1]Corresponding author: 3027 BSRB, 109 Zina Pitcher Place, Ann Arbor, MI 48109. E-mail: pathu@umich.edu

FoxO3 polymorphisms are associated with extreme longevity in multiple independent cohorts of centenarians (Lunetta *et al.* 2007; Willcox *et al.* 2008; Anselmi *et al.* 2009; Flachsbart *et al.* 2009; Li *et al.* 2009; Pawlikowska *et al.* 2009). The evolutionary conservation of FoxO functions in promoting longevity suggests that understanding the molecular basis for FoxO transcription factor action will illuminate fundamental mechanisms that govern aging.

The well-established role of FoxO transcription factors as targets of insulin-like signaling first came to light from studies in *Caenorhabditis elegans*, where the insulin/insulin-like growth factor receptor (IGFR) ortholog DAF-2 promotes reproductive development and limits adult life span by inhibiting the FoxO transcription factor DAF-16 via a conserved phosphoinositide 3-kinase (PI3K)/Akt pathway-dependent mechanism. Engagement of DAF-2/IGFR by agonist insulin-like ligands activates the PI3K/Akt pathway, resulting in Akt-dependent phosphorylation of three DAF-16/FoxO amino acid residues that lie within conserved RxRxxS/T motifs. Phosphorylated DAF-16/FoxO is subsequently exported from the nucleus and sequestered in the cytoplasm. When DAF-2/IGFR pathway activity is reduced, unphosphorylated DAF-16/FoxO translocates to the nucleus, where it regulates the expression of numerous genes, including those that control metabolism, immunity, and detoxification (Murphy and Hu 2013). The inhibition of FoxO by insulin-like signaling is evolutionarily conserved, as reduction of FoxO activity ameliorates biological phenotypes associated with reduced insulin-like signaling in flies (Junger *et al.* 2003; Slack *et al.* 2011; Yamamoto and Tatar 2011) and mice (Kitamura *et al.* 2002; Nakae *et al.* 2002; Dong *et al.* 2008; Cheng *et al.* 2009).

DAF-16/FoxO also promotes life span extension in animals lacking a germline (Hsin and Kenyon 1999). Although DAF-2/IGFR and the germline both control DAF-16/FoxO activity by regulating its subcellular localization (Henderson and Johnson 2001; Lee *et al.* 2001; Lin *et al.* 2001), they may do so through distinct mechanisms, as the molecular requirements for DAF-16/FoxO regulation by DAF-2/IGFR signaling and the germline differ (Berman and Kenyon 2006; Ghazi *et al.* 2009).

Work from multiple groups has identified hundreds of genes that are regulated by DAF-16/FoxO in the context of reduced DAF-2/IGFR signaling (Lee *et al.* 2003; McElwee *et al.* 2003; Murphy *et al.* 2003). Our understanding of the functional significance of DAF-16/FoxO target genes in mediating DAF-16/FoxO-dependent longevity is based primarily on a study in which nearly 60 DAF-16/FoxO target genes were tested for roles in DAF-16/FoxO-dependent life span extension using RNAi-based assays. This revealed that most single gene RNAi knockdowns have relatively small effects on longevity, leading to the conclusion that DAF-16/FoxO promotes longevity through the cumulative regulation of hundreds of genes (Murphy *et al.* 2003).

The roles of most individual DAF-16/FoxO-dependent gene regulatory events in life span control have not been assessed experimentally. This may be due in large part to the abundance of genes regulated by DAF-16/FoxO. Efforts to prioritize DAF-16/FoxO target genes based on direct binding of DAF-16/FoxO to promoters succeeded in identifying *aakg-4* as a gene that is directly induced by DAF-16/FoxO and required for DAF-16/FoxO-dependent life span extension (Schuster *et al.* 2010; Tullet *et al.* 2014). Therefore, strategies to prioritize subsets of DAF-16/FoxO target genes can lead to the discovery of new longevity genes by permitting detailed functional analysis of a relatively small number of genes.

The *daf-16* genomic locus encodes three groups of transcripts (a, b, and d/f/h) that are transcribed from distinct promoters (Lin *et al.* 1997; Ogg *et al.* 1997; Kwon *et al.* 2010). The encoded proteins possess phosphorylation sites conserved in humans and other species (Supporting Information, Figure S1, A and B). *daf-16d*, *f*, and *h* are transcribed from the same promoter but have distinct 5′ ends and translational start sites (Figure S1C; Figure S2; WormBase, www.wormbase.org) (Kwon *et al.* 2010; Murphy and Hu 2013). For clarity, we refer to the *d/f/h* group of transcripts and polypeptides collectively as *daf-16f* and DAF-16F, respectively. In animals with diminished DAF-2/IGFR signaling, mutations that reduce *daf-16a* and *f* but not *daf-16b* activity shorten life span to the same extent as *daf-16* null mutations (Lee *et al.* 2001). Furthermore, overexpression of DAF-16B under the control of its endogenous promoter does not extend the life span of *daf-16/FoxO* null mutants (Lee *et al.* 2001; Kwon *et al.* 2010). These data implicate DAF-16A and DAF-16F as the critical targets of DAF-2/IGFR in life span control. Analysis of functional isoform-specific DAF-16::GFP reporters demonstrates that DAF-16A and DAF-16F have overlapping spatiotemporal expression patterns and are both expressed in multiple tissues (Kwon *et al.* 2010). Notably, although the set of genes collectively regulated by DAF-16/FoxO is well defined, the roles of specific DAF-16/FoxO isoforms in gene regulation are obscure.

In light of the differential influence of DAF-16/FoxO isoforms on longevity (Kwon *et al.* 2010), we hypothesized that detailed characterization of isoform-specific *daf-16/FoxO* mutants would illuminate the molecular basis for DAF-16/FoxO action in life span control by enabling the prioritization of a subset of DAF-16/FoxO target genes for further investigation.

Materials and Methods

C. elegans strains and maintenance

Strains used in this study are listed in Table S17; Table S20. Animals were maintained at 15° on nematode growth media (NGM) plates seeded with *Escherichia coli* OP50. Double mutants were constructed using standard genetic techniques. Genotypes were confirmed by PCR amplification to detect restriction fragment length or PCR polymorphisms. Percival I-36NL incubators (Percival Scientific, Perry, IA) were used for maintenance, dauer arrest assays, and life span assays.

RNA isolation

Animals were washed twice in M9 buffer. Total RNA was isolated using TRIzol reagent (Invitrogen) and purified using

an RNeasy kit (Qiagen, Valencia, CA) according to the manufacturer's instructions.

Quantitative real-time reverse-transcriptase PCR

cDNA was synthesized using a SuperScript III Reverse Transcriptase kit and random hexamers (Invitrogen, Carlsbad, CA). Real-time PCR was then performed in triplicate using Power SYBR Green PCR master mix (Applied Biosystems, Warrington, UK) and a Mastercycler ep realplex thermal cycler (Eppendorf North America, Westbury, NY). A total of 10 ng of cDNA was used as a template in 15 μl reaction volume. Primers were selected initially using GETPrime (Gubelmann *et al.* 2011) and Primer-BLAST (http://www.ncbi.nlm.nih.gov/tools/primer-blast/) and subsequently validated by melt curve analysis and agarose gel electrophoresis. Primer sequences are listed in Table S21. Relative expression levels and technical error were determined by the $\Delta\Delta 2C_t$ method (Nolan *et al.* 2006). Gene expression levels were normalized to actin (*act-1*), and the ratio of expression relative to *act-1* was then compared to the same ratio in N2 Bristol wild type. Statistical analysis was performed in GraphPad Prism (GraphPad Software, La Jolla, CA) using the paired ratio *t*-test.

Rapid amplification of complementary DNA (cDNA) ends

Total RNA was isolated from young adult animals. *daf-16a* and *daf-16f* cDNA was prepared using a 5′ rapid amplificiation of cDNA ends (RACE) system version 2.0 (Invitrogen). First-strand cDNA was synthesized using a *daf-16a/f* gene-specific primer and SuperScript II. The original mRNA template was degraded by RNase H and RNase T1. After purification, a homopolymeric tail was added using terminal deoxynucleotidyl transferase to the 3′ end of cDNA. Standard PCR was performed using Taq DNA polymerase, a nested *daf-16a* or *daf-16f*-specific primer, and the abridged anchor primer complementary to the homopolymeric tail. After visualization of products on a standard agarose gel, the reaction mix was cloned into pCR4-TOPO vector using a TOPO TA Cloning kit (Invitrogen) and transformed into chemically competent *E. coli* DH5α. Clones were selected on LB plates containing 50 μg/ml ampicillin, and plasmids were analyzed by Sanger sequencing. Numbers of clones analyzed for each strain are indicated in Table S22.

Dauer arrest assays

Dauer assays were performed at 25° as previously described (Hu *et al.* 2006). Briefly, animals were synchronized in a 4-hr egglay at 15° and grown at 25° on NGM plates. Animals were scored when wild-type animals were gravid adults and *daf-2* animals had arrested as dauers (∼60–72 h after egglay). Statistical significance was assessed using a two-tailed, unpaired *t*-test with Welch's correction.

Life span assays

Life span assays were performed as previously described (Chen *et al.* 2013a), with minor modifications. Animals derived from a synchronized 4-hr egglay were grown at 15° until the L4 larval stage and then shifted to 20°. Plates harboring any males were discarded. Animals were grown for an additional 20–24 hr to day 1 of adulthood and then placed on life span plates containing 25 μg/ml 5-fluoro-2′-deoxyuridine (FUDR) (Sigma-Aldrich, St. Louis) to prevent progeny growth. *glp-1* mutant animals were raised for 48 hr at the restrictive temperature (25°) to ablate the germline and then shifted to 20°. Statistical significance was assessed using the standard chi-square-based log-rank test in GraphPad Prism.

RNAi

RNAi clones were identical to previously published isoform-specific and pan-*daf-16* RNAi clones (Kwon *et al.* 2010). Feeding RNAi was performed using standard procedures (Kamath *et al.* 2001). All RNAi NGM plates contained 5 mM IPTG and 25 μg/ml carbenicillin. NGM plates were seeded with an overnight culture of *E. coli* HT115 with either control L4440 vector or RNAi plasmid. For RNAi life span assays, HT115 was concentrated 5×. Plasmids from *E. coli* clones were sequenced for every experimental replicate to confirm their identity.

MosI-mediated single copy insertion

Using the full build service platform at Knudra Transgenics, the plasmids pNU164 and pNU191 were constructed by inserting *daf-16* cargo into MosI-mediated single copy insertion (MosSCI) vector backbones. For pNU164, the *daf-16a* cDNA was PCR amplified from yk13f11/yk1006c10 plasmid, and the full-length *daf-16* 3′ UTR was PCR amplified from wild-type genomic DNA. These two were ligated by PCR-mediated overlap extension (Heckman and Pease 2007) and cloned into a pCFJ151 plasmid. A hybrid segment composed of the 3′ portion of the cDNA and the 3′ UTR was amplified from this plasmid, while *daf-16a* promoter segments and partial *daf-16a* genomic sequence was PCR amplified from wild-type genomic DNA. All parts were then inserted into the multiple cloning site (MCS) of pCFJ151 via Gibson ligation. For pNU191, the promoter and unique *daf-16f* exons were PCR amplified from wild-type genomic DNA. The common *daf-16a/f* coding segment and the end of the coding region through the 3′ UTR were amplified from pNU164. All parts were then inserted into the MCS of pCFJ151 via Gibson ligation. All coding regions of plasmids were verified by Sanger sequencing. For production of transgenic animals, plasmids were used in a MosSCI injection mix and used to create single copy insertions at the ttTi5605 locus as per published methods (Frokjaer-Jensen *et al.* 2008).

Stress-resistance assays

For all stress assays, animals derived from a synchronized 4-hr egglay were grown at 15° until the late L3 larval stage and then shifted to 20° and grown for an additional 12 hr until the L4 larval stage. Plates harboring any males were discarded.

For oxidative stress, animals were transferred to plates containing 7.5 mM *tert*-butyl hydroperoxide (*t*-BOOH) (Sigma-Aldrich) and scored approximately three times per

day for survival. For ultraviolet (UV) stress, animals were transferred to plates lacking bacteria and irradiated with 1200 J/m^2 UV-C using a Stratalinker 2400 UV crosslinker (Stratagene). UV-treated animals were then transferred to seeded plates containing 25 μg/ml FUDR and scored daily for survival. For thermotolerance, animals were transferred to seeded plates containing 25 μg/ml FUDR, grown for an additional 12 hr at 20°, shifted to 33°, and scored approximately four times per day for survival. For all assays, animals that dessicated on the side of plates were censored. Statistical significance was assessed in GraphPad Prism using the standard chi-square-based log-rank test.

Whole transcriptome profiling (RNA-Sequencing)

Animals were grown as described for life span assays. After picking a subset of the population for life span assays, the remaining animals were harvested for isolation of total RNA. The Agilent TapeStation was used to assess RNA quality. Samples with RNA integrity numbers (RINs) of eight or greater were prepped using the Illumina TruSeq mRNA Sample Prep v2 kit (catalog nos. RS-122-2001 and RS-122-2002). Messenger RNA (mRNA) was isolated from 0.1 to 3 μg of total RNA by polyA$^+$ purification, fragmented, and copied into first-strand cDNA using reverse transcriptase and random primers. The 3′ cDNA ends were then adenylated and adapters were ligated. One of the adapters contained a six-nucleotide barcode to enable multiplexing of samples. Products were purified and enriched by PCR to create the final cDNA library. Libraries were checked for quality and quantity by Agilent TapeStation and quantitative PCR (qPCR) using a library quantification kit for Illumina sequencing platforms (catalog no. KK4835, Kapa Biosystems, Wilmington, MA). Clonal clusters were generated using cBot (Illumina, San Diego). Quadriplexed samples were sequenced using the HiSequation 2000 system (Illumina) with a 100-cycle paired-end run in high output mode using version 3 reagents according to manufacturer's protocols.

RNA-seq analysis

Individual read files for each sample were concatenated into a single .fastq file. Raw reads data for each sample were checked using FastQC (version 0.10.0, Babraham Bioinformatics, Cambridge, United Kingdom; http://www.bioinformatics.bbsrc.ac.uk/projects/fastqc/) to identify features potentially indicative of quality issues (*e.g.*, low-quality scores, overrepresented sequences, and inappropriate GC content). We used the Tuxedo Suite (Langmead *et al.* 2009; Trapnell *et al.* 2009, 2013) for alignment, differential expression analysis, and postanalysis diagnostics. Briefly, reads were aligned to the reference genome (University of California Santa Cruz, UCSC ce10; http://genome.ucsc.edu/) using TopHat (version 2.0.9) (Trapnell *et al.* 2009) and Bowtie (version 2.1.0.0) (Langmead 2010). Alignments were performed using default parameter settings, with the exception of "–b2-very-sensitive" and "–no-coverage-search." Additionally, the "max_intron_length" parameter was set to 25 kb to minimize false positive splice junction discovery. A second round of quality control was then performed using FastQC to ensure that only high-quality data were analyzed further. Cufflinks/CuffDiff (version 2.1.1) (Trapnell *et al.* 2013) was used for quantification of expression and differential expression analysis, using UCSC ce10.fa as the reference genome and UCSC ce10.gtf as the reference transcriptome (http://genome.ucsc.edu/). For this analysis, we used parameter settings "–multi-read-correct" to adjust expression calculations for reads that map to more than one locus, as well as "–compatible-hits-norm" and "–upper-quartile –norm" for normalization of expression values. We generated diagnostic plots using the CummeRbund package (Trapnell *et al.* 2012) as a quality check on normalized data.

RNA-seq reads were examined using the Integrative Genomics Viewer version 2.3.39 (Broad Institute) (Robinson *et al.* 2011; Thorvaldsdottir *et al.* 2013). The annotated gene expression data output from CuffDiff was read into R (http://www.r-project.org/) for six comparisons: *daf-2(e1370)* compared to wild type, *daf-16(mu86);daf-2*, *daf-16a/f(mg54);daf-2*, *daf-16a(tm5030);daf-2*, *daf-16a(tm5032);daf-2*, and *daf-16f(tm6659);daf-2*. DAF-16A/F targets were defined by the following criteria: (1) fold change (FC) $\geq \pm 1.5$ for wild type *vs.* *daf-2*, and (2) FC ≥ 2 in the opposite direction as wild type *vs.* *daf-2* for both *daf-2 vs. daf-16(mu86);daf-2* and *daf-2 vs. daf-16a/f(mg54);daf-2*. We required FDR < 0.05 for only one of the three comparisons for three reasons: (1) nearly all genes showed concordance in FC for all three comparisons even if they did not satisfy FDR < 0.05 for all three; (2) some known DAF-16/FoxO targets only satisfied FDR < 0.05 in one or two comparisons; and (3) the choice of requiring FDR < 0.05 for one, two, or three comparisons did not significantly affect the categorization of DAF-16A/F target genes (Table S23; see below). FC ≥ 2 instead of 1.5 was chosen for the *daf-2 vs. daf-16;daf-2* comparisons to improve quantification of the effects of *daf-16a* and *daf-16f* mutations on gene expression.

For functional enrichment testing, we identified enriched Gene Ontology (GO) biological process terms (Ashburner *et al.* 2000) and Kyoto Encyclopedia of Genes and Genomes (KEGG) pathways (Kanehisa and Goto 2000) using LRpath, a logistic regression method that overcomes limitations associated with the use of arbitrary significance cutoff values by taking into account the distribution of significance levels of all profiled genes (Sartor *et al.* 2009). Enriched GO terms and KEGG pathways were defined as those having a false discovery rate of <0.01. We used a directional LRpath test to distinguish between up-regulated and down-regulated functions. Overlapping and redundant GO terms were clustered semantically with REVIGO (Supek *et al.* 2011). We employed a semantic similarity (SimRel) cutoff of 0.7 to define representative terms. LRpath and REVIGO outputs are shown in Table S15.

To define classes of DAF-16A/F targets, A and F indices (I_A and I_F) were calculated for 399 DAF-16A/F targets. Given high correlation in gene expression between *daf-16a(tm5030);daf-2* and *daf-16a(tm5032);daf-2* (Figure S17),

a combined *daf-16a;daf-2* gene expression profile was generated by calculating the mean fragments per kilobase per million reads (FPKM) for each gene. I_A for each gene was defined as the absolute FPKM difference between *daf-2(e1370)* and *daf-16a; daf-2*, divided by the absolute FPKM difference between *daf-2(e1370)* and *daf-16a/f(mg54);daf-2*. Likewise, I_F for each gene was defined as the FPKM difference between *daf-2(e1370)* and *daf-16f(tm6659);daf-2*, divided by the FPKM difference between *daf-2(e1370)* and *daf-16a/f(mg54);daf-2*.

Classes of DAF-16A/F targets were defined by the following criteria: DAF-16A-specific, $I_A > 0.8$ and $I_F < 0.2$; DAF-16F-specific, $I_F > 0.8$ and $I_A < 0.2$; and redundantly regulated, $I_A < 0.2$ and $I_F < 0.2$. Genes not binned into these three categories were partitioned into one of the following three groups: shared A-dominant (shared A > F), $I_A/I_F > 2$; shared F-dominant (shared F > A), $I_F/I_A > 2$; or equally shared (shared A = F), $0.5 \leq I_A/I_F \leq 2$.

RNAi-defective assays

Assays were performed essentially as described (Billi *et al.* 2012). L1 larvae were picked onto RNAi plates (5 mM IPTG, 25 μg/ml carbenicillin) seeded with an overnight culture of *E. coli* HT115 containing a *pos-1* RNAi plasmid, which causes embryonic lethality (Tabara *et al.* 1999). *rde-4(ne301)* was used as an RNAi-defective (rde) control (Tabara *et al.* 2002). Animals were grown for 84 hr at 20° to allow for development and egglaying and then removed from the plate. Eggs were counted immediately, live progeny were counted 48 hr later, and percentage of nonviable eggs was calculated.

Data availability

Strains are available upon request. Whole transcriptome profiling data are available at GEO with the accession number: GSE72426.

Results

Molecular characterization of isoform-specific daf-16/FoxO mutants

To isolate *daf-16a*- and *daf-16f*-specific mutant alleles, we screened for mutants with deletions in the unique N-terminal exons of each isoform (Gengyo-Ando and Mitani 2000). Two independent alleles, *tm5030* and *tm5032*, are deletions in the *daf-16a*-specific exon (Figure 1). The 5′ RACE analysis shows that these mutations result in frameshifts and predicted early translation termination (Figure 1B, Figure S3, Figure S4, and Figure S5). As expected, both *tm5030* and *tm5032* significantly reduced *daf-16a* transcript levels as measured by quantitative real-time reverse transcriptase PCR (qPCR; Figure S6 A and B; Table S1), consistent with nonsense-mediated decay secondary to premature translation termination. Neither mutation influenced the integrity or quantity of *daf-16b* or *daf-16f* transcripts (Figure S6, C and D; Table S1). *tm6659* is a deletion that spans all four *daf-16f*-specific exons, including all three putative transcriptional and translational start sites

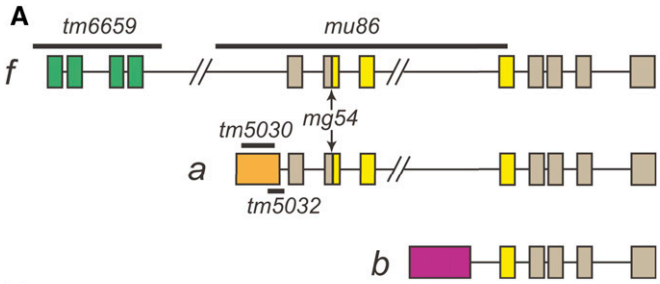

B

Allele	Referred to as	Isoform(s) affected	Predicted effect on protein
mu86	*daf-16(null)*	a, b, f	elimination of DAF-16F Forkhead domain, elimination of all DAF-16A and DAF-16B
mg54	*daf-16a/f*	a, f	Y 147 ➔ STOP
tm5030	*daf-16a #1*	a	frameshift after 7 aa ➔STOP after 91 aa
tm5032	*daf-16a #2*	a	translation into intron after 58 aa ➔STOP after 6 aa
tm6659	*daf-16f*	f	no protein due to elimination of transcriptional and translational start sites

Figure 1 *daf-16/FoxO* isoforms and isoform-specific mutations. (A) *daf-16/FoxO* genomic structure with isoform-specific mutations. Colors indicate unique N-terminal exons (green and orange) and Forkhead domains (yellow) that correspond to DAF-16/FoxO protein domains in Figure S1A. (B) Summary of isoform-specific mutant alleles. See text for details.

(Figure 1A; Figure S1C) (Kwon *et al.* 2010; Murphy and Hu 2013). *daf-16f* transcripts were undetectable in animals harboring *tm6659* by 5′ RACE and qPCR (Figure S3; Figure S6D; Table S1), and neither *daf-16a* nor *daf-16b* transcripts were affected (Figure S6 A–C; Table S1). Total *daf-16* levels are sharply reduced in *tm6659* mutants (Figure S6 E and F; Table S1). Importantly, our data show no compensatory increase in *daf-16f* transcripts in either *daf-16a(tm5030)* or *daf-16a (tm5032)* (Figure S6D) and no increase in *daf-16a* transcripts in *daf-16f(tm6659)* (Figure S6, A and B).

Taken together, these data strongly suggest that *tm5030*, *tm5032*, and *tm6659* are *bona fide* isoform-specific loss-of-function alleles. These isoform-specific alleles are henceforth referred to as *daf-16a* no. 1 *(tm5030)*, *daf-16a* no. 2 *(tm5032)*, and *daf-16f (tm6659)*.

DAF-16A promotes dauer arrest in animals with reduced DAF-2/IGFR signaling

In response to adverse environmental conditions, *C. elegans* larvae undergo developmental arrest in an alternative larval stage known as dauer (Riddle 1988). *daf-2/IGFR* and *daf-16/FoxO* mutants were first isolated in genetic screens for animals with dauer-constitutive (Daf-c) and dauer-defective (Daf-d) phenotypes, respectively (Riddle *et al.* 1981). *daf-2/IGFR* mutants constitutively arrest as dauers at 25° in a *daf-16/FoxO*-dependent manner (Riddle *et al.* 1981; Vowels and Thomas 1992; Gottlieb and Ruvkun 1994).

To examine the roles of distinct DAF-16/FoxO isoforms in dauer regulation, we determined the influence of isoform-specific *daf-16/FoxO* mutations on dauer-constitutive phenotypes in two *daf-2/IGFR* mutant backgrounds: *e1368*, a missense mutation in the DAF-2/IGFR extracellular ligand-binding domain, and *e1370*, a missense mutation in the cytoplasmic tyrosine kinase domain (Kimura *et al.* 1997). *e1370* may be a stronger loss-of-function allele than *e1368*, as it causes a more penetrant dauer-constitutive phenotype and extends life span to a greater extent than *e1368* (Figure 2 and Figure 3) (Gems *et al.* 1998).

As previously shown, the dauer-constitutive phenotype caused by both *daf-2/IGFR* mutations is fully suppressed by the null *daf-16/FoxO* allele *mu86* (*Lin et al. 1997*) as well as by *mg54* (Figure 2; Table S2; Table S3; Table S4), a nonsense mutation that affects *daf-16a* and *daf-16f* but not *daf-16b* (Figure 1, A and B) (Ogg *et al.* 1997; Lee *et al.* 2001). *daf-16(mu86)* and *daf-16(mg54)* are henceforth referred to as "*daf-16* null" and "*daf-16a/f* mutation" for purposes of clarity. These results indicate that DAF-16B does not suffice to promote dauer arrest in animals with reduced DAF-2/IGFR signaling, implicating DAF-16A and/or DAF-16F in dauer regulation.

Both *daf-16a* mutations completely suppress the dauer-constitutive phenotype of *daf-2(e1368)* mutants, whereas *daf-16f* mutation does not influence *daf-2(e1368)* dauer arrest (Figure 2A; Table S2; Table S3). Thus, in this context, DAF-16A is the critical isoform that regulates dauer arrest. This result is consistent with the observation that in *daf-2(e1368)* animals, DAF-16A translocates to nuclei, whereas DAF-16F remains cytoplasmic (Bansal *et al.* 2014). In *daf-2(e1370)* mutants, *daf-16a* no. 1 and no. 2 mutations suppress dauer arrest by 22% ($P = 0.0204$) and 24% ($P = 0.0408$), respectively, whereas *daf-16f* mutation has no effect on dauer arrest (Figure 2B; Table S2; Table S4). Since *daf-16a/f* mutation fully suppresses *daf-2(e1370)* dauer arrest (Figure 2B; Table S2; Table S4), DAF-16A and DAF-16F act redundantly to promote dauer arrest in *daf-2(e1370)* mutant animals.

DAF-16A promotes longevity in animals with reduced DAF-2/IGFR signaling

DAF-16/FoxO is required for life span extension both in animals with reduced DAF-2/IGFR activity (Kenyon *et al.* 1993) and in animals lacking a germline (Hsin and Kenyon 1999). Experiments involving RNAi-based knockdown and transgenic overexpression of DAF-16/FoxO isoforms suggest that both DAF-16A and DAF-16F promote longevity in *daf-2/IGFR* mutants (Kwon *et al.* 2010). We determined the effect of *daf-16a* and *daf-16f* mutations on life span in *daf-2(e1368)* and *daf-2(e1370)* mutants. As previously shown, life span extension induced by *daf-2/IGFR* mutation was fully suppressed by *daf-16* null mutation as well as by *daf-16a/f* mutation (Figure 3, A–D; Table S5; Table S6) (Lee *et al.* 2001; Lin *et al.* 2001).

daf-16a no. *1* and no. *2* mutations partially reduced mean life spans of both *daf-2(e1368)* and *daf-2(e1370)* mutants, whereas *daf-16a/f* mutation decreased mean life spans to the same extent as *daf-16* null mutation (Figure 3, A and C; Table S5; Table S6). These results indicate that DAF-16A is partially required for the longevity of *daf-2/IGFR* mutants. In contrast, *daf-16f* mutation did not reproducibly influence life span in either *daf-2/IGFR* mutant background (Figure 3, B and D; Table S5; Table S6). This finding was unexpected in light of previous studies implicating DAF-16F in life span control by the DAF-2/IGFR pathway (Kwon *et al.* 2010; Bansal *et al.* 2014). Taken with our finding that the *tm6659* mutation likely fully eliminates *daf-16f* activity (Figure 1, A and B; Figure S1C; Figure S6D), our data are consistent with a hierarchical model of DAF-16/FoxO isoform function in promoting longevity in the context of reduced DAF-2/IGFR signaling. DAF-16A is necessary for full life span extension. However, DAF-16F is dispensable for longevity, as DAF-16A is sufficient to fully extend life span even when *daf-16f* is mutated.

Given that *daf-16a/f* mutation shortens life span in animals with reduced DAF-2/IGFR activity to a much greater extent than *daf-16a* mutation alone (Figure 3, A and C; Table S5; Table S6), we tested the possibility that DAF-16F is required for life span extension in the absence of DAF-16A by performing isoform-specific *daf-16/FoxO* RNAi (Kwon *et al.* 2010). As previously shown, inactivation of either *daf-16a* or *daf-16f* alone by RNAi had a modest effect on the longevity of *daf-2/IGFR* mutant animals compared to RNAi of all *daf-16/FoxO* isoforms ("pan-*daf-16* RNAi"; Figure S7A; Table S7) (Kwon *et al.* 2010). However, *daf-16f* RNAi shortened the mean life span of *daf-16a;daf-2* double mutant animals to nearly the same extent as *pan-daf-16* RNAi (Figure 3E; Table S7). Therefore, although DAF-16F is dispensable for longevity in the presence of DAF-16A, it is required for life span extension in animals lacking DAF-16A. The life span shortening effect of *daf-16a* RNAi in *daf-16a;daf-2* double mutants may be a consequence of off-target RNAi effects (Ma *et al.* 2006).

We also wished to determine the extent to which longevity in *daf-16f;daf-2* double mutants requires DAF-16A. To address this question, we performed isoform-specific *daf-16/FoxO* RNAi on *daf-16f;daf-2* double mutants. *daf-16a* RNAi shortened the mean life span of *daf-16f;daf-2* double mutant animals by nearly the same amount as *pan-daf-16* RNAi (Figure 3F; Table S7). In contrast, *daf-16f* RNAi had a negligible effect on *daf-16f;daf-2* mean life span. Therefore, when DAF-16F is absent, DAF-16A is likely the sole FoxO isoform that promotes longevity. In aggregate, our results indicate that DAF-16A is the primary isoform that controls *C. elegans* aging in the context of reduced DAF-2/IGFR signaling. DAF-16F is not required for longevity when DAF-16A is present, but it promotes long life in the absence of DAF-16A.

Rescue of mutant phenotypes with single-copy isoform-specific DAF-16/FoxO transgenes

Our data on DAF-16/FoxO isoform function are in agreement with a previous study implicating both DAF-16A and DAF-16F in dauer regulation in the *daf-2(e1370)* mutant background (Kwon *et al.* 2010). However, our results contradict the contention that DAF-16F plays a more prominent role in life span control than DAF-16A (Kwon *et al.* 2010; Bansal

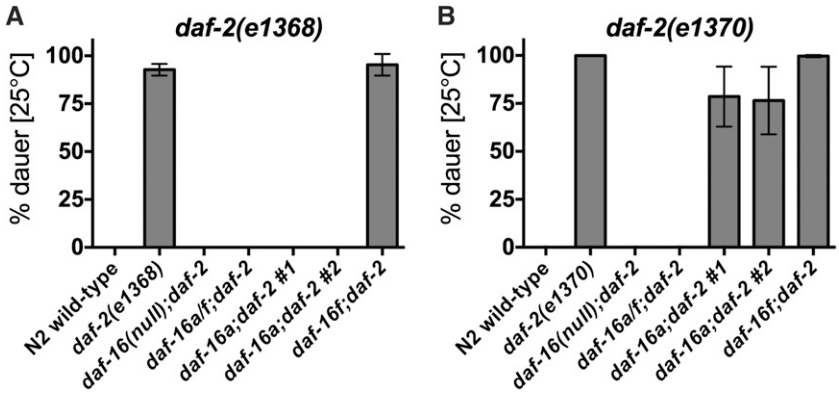

Figure 2 *daf-16a*-specific mutations suppress dauer arrest in *daf-2/IGFR* mutants. (A) The dauer-constitutive phenotype of *daf-2(e1368)* animals is fully suppressed by *daf-16a/f* mutation and both *daf-16a* mutations but is unaffected by *daf-16f* mutation. (B) The dauer-constitutive phenotype of *daf-2(e1370)* animals is fully suppressed by *daf-16a/f* mutation, partially suppressed by both *daf-16a* mutations, and unaffected by *daf-16f* mutation. Mean and standard deviation for at least three biological replicates are presented. Statistics and raw data are presented in Table S2; Table S3; Table S4.

et al. 2014). This discrepancy may be a consequence of distinct experimental strategies used to assess the function of DAF-16/FoxO isoforms in life span control. We used isoform-specific deletion mutants in which other *daf-16/FoxO* isoforms remained under the control of endogenous regulatory elements and continued to be expressed at physiological levels (Figure S6). In contrast, Kwon *et al.* (2010) based their analysis on strains harboring both a *daf-16/FoxO* null mutation and transgenes overexpressing cDNAs encoding individual *daf-16/FoxO* isoforms.

In an effort to reconcile our results with those of Kwon *et al.* (2010), we generated integrated transgenic strains expressing either *daf-16a* or *daf-16f* under the control of their native promoters (Figure S8). These transgenes were modeled after those reported by Kwon *et al.* (2010). To minimize potentially confounding influences pertaining to overexpression and/or differences in genomic integration sites, we constructed these strains using MosSCI (Frokjaer-Jensen *et al.* 2008). We crossed these single-copy transgenes into *daf-16a/f* and *daf-16a* mutant backgrounds to assess their relative activity in promoting longevity and dauer arrest.

To test the *daf-16a* transgene in life span control, we crossed it into *daf-16a/f;daf-2* double mutant animals that lack both DAF-16A and DAF-16F. *daf-16a/f;daf-2* double mutant animals containing the single-copy *daf-16a* transgene lived longer than nontransgenic siblings but significantly shorter than *daf-2* single mutants (Figure 3G; Figure S9A; Table S8) (and by inference, *daf-16f;daf-2* double mutants) (Figure 3D). Furthermore, this transgene did not fully rescue life span extension in *daf-16a;daf-2* double mutants (Figure S9, B and C; Table S8). Therefore, the *daf-16a* transgene promotes life span extension modestly in comparison to endogenous *daf-16a*, which extends life span fully in *daf-16f; daf-2* double mutants (Figure 3F). Similarly, although this *daf-16a* transgene rescued the dauer-constitutive phenotype of *daf-16a;daf-2(e1370)* double mutants (Figure S10B; Table S11), it did not rescue dauer arrest in *daf-16a;daf-2(e1368)* double mutants (Figure S10D; Table S11), nor did it fully rescue dauer arrest in *daf-16a/f;daf-2* double mutants (Figure S10, A and C; Table S11). In concert, these data indicate that this single-copy *daf-16a* transgene is less active than the endogenous *daf-16a* locus.

Promoter-swap experiments show that *daf-16a* or *daf-16f* transgenes driven by the *daf-16f* promoter rescue longevity to a greater extent than the same transgenes driven by the *daf-16a* promoter (Kwon *et al.* 2010). Intriguingly, WormBase (www.wormbase.org) annotations document the existence of *daf-16a* transcripts that originate from the *daf-16f* promoter. We verified this in two ways. First, we used PCR amplification and sequencing to identify splice junctions unique to these transcripts (Figure S11, A and B). Furthermore, we identified sequence reads in whole transcriptome profiling data that correspond to such transcripts (Figure S11B). Therefore, *daf-16a* is transcribed from two promoters, one of which is the same promoter that drives expression of *daf-16f*. As primary transcripts originating from the *daf-16f* promoter contain all *daf-16a* exons (Figure 1A), alternative splicing of such pre-mRNAs may generate mature *daf-16a* transcripts. Taken together with the relative importance of the *daf-16f* promoter in extending life span (Kwon *et al.* 2010), this finding could explain why our single-copy *daf-16a* transgene (Figure S8) has less activity than the endogenous *daf-16a* locus (Figure 3G; Figure S9, A–C; Figure S10, A–D).

To test the activity of our single-copy *daf-16f* transgene, we constructed *daf-16a/f;daf-2(e1368)* and *daf-16a/f;daf-2(e1370)* animals harboring the *daf-16f* transgene. The life spans of these animals were comparable to the life spans of *daf-16a;daf-2* double mutant animals (Figure 3H; Figure S9D; Table S8). Since *daf-16f* activity is the major contributor to longevity in *daf-16a;daf-2* double mutants (Figure 3E), the activity of *daf-16f* encoded by this single-copy transgene is comparable to the activity of the endogenous *daf-16f* locus. Dauer arrest phenotypes of these animals also mirrored those of *daf-16a;daf-2* double mutants (Figure S10, E and F). As previously observed in strains harboring multicopy *daf-16* transgenes (Kwon *et al.* 2010), animals with the *daf-16f* transgene lived much longer than those with the *daf-16a* transgene (Figure 3, G and H; Table S8). Notably, the *daf-16f* transgene significantly increased both the life span and the penetrance of the dauer-constitutive phenotype of *daf-16a;daf-2(e1370)* double mutant animals that contain intact endogenous *daf-16f* (Figure 3H; Figure S10E). Therefore, the longevity and dauer-constitutive phenotypes of *daf-2* mutant animals are highly sensitive to *daf-16f* gene dosage.

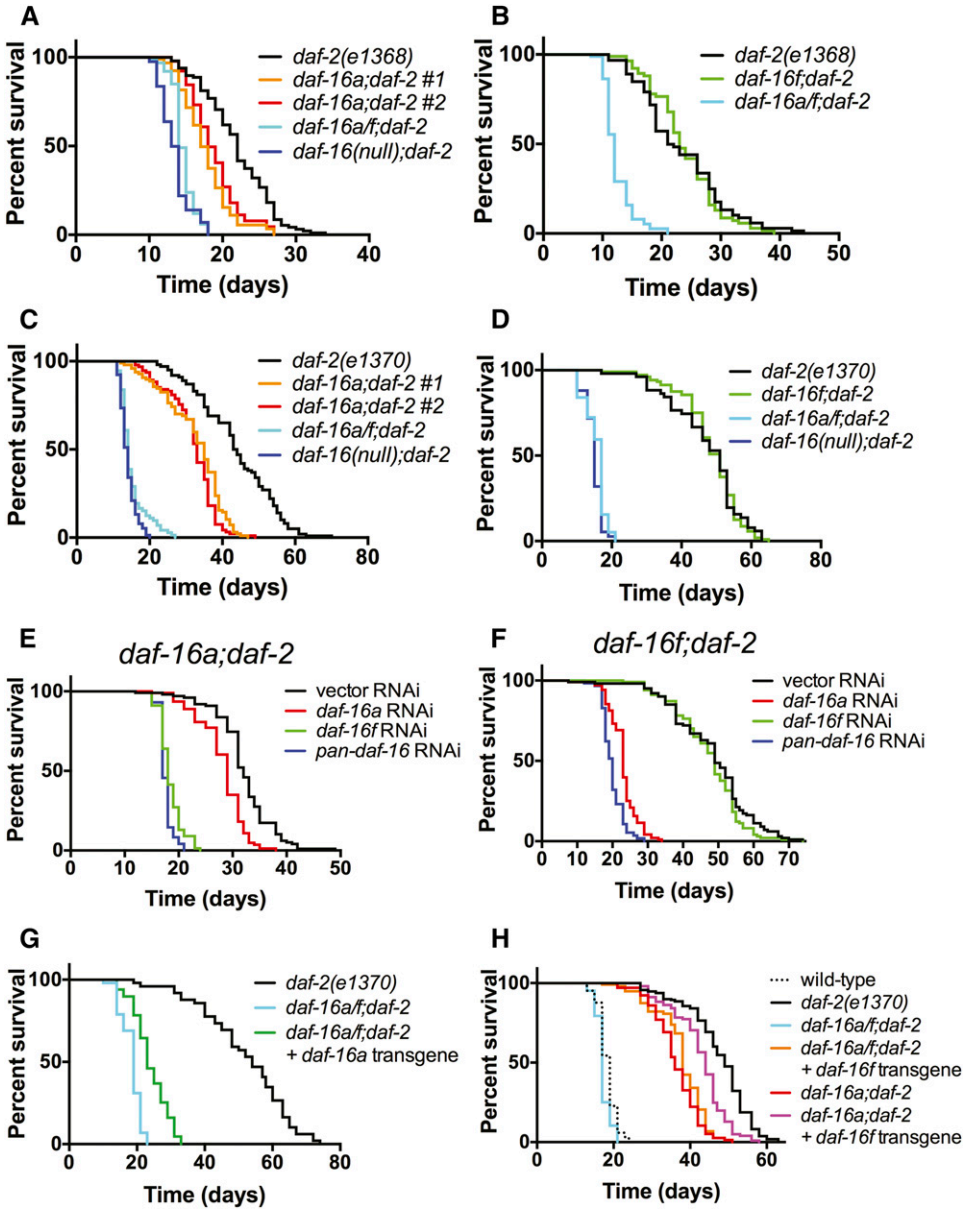

Figure 3 Effects of *daf-16a*- and *daf-16f*-specific mutations, RNAi, and single-copy transgenic rescues on *daf-2/IGFR* life span. (A–D) Effects of *daf-16a* (A and C) and *daf-16f* (B and D) mutations on life spans of *daf-2(e1368)* (A and B) and *daf-2 (e1370)* (C and D). (E and F) *daf-16f* is required for *daf-16a;daf-2* longevity and *vice versa*. Survival curves are presented for (E) *daf-16a;daf-2(e1370)* and (F) *daf-16f;daf-2 (e1370)* mutant animals upon exposure to isoform-specific *daf-16* RNAi. Figure S7A shows control *daf-2(e1370)* survival when treated with isoform-specific *daf-16* RNAi. (G) Effect of a single-copy *daf-16a* transgene on *daf-16a/f;daf-2(e1370)* life span. (H) Effect of a single-copy *daf-16f* transgene on *daf-16a/f;daf-2(e1370)* and *daf-16a;daf-2(e1370)* life span. See text for details. Statistics and raw data are presented in Table S5; Table S6; Table S7; Table S8.

Collectively, our results with single-copy isoform-specific *daf-16/FoxO* transgenes, while consistent with published results using multicopy transgenes (Kwon *et al.* 2010; Bansal *et al.* 2014), strongly suggest that the previously reported difference in longevity-promoting activity of multicopy *daf-16a*- and *daf-16f*-specific transgenes (Kwon *et al.* 2010; Bansal *et al.* 2014) is due to both overexpression of *daf-16f* as well as the failure of the *daf-16a*-specific transgene to recapitulate endogenous *daf-16a* activity.

DAF-16A promotes longevity in animals lacking a germline

Although DAF-16/FoxO is also required for longevity in animals lacking a germline (Hsin and Kenyon 1999), life span extension caused by germline ablation requires molecules such as KRI-1 and TCER-1 that are not necessary for longevity in *daf-2/IGFR* mutants (Berman and Kenyon 2006; Ghazi *et al.* 2009). These observations suggest that DAF-2/IGFR and the germline could control life span by coupling to distinct DAF-16/FoxO isoforms. To test this hypothesis, we determined the effect of isoform-specific *daf-16/FoxO* mutations on life span in animals harboring a temperature-sensitive *glp-1* mutation that develops without a germline when grown at 25° (Arantes-Oliveira *et al.* 2002). As we observed in animals with reduced DAF-2/IGFR activity, the life spans of germline-ablated animals were modestly reduced by *daf-16a* mutation (Figure 4A; Table S9). *daf-16f* mutation did not influence the life span of germline-ablated animals in a consistent manner (Figure 4B; Table S9).

RNAi-based inactivation of either *daf-16a* or *daf-16f* in animals lacking a germline revealed phenotypes similar to those observed in *daf-2/IGFR* mutants. Compared to pan-*daf-16*

RNAi, *daf-16a*, or *daf-16f* RNAi partially shortened median life spans of germline-ablated animals (Figure S7B; Table S10). In contrast, *daf-16f* RNAi shortened the life span of *daf-16a;glp-1* double mutant animals to the same extent as pan-*daf-16* RNAi (Figure 4C; Table S10). Likewise, *daf-16a* RNAi suppressed longevity to nearly the same degree as pan-*daf-16* RNAi in *daf-16f;glp-1* double mutants (Figure 4D; Table S10).

Collectively, these data show that DAF-16A is also the main FoxO isoform that promotes longevity in animals lacking a germline, while DAF-16F is not required for life span extension in this context. Furthermore, they demonstrate that the distinct molecular requirements for life span extension in *daf-2/IGFR* mutants and germline-ablated animals (Berman and Kenyon 2006; Ghazi *et al.* 2009) cannot be explained by the coupling of these upstream pathways to disparate DAF-16/FoxO isoform outputs.

DAF-16A promotes stress resistance in animals with reduced DAF-2/IGFR signaling

As DAF-16/FoxO is required for the resistance of *daf-2/IGFR* mutants to various environmental insults (Murakami and Johnson 1996; Honda and Honda 1999; McColl *et al.* 2010), we determined the impact of *daf-16a*- and *daf-16f*-specific mutations on the sensitivity of *daf-2(e1370)* mutants to heat, oxidative stress, and UV radiation. The effect of these mutations on stress tolerance was similar in each condition. As expected, the *daf-2/IGFR* mutant was significantly more resistant to heat, oxidative stress, and UV radiation (Figure S12; Table S12) than wild-type animals. *daf-16a/f* mutation completely abolished the resistance of the *daf-2/IGFR* mutant to heat and oxidative stress and strongly suppressed its resistance to UV radiation. In all three contexts, *daf-16a* mutation partially suppressed stress resistance of the *daf-2/IGFR* mutant, whereas *daf-16f* mutation did not influence its ability to withstand insult. These results mirror the impact of isoform-specific mutations on life span (Figure 3; Figure 4).

DAF-16/FoxO target gene regulation by DAF-16A and DAF-16F

To illuminate the mechanistic basis for DAF-16/FoxO isoform-specific functions in life span control, we performed whole transcriptome profiling of young adult *daf-2(e1370)* mutant animals in the context of wild-type *daf-16/FoxO* and isoform-specific *daf-16/FoxO* mutant alleles. A subset of animals from each experimental replicate was subjected to life span assays to confirm that all mutants from which RNA was isolated had the expected life span phenotypes. Identification of genes that were differentially expressed in wild type and *daf-2(e1370)* and differentially expressed in the opposite direction in both *daf-16(null);daf-2* and *daf-16a/f;daf-2* double mutants compared to *daf-2* mutants defined a set of 399 genes that are targets of DAF-16A and/or DAF-16F (Figure 5; Table S13; henceforth referred to as "DAF-16A/F target genes"). We validated our profiling results by measuring transcript levels corresponding to 15 genes that emerged from this analysis using qPCR. DAF-16/FoxO-dependent regulation was confirmed for all 15 of these genes (Figure 6; Figure S13; Table S14).

To estimate the influence of specific DAF-16/FoxO isoforms on aspects of whole organism physiology, we performed gene set enrichment analysis of DAF-16A/F target genes using GO biological process terms (Ashburner *et al.* 2000) and KEGG pathways (Kanehisa and Goto 2000) (Figure S14; Table S15). GO analysis revealed specific up-regulation of ribosome biogenesis genes and specific down-regulation of replication and cell death genes in the *daf-16f* mutant. Immune response genes were up-regulated in *daf-16a* mutants and down-regulated in the *daf-16f* mutant (Figure S14A; Table S15). KEGG analysis also unveiled enrichment of genes involved in ribosome biogenesis in the *daf-16f* mutant while showing reduction of genes involved in glycolysis and gluconeogenesis in *daf-16a* mutants. Genes involved in cysteine and methionine metabolism were depleted in the *daf-16f* mutant but enriched in *daf-16a* mutants (Figure S14B; Table S15).

To gain insight into the relative magnitude of DAF-16A- and DAF-16F-specific contributions to the regulation of individual DAF-16A/F target genes, we compared the effect of either *daf-16a* or *daf-16f* mutation on DAF-2/IGFR-dependent gene regulation to the effect of *daf-16a/f* mutation on DAF-2/IGFR-dependent gene regulation, thus calculating an "A-index" (I_A) and "F-index" (I_F) for each DAF-16A/F target gene (see *Materials and Methods*). Hypothetically, an idealized DAF-16A-specific target gene would have $I_A = 1.0$ and $I_F = 0$, whereas a DAF-16F-specific target gene would have $I_A = 0$ and $I_F = 1.0$ (Figure 5A). I_A and I_F calculated using FPKM values from whole transcriptome profiling correlated well with I_A and I_F derived from qPCR data for 15 genes tested (Figure 6; Figure S13; Table S13; Table S16).

We first generated a scatterplot of I_A and I_F for the entire set of 399 DAF-16A/F target genes (Figure 5B; Figure S15). This depiction indicates that $I_A > I_F$ for most genes, suggesting that DAF-16A plays a larger role in gene regulation than DAF-16F. To further explore this question, we plotted I_A and I_F of the entire set of DAF-16A/F target genes from lowest to highest I_A (Figure 5C) and I_F (Figure 5D). This allowed us to visualize the magnitude of isoform-specific regulation for both DAF-16A and DAF-16F across the entire set of target genes while potentially revealing relationships between the isoforms in target gene regulation. These illustrations confirm that for most target genes, DAF-16A has a greater impact on expression than DAF-16F. Furthermore, they reveal no obvious global relationship between the degree of regulation of any single gene by one isoform and the impact of the other isoform on its expression.

Categorization of DAF-16A/F target genes

The life span phenotypes of *daf-16a/f*, *daf-16a*, and *daf-16f* mutants (Figure 3) suggested that sorting of DAF-16A/F target genes into categories based on their regulation by DAF-16A and/or DAF-16F might help to prioritize subsets of DAF-16/FoxO genes that are likely to contribute significantly to longevity. Therefore, we placed each DAF-16A/F target gene into one of four categories based on the impact of each

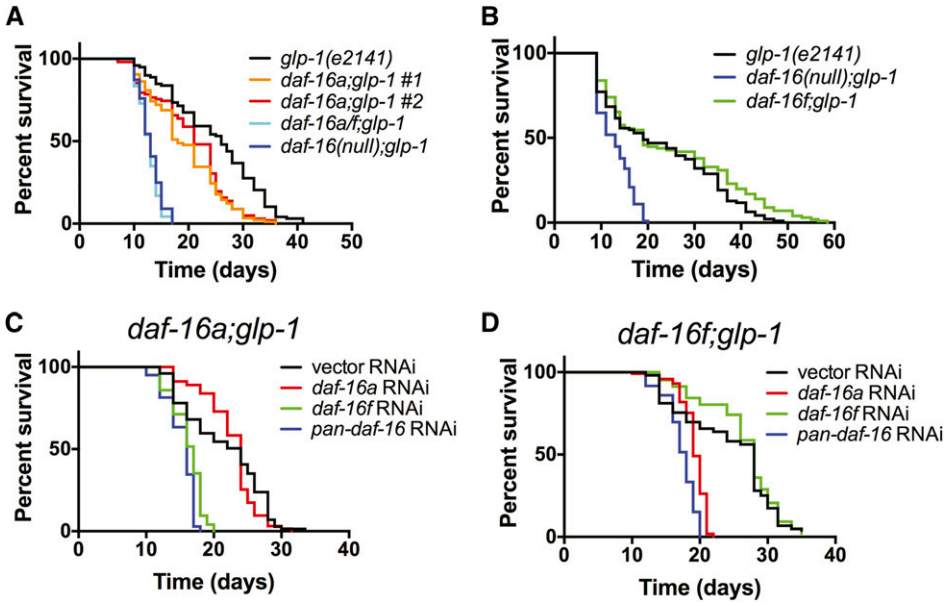

Figure 4 Effects of *daf-16a*- and *daf-16f*-specific mutations and RNAi on life span in animals lacking a germline. (A and B) Effects of *daf-16a* (A) and *daf-16f* (B) mutations on life spans of germline-ablated *glp-1(e2141)* animals. (C and D) *daf-16f* is required for *daf-16a;glp-1* longevity and *vice versa*. Survival curves are presented for (C) *daf-16a;glp-1* and (D) *daf-16f;glp-1* mutant animals upon exposure to isoform-specific *daf-16* RNAi. Figure S7B shows control *glp-1(e2141)* survival when treated with isoform-specific *daf-16* RNAi. See text for details. Statistics and raw data are presented in Table S9; Table S10.

isoform on expression: DAF-16A-specific ($I_A > 0.8$ and $I_F < 0.2$), DAF-16F-specific ($I_F > 0.8$ and $I_A < 0.2$), redundant (I_A and I_F both < 0.2), and shared (all others). We further subdivided genes in the "shared" category into three subgroups: genes for which DAF-16A plays a greater role than DAF-16F in regulation (shared A > F; $I_A/I_F > 2.0$), genes for which DAF-16F has a greater impact on regulation than DAF-16A (shared F > A; $I_F/I_A > 2.0$), and genes that are regulated by both isoforms (shared A = F; $0.5 \leq I_A/I_F \leq 2.0$) (Figure 5, E and F).

Fifty-seven genes are DAF-16A-specific targets (Figure 5, E and F; Table S13). This group includes *far-3* (Figure 6A; Table S14), which encodes a fatty acid/retinol binding protein (Garofalo *et al.* 2003), as well as the *lipl-1* gene encoding a lysosomal acid lipase, which is transcriptionally up-regulated and promotes the mobilization of lipid stores in response to starvation (O'Rourke and Ruvkun 2013). Overexpression of *lipl-1* extends life span (O'Rourke and Ruvkun 2013). Eight genes are DAF-16F-specific targets (Figure 5, E and F; Table S13), including *lea-1* (Figure 6B; Table S14), which encodes a homolog of human perilipin-4 that promotes resistance to dehydration stress (Gal *et al.* 2004).

Most DAF-16A/F target genes are regulated by both DAF-16A and DAF-16F (Figure 5, E and F). Thirty-five genes are redundantly regulated by DAF-16A and DAF-16F (Figure 5, E and F; Table S13), including *hen-1* (Figure 6C; Table S14), a secreted protein required for sensory integration and learning (Ishihara *et al.* 2002), and the established DAF-16/FoxO target genes *lys-7* and *dod-17* (Figure S13, D–E; Table S14) (Murphy *et al.* 2003).

The remaining 299 DAF-16A/F target genes are categorized as those with shared regulation by DAF-16A and DAF-16F (Figure 5, E and F; Table S13). A total of 73% of these (219/299) are primarily regulated by DAF-16A (Figure 5, E and F; Table S13). This subgroup comprises the largest subset of target genes and includes the established DAF-16/FoxO targets *sod-3* (Figure 6D; Table S14), *mtl-1* (Figure 6E; Table S14), *fat-7* (Figure S13F; Table S14), *hsp-12.6*, *dod-3*, *dod-23*, and *dod-24* (Murphy *et al.* 2003) and the lipase-like gene *lipl-2* (Figure S13G; Table S14). It also includes *aakg-4*, which encodes an atypical AMP kinase gamma subunit that participates in a positive feedback loop to promote DAF-16/FoxO activity (Chen *et al.* 2013b; Tullet *et al.* 2014), *akt-2*, which acts together with *akt-1* to inhibit DAF-16/FoxO (Paradis and Ruvkun 1998), and *ins-7*, which encodes an insulin-like peptide that is repressed by DAF-16/FoxO as part of a feedback loop that coordinates organism-wide DAF-16/FoxO activation (Murphy *et al.* 2003, 2007). Among the 20 shared target genes that are primarily regulated by DAF-16F are the S-adenosyl methionine synthase gene *sams-5* (Figure 6F; Table S14) and five collagen genes (Figure 5, E and F; Table S13). Finally, 60 target genes are regulated to a comparable extent by DAF-16A and DAF-16F (Figure 5, E and F; Table S13). Within this subgroup are *lipl-3* and *lipl-4*, which encode lipases that, along with the DAF-16A-specific target *lipl-1*, are transcriptionally induced in response to fasting (O'Rourke and Ruvkun 2013), and *mdl-1*, a Mad transcription factor family member that promotes DAF-16/FoxO-dependent longevity (Riesen *et al.* 2014).

Collectively, these classifications indicate that DAF-16A plays an important role in regulating 93% of DAF-16A/F target genes ("DAF-16A specific," "redundant," "shared A > F," and "shared A = F" categories; 371/399 genes), whereas DAF-16F strongly influences the expression of just over 30% of target genes ("DAF-16F specific," redundant, "shared F > A," and shared A = F categories; 123/399 genes).

Two DAF-16A-specific target genes play important roles in life span control

Our main goal at the outset of this line of inquiry was to prioritize a tractable subset of DAF-16/FoxO target genes for functional analysis. Based on the life span phenotypes of isoform-specific *daf-16/FoxO* mutants (Figure 3; Figure 4),

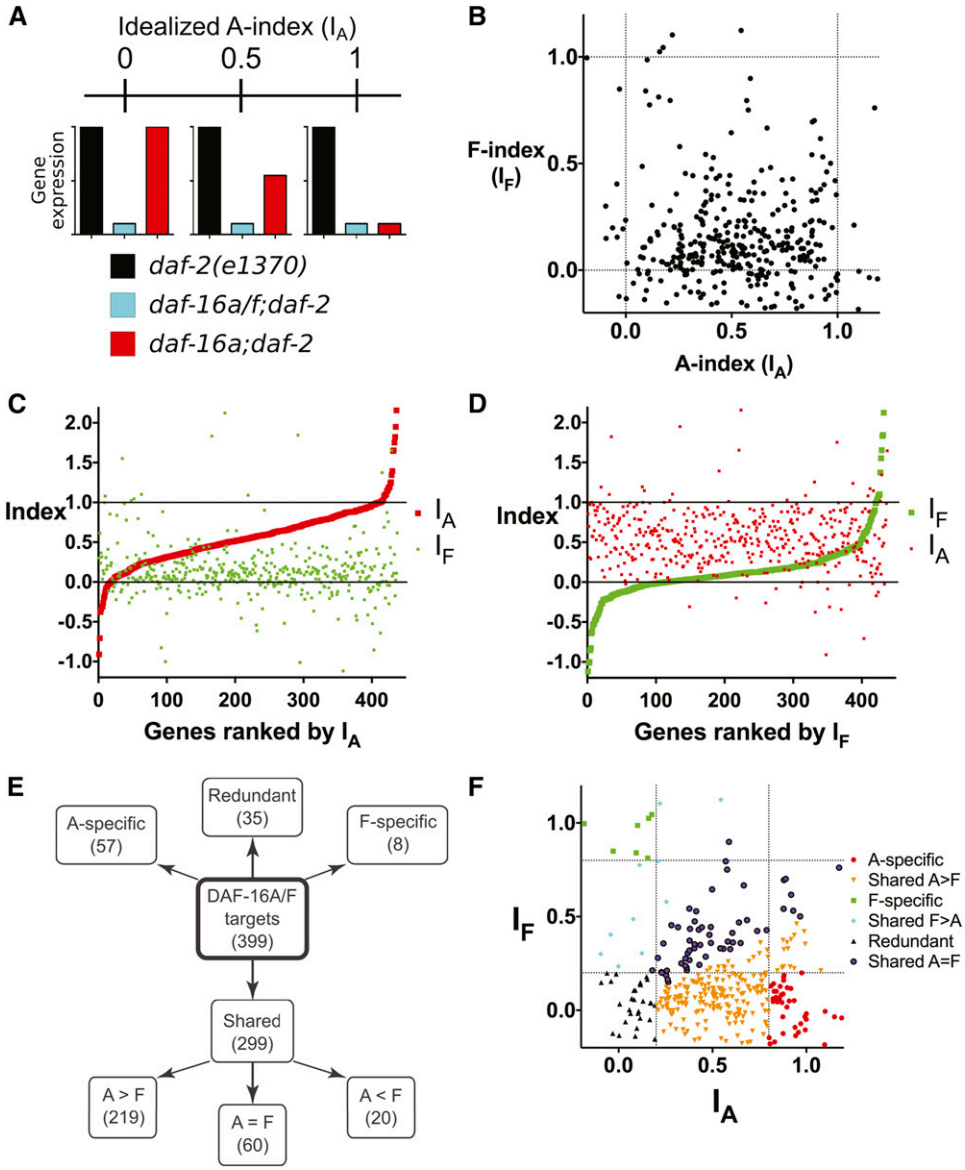

Figure 5 DAF-16A and DAF-16F target genes identified by whole transcriptome profiling. (A) Depiction of the A-index (I_A) for three hypothetical target genes with I_A = 0, 0.5, and 1.0. Idealized expression profiles in *daf-2(e1370)*, *daf-16a/f;daf-2*, and *daf-16a;daf-2* are shown for all three genes. (B) Scatterplot comparing I_A and I_F for DAF-16A/F target genes. Dashed lines indicate I_A and I_F = 0 or 1. Only genes with indices from −0.2 to 1.2 are shown; a scatterplot with a wider range of indices is shown in Figure S15. I_A and I_F for all genes are listed in Table S13. (C and D) Plots of I_A and I_F for all DAF-16A/F target genes from lowest to highest I_A (C) or I_F (D). Solid lines correspond to indices of 0 and 1. Three genes with indices >2.2 or < −1.2 were omitted for presentation purposes. Gene rankings are listed in Table S13. (E) Tree diagram summarizing the categorization system for DAF-16A and DAF-16F target genes. See text and *Materials and Methods* for details. (F) Scatterplot from B, with individual genes color coded according to categories depicted in E. Dashed lines indicate I_A or I_F values of 0.2 or 0.8, corresponding to the cutoffs used to define redundantly regulated, A-specific, and F-specific targets.

we surmised that the subgroups of 57 DAF-16A-specific and 35 redundant target genes had a high probability of containing genes that would impact longevity significantly. DAF-16A-specific genes likely contribute to the life span differential between *daf-16a;daf-2* and *daf-2* mutants, whereas redundantly regulated genes might be expected to account for the difference in the life spans of *daf-16a/f;daf-2* and *daf-16a;daf-2* double mutants (Figure 3, A and C).

To test this hypothesis, we obtained strains readily available to the community that harbored probable strong loss-of-function mutations in twenty DAF-16A-specific, two DAF-16F-specific, and nine redundant target genes (Table S17). Life spans were assayed after exposure to either control bacteria or bacteria engineered to synthesize double-stranded RNA corresponding to the *daf-2* gene (*daf-2* RNAi). In control experiments, life span extension induced by *daf-2* RNAi was completely abrogated in *daf-16* null mutants and partially reduced in *daf-16a*-specific mutants (Figure 7, A and B).

Among 19 strains harboring mutations in genes induced by DAF-16/FoxO, *daf-2*-RNAi-induced life span extension was significantly less than that observed in wild-type controls in a strain harboring a mutation in *gst-20* (Figure 7C; Table S18). This strain was not RNAi defective (Rde; Figure S16), indicating that the reduced life span extension upon exposure to *daf-2* RNAi is unlikely to be a consequence of a background mutation that reduces the efficiency of *daf-2* inactivation by RNAi. Furthermore, examination of the mutational load in this strain, which was generated as part of the Million Mutation Project (Thompson *et al.* 2013), revealed no obvious strong loss-of-function mutations in genes known to influence aging or RNAi (Table S19).

To verify this result, we constructed a *gst-20;daf-2(e1368)* double mutant and compared its life span to that of *gst-20* and *daf-2* single mutant siblings. *gst-20* mutation did not significantly shorten life span in animals with wild-type *daf-2* (Figure 7, D and E; Table S18), indicating that this mutation does not cause general frailty or sickness. Intriguingly, *gst-20* mutation significantly

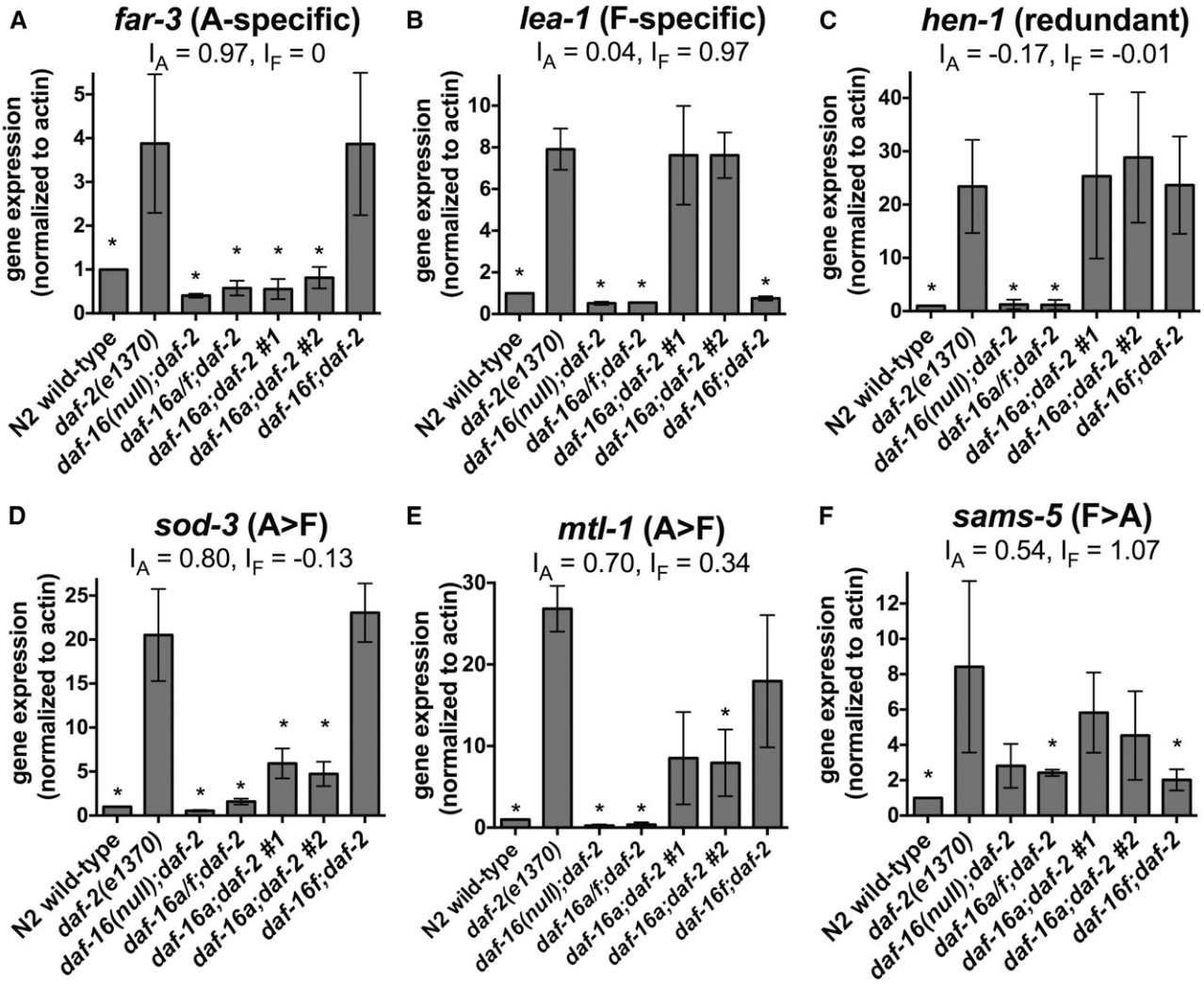

Figure 6 qPCR validation of target gene regulation by DAF-16A and DAF-16F. (A–F) Expression of six DAF-16A/F target genes quantified by qPCR using RNA isolated from day 1 young adult animals. Values represent the mean from three biological replicates. Error bars represent standard deviation. Asterisks indicate statistically significant changes ($P < 0.05$ by paired ratio *t*-test). I_A and I_F were calculated using mean expression values measured by qPCR, and correlate with indices calculated using RNA-seq measurements (Table S16). Statistics and data are summarized in Table S14.

reduced life span extension caused by *daf-2* mutation when animals were fed *E. coli* HT115 (Figure 7D; Table S18) but did not influence the life span of *daf-2(e1368)* mutants when they were fed *E. coli* OP50 (Figure 7E; Table S18).

gst-20 encodes a glutathione-S-transferase family member homologous to human hematopoietic prostaglandin D synthase, an enzyme that catalyzes the glutathione-dependent isomerization of prostaglandin H2 to prostaglandin D2 (Kanaoka and Urade 2003). We hypothesize that the induction of *gst-20* by DAF-16A (Figure S13A; Table S14) contributes to DAF-16/FoxO-dependent life span extension in a manner dependent upon bacterial food source.

Among 12 strains with mutations in genes repressed by DAF-16/FoxO, one strain containing a mutation in *srr-4* lived significantly longer than wild-type animals exposed to control RNAi. This strain also did not contain strong loss-of-function mutations in genes that affect aging (Table S19). Life span assays with outcrossed *srr-4* mutant animals and wild-type siblings verified that *srr-4* mutation extends life span (Figure 7F; Table S18). As observed for *gst-20* mutation, we found that the impact of *srr-4* mutation on life span was also dependent upon bacterial food source; *srr-4* mutation extended life span significantly when animals were fed *E. coli* HT115 (Figure 7F; Table S18) but had less of an effect on longevity when animals were fed *E. coli* OP50 (Figure 7G; Table S18). *srr-4* encodes a putative seven-transmembrane G-protein-coupled receptor that is repressed by DAF-16A (Figure S13B; Table S14). The SRR-4 protein is conserved in other *Caenorhabditis* species and is predicted to contain a DUF267 (**d**omain of **u**nknown **f**unction) domain. We postulate that DAF-16A may promote longevity in part by reducing *srr-4* expression.

Discussion

Over 20 yr after the initial demonstration that DAF-16/FoxO promotes longevity (Kenyon *et al.* 1993), the question of

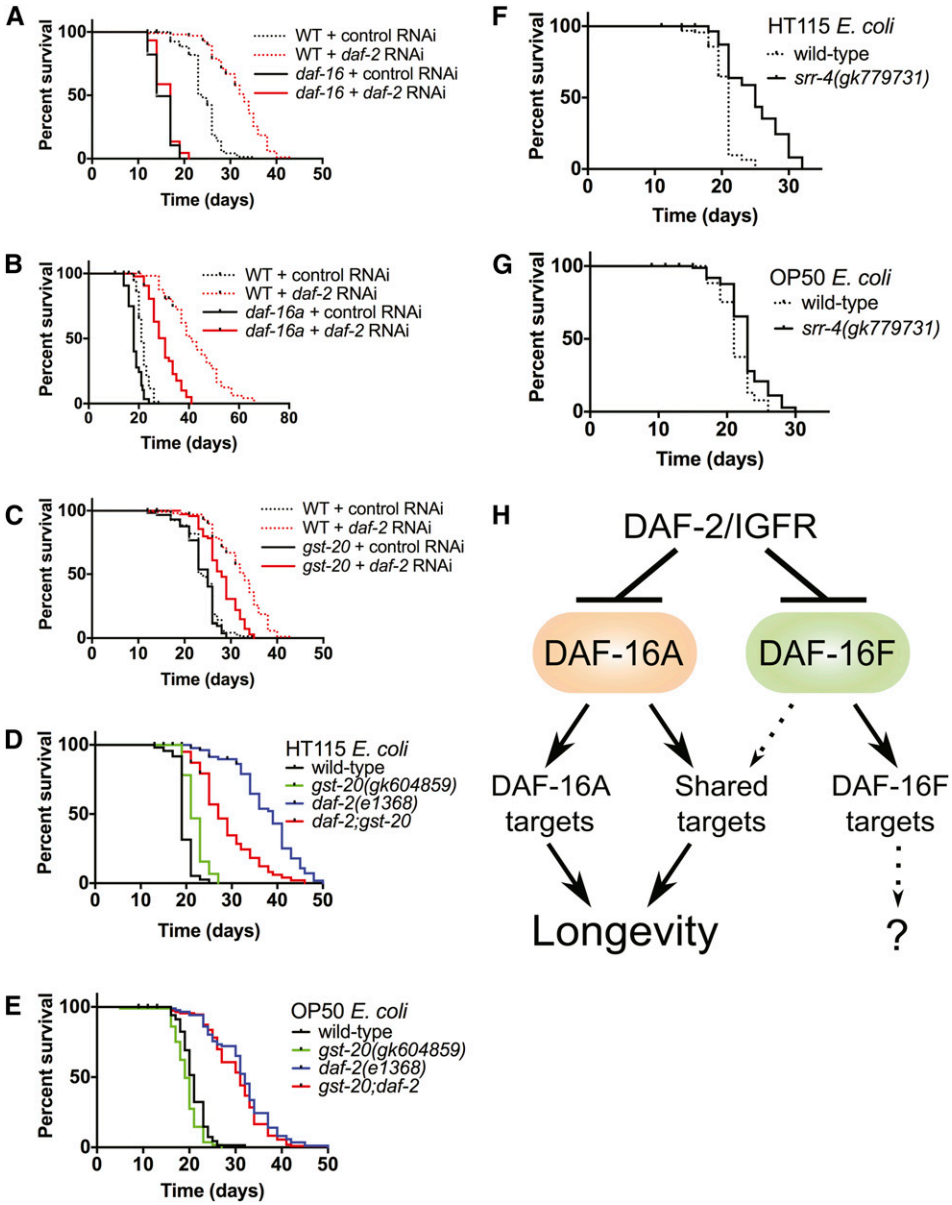

Figure 7 DAF-16A-specific targets influence life span. *daf-16* (A) and *daf-16a* (B) are required for longevity induced by *daf-2/IGFR* RNAi. (C) The DAF-16A up-regulated target gene *gst-20* is required for full life span extension induced by *daf-2/IGFR* RNAi. *gst-20* promotes longevity in *daf-2(e1368)* mutants grown on *E. coli* HT115 (D) but not in animals grown on *E. coli* OP50 (E). The DAF-16A down-regulated target gene *srr-4* limits longevity in animals grown on HT115 (F) but does not influence life span in animals grown on OP50 (G). (H) Model of life span control and gene regulation by DAF-16A and DAF-16F. See text for details. Life span statistics and data are presented in Table S18.

which DAF-16/FoxO target genes are important for life span extension remains unanswered. Efforts to address this important issue have been hindered by the prodigious number of genes that are regulated by DAF-16/FoxO. Most of the hundreds of DAF-16/FoxO target genes that are regulated by DAF-2/IGFR signaling (Lee *et al.* 2003; McElwee *et al.* 2003; Murphy *et al.* 2003) have not been interrogated for roles in life span control.

Approaches to prioritize subsets of DAF-16/FoxO target genes for detailed investigation have succeeded in identifying DAF-16/FoxO target genes with previously unappreciated functions in promoting longevity (Schuster *et al.* 2010; Tullet *et al.* 2014). We have combined phenotypic analysis and whole transcriptome profiling of isoform-specific *daf-16/FoxO* mutants to define a subset of 92 DAF-16/FoxO target genes (composed of 57 DAF-16A-specific and 35 redundant target genes; Figure 5, E and F; Table S13) that we have prioritized for further study. We hypothesize that this subset may be enriched in genes likely to play important roles in life span control; regulation of DAF-16A-specific genes may account for the difference in life span between *daf-2* mutants and *daf-16a;daf-2* double mutants (Figure 3, A and C), and regulation of redundant genes may contribute to life span differences between *daf-16a/f;daf-2* double mutants and both *daf-16a;daf-2* (Figure 3, A and C) and *daf-16f;daf-2* double mutants (Figure 3, B and D).

Our initial phenotypic analysis of 29 strains harboring strong loss-of-function mutations in genes from this subset has revealed potentially important functions for two DAF-16/FoxO target genes, *gst-20* and *srr-4*, in controlling life span. Neither of these genes had previously been implicated in DAF-16/FoxO-dependent longevity. Our discovery of these new longevity genes underscores the efficacy of our integrative strategy in identifying DAF-16/FoxO target genes that

are likely to influence life span. We anticipate that functional analysis of the remaining 63 genes within this prioritized subset of DAF-16/FoxO targets will reveal further insights into the mechanistic basis for life span extension by DAF-16/FoxO. As most transcription factors regulate the expression of hundreds of genes, our strategy may be generally applicable to the study of target genes and their relative importance in mediating transcription factor function.

Notably, our life span assays revealed diet-dependent effects of *gst-20* and *srr-4* on longevity. Mutations in both genes influenced life span when animals were fed *E. coli* HT115 but did not significantly affect longevity when animals were fed *E. coli* OP50 (Figure 7; Table S18). Given that the main RNAi library used in the *C. elegans* field was constructed using *E. coli* HT115 (Kamath *et al.* 2003), which is distinct from the standard OP50 strain used in *C. elegans* studies, our findings underscore the importance of verifying RNAi-based life span assays in the context of *E. coli* OP50.

Although we have focused our efforts on genes within the DAF-16A-specific and redundant categories of DAF-16/FoxO targets (Figure 5E; Table S13), genes in other categories may also influence life span significantly. Indeed, *aakg-4*, which encodes an atypical AMP-activated protein kinase gamma isoform that promotes longevity in the context of reduced DAF-2/IGFR activity (Chen *et al.* 2013b; Tullet *et al.* 2014), emerged from our analysis in the shared A > F category, which was the largest subset of DAF-16/FoxO targets (Figure 5E; Table S13). We are exploring complementary integrative approaches to define other subsets of DAF-16/FoxO target genes that may direct our attention to specific genes within the larger subsets generated in this study.

Our analysis of isoform-specific *daf-16/FoxO* mutants indicates that DAF-16A is the major FoxO isoform that controls dauer arrest (Figure 2), longevity (Figure 3; Figure 4), and stress resistance (Figure S12). In the presence of physiologic levels of DAF-16A, DAF-16F is dispensable for dauer regulation, life span control, and stress resistance. In the absence of DAF-16A, DAF-16F promotes dauer arrest and longevity, as demonstrated by the incomplete suppression of dauer-constitutive and life span extension phenotypes by *daf-16a* mutation (Figure 2B; Figure 3, A and C; Figure 4A) and the influence of *daf-16f* RNAi on life span in *daf-2/IGFR* mutant animals and germline-ablated animals that lack *daf-16a* (Figure 3E; Figure 4C).

These conclusions are at odds with previous suggestions that DAF-16F is the major isoform that promotes longevity in the context of reduced DAF-2/IGFR signaling (Kwon *et al.* 2010; Bansal *et al.* 2014). As this interpretation of the primacy of DAF-16F in life span control was based in large part on life span phenotypes of transgenes overexpressing either *daf-16a* or *daf-16f* (Kwon *et al.* 2010; Bansal *et al.* 2014), we conducted our own investigations of single-copy *daf-16a* and *daf-16f* transgenes driven by the same promoters used by Kwon *et al.* (2010) (Figure S8). Our results (Figure 3, G and H; Figure S9; Figure S10) strongly suggest that the difference in the longevity-promoting activities of *daf-16a* and *daf-16f* transgenes that they observed is a consequence of both the sensitivity of the *daf-16f* transgene to dosage (Figure 3H; Figure S10E) as well as the failure of the *daf-16a* transgene to fully recapitulate the activity of the endogenous *daf-16a* locus (Figure 3G; Figure S9A; Figure S10, A–D), rather than greater longevity-promoting activity *per se* of *daf-16f* compared to *daf-16a*.

The expression profiling experiments presented here are the first to define the relative contributions of endogenous DAF-16/FoxO isoforms to the regulation of DAF-16/FoxO target genes. They reveal a dominant role for DAF-16A relative to DAF-16F in regulating gene expression in young adult animals (Figure 5; Table S13) that is commensurate with the relative influence of DAF-16A and DAF-16F on adult life span (Figure 3; Figure 4). These results further support the conclusion that DAF-16A is the major FoxO isoform that promotes longevity in *C. elegans*.

Based on our results, we propose a hierarchical model of DAF-16/FoxO isoform function in life span control (Figure 7H). DAF-2/IGFR inhibits both DAF-16A and DAF-16F (Kwon *et al.* 2010). In the context of reduced DAF-2/IGFR signaling, both DAF-16A and DAF-16F contribute to longevity and the regulation of DAF-16/FoxO target genes. In the absence of DAF-16A, the altered expression of genes regulated mainly by DAF-16A shortens life span. When DAF-16F is inactive, genes regulated primarily by DAF-16F are misregulated, but this does not influence life span. When neither DAF-16A nor DAF-16F is present, DAF-2/IGFR mutation does not promote longevity due to the misregulation of both DAF-16A-specific target genes as well as genes that are regulated by both DAF-16A and DAF-16F.

The conserved role of IGFR signaling and FoxO transcription factors in life span control was first discovered in *C. elegans* (Friedman and Johnson 1988a,b; Johnson 1990; Kenyon *et al.* 1993). Decades later, how FoxO transcription factors extend life span remains poorly understood. Here we report a novel approach to delineate the contributions of specific FoxO target genes to FoxO-dependent longevity. IGFR signaling is now known to influence aging in mammals (Bluher *et al.* 2003; Holzenberger *et al.* 2003) and possibly humans (Suh *et al.* 2008; Tazearslan *et al.* 2011), and the prolongevity function of FoxO that is conserved in invertebrates (Kenyon *et al.* 1993; Giannakou *et al.* 2004; Hwangbo *et al.* 2004; Slack *et al.* 2011; Yamamoto and Tatar 2011) and mice (Shimokawa *et al.* 2015) is likely relevant to human aging and aging-related diseases. By directing focus to a subset of target genes, our strategy will facilitate the elucidation of the molecular basis for life span extension by FoxO transcription factors. Further investigation of DAF-16/FoxO target gene function in *C. elegans* promises to illuminate phyletically general functions of FoxO transcription factors in controlling aging.

Acknowledgments

We thank Robert Lyons and Jeanne Geskes at the University of Michigan (UM) DNA Sequencing Core for their assis-

tance with whole transcriptome profiling, the UM Bioinformatics Core and Mallory Freeberg for help with analysis of transcriptome profiling data, and John Kim and Colin Delaney for comments on the manuscript. Some strains were provided by the *Caenorhabditis* Genetics Center, which is funded by the National Institutes of Health (NIH) Office of Research Infrastructure Programs (P40 OD010440). This work was supported by the Biology of Aging training grant T32AG000114, awarded to the UM Geriatrics Center by the National Institute on Aging (A.T.-Y.C.), the Functional Assessment Core of the UM Nathan Shock Center of Excellence in the Basic Biology of Aging, research scholar grant DDC-119640 from the American Cancer Society (P.J.H.), and R01 grant AG041177 from the NIH (P.J.H.).

Literature Cited

Accili, D., and K. C. Arden, 2004 FoxOs at the crossroads of cellular metabolism, differentiation, and transformation. Cell 117: 421–426.

Ambrogini, E., M. Almeida, M. Martin-Millan, J. H. Paik, R. A. Depinho *et al.*, 2010 FoxO-mediated defense against oxidative stress in osteoblasts is indispensable for skeletal homeostasis in mice. Cell Metab. 11: 136–146.

Anselmi, C. V., A. Malovini, R. Roncarati, V. Novelli, F. Villa *et al.*, 2009 Association of the FOXO3A locus with extreme longevity in a southern Italian centenarian study. Rejuvenation Res. 12: 95–104.

Arantes-Oliveira, N., J. Apfeld, A. Dillin, and C. Kenyon, 2002 Regulation of life-span by germ-line stem cells in Caenorhabditis elegans. Science 295: 502–505.

Ashburner, M., C. A. Ball, J. A. Blake, D. Botstein, H. Butler *et al.*, 2000 Gene ontology: tool for the unification of biology. The Gene Ontology Consortium. Nat. Genet. 25: 25–29.

Bansal, A., E. S. Kwon, D. Conte, Jr., H. Liu, M. J. Gilchrist *et al.*, 2014 Transcriptional regulation of Caenorhabditis elegans FOXO/DAF-16 modulates lifespan. Longev. Healthspan 3: 5.

Barthel, A., D. Schmoll, and T. G. Unterman, 2005 FoxO proteins in insulin action and metabolism. Trends Endocrinol. Metab. 16: 183–189.

Berman, J. R., and C. Kenyon, 2006 Germ-cell loss extends C. elegans life span through regulation of DAF-16 by kri-1 and lipophilic-hormone signaling. Cell 124: 1055–1068.

Billi, A. C., A. F. Alessi, V. Khivansara, T. Han, M. Freeberg *et al.*, 2012 The Caenorhabditis elegans HEN1 ortholog, HENN-1, methylates and stabilizes select subclasses of germline small RNAs. PLoS Genet. 8: e1002617.

Bluher, M., B. B. Kahn, and C. R. Kahn, 2003 Extended longevity in mice lacking the insulin receptor in adipose tissue. Science 299: 572–574.

Chen, A. T., C. Guo, K. J. Dumas, K. Ashrafi, and P. J. Hu, 2013a Effects of Caenorhabditis elegans sgk-1 mutations on lifespan, stress resistance, and DAF-16/FoxO regulation. Aging Cell 12: 932–940.

Chen, D., P. W. Li, B. A. Goldstein, W. Cai, E. L. Thomas *et al.*, 2013b Germline signaling mediates the synergistically prolonged longevity produced by double mutations in daf-2 and rsks-1 in C. elegans. Cell Reports 5: 1600–1610.

Cheng, Z., S. Guo, K. Copps, X. Dong, R. Kollipara *et al.*, 2009 Foxo1 integrates insulin signaling with mitochondrial function in the liver. Nat. Med. 15: 1307–1311.

Dong, X. C., K. D. Copps, S. Guo, Y. Li, R. Kollipara *et al.*, 2008 Inactivation of hepatic Foxo1 by insulin signaling is required for adaptive nutrient homeostasis and endocrine growth regulation. Cell Metab. 8: 65–76.

Flachsbart, F., A. Caliebe, R. Kleindorp, H. Blanche, H. von Eller-Eberstein *et al.*, 2009 Association of FOXO3A variation with human longevity confirmed in German centenarians. Proc. Natl. Acad. Sci. USA 106: 2700–2705.

Friedman, D. B., and T. E. Johnson, 1988a A mutation in the age-1 gene in Caenorhabditis elegans lengthens life and reduces hermaphrodite fertility. Genetics 118: 75–86.

Friedman, D. B., and T. E. Johnson, 1988b Three mutants that extend both mean and maximum life span of the nematode, Caenorhabditis elegans, define the age-1 gene. J. Gerontol. 43: B102–B109.

Frokjaer-Jensen, C., M. W. Davis, C. E. Hopkins, B. J. Newman, J. M. Thummel *et al.*, 2008 Single-copy insertion of transgenes in Caenorhabditis elegans. Nat. Genet. 40: 1375–1383.

Gal, T. Z., I. Glazer, and H. Koltai, 2004 An LEA group 3 family member is involved in survival of C. elegans during exposure to stress. FEBS Lett. 577: 21–26.

Gan, B., C. Lim, G. Chu, S. Hua, Z. Ding *et al.*, 2010 FoxOs enforce a progression checkpoint to constrain mTORC1-activated renal tumorigenesis. Cancer Cell 18: 472–484.

Garofalo, A., M. C. Rowlinson, N. A. Amambua, J. M. Hughes, S. M. Kelly *et al.*, 2003 The FAR protein family of the nematode Caenorhabditis elegans. Differential lipid binding properties, structural characteristics, and developmental regulation. J. Biol. Chem. 278: 8065–8074.

Gems, D., A. J. Sutton, M. L. Sundermeyer, P. S. Albert, K. V. King *et al.*, 1998 Two pleiotropic classes of daf-2 mutation affect larval arrest, adult behavior, reproduction and longevity in Caenorhabditis elegans. Genetics 150: 129–155.

Gengyo-Ando, K., and S. Mitani, 2000 Characterization of mutations induced by ethyl methanesulfonate, UV, and trimethylpsoralen in the nematode Caenorhabditis elegans. Biochem. Biophys. Res. Commun. 269: 64–69.

Ghazi, A., S. Henis-Korenblit, and C. Kenyon, 2009 A transcription elongation factor that links signals from the reproductive system to lifespan extension in Caenorhabditis elegans. PLoS Genet. 5: e1000639.

Giannakou, M. E., M. Goss, M. A. Junger, E. Hafen, S. J. Leevers *et al.*, 2004 Long-lived Drosophila with overexpressed dFOXO in adult fat body. Science 305: 361.

Gottlieb, S., and G. Ruvkun, 1994 daf-2, daf-16 and daf-23: genetically interacting genes controlling Dauer formation in Caenorhabditis elegans. Genetics 137: 107–120.

Gubelmann, C., A. Gattiker, A. Massouras, K. Hens, F. David *et al.*, 2011 GETPrime: a gene- or transcript-specific primer database for quantitative real-time PCR. Database (Oxford) 2011: bar040.

Heckman, K. L., and L. R. Pease, 2007 Gene splicing and mutagenesis by PCR-driven overlap extension. Nat. Protoc. 2: 924–932.

Henderson, S. T., and T. E. Johnson, 2001 daf-16 integrates developmental and environmental inputs to mediate aging in the nematode Caenorhabditis elegans. Curr. Biol. 11: 1975–1980.

Holzenberger, M., J. Dupont, B. Ducos, P. Leneuve, A. Geloen *et al.*, 2003 IGF-1 receptor regulates lifespan and resistance to oxidative stress in mice. Nature 421: 182–187.

Honda, Y., and S. Honda, 1999 The daf-2 gene network for longevity regulates oxidative stress resistance and Mn-superoxide dismutase gene expression in Caenorhabditis elegans. FASEB J. 13: 1385–1393.

Hsin, H., and C. Kenyon, 1999 Signals from the reproductive system regulate the lifespan of C. elegans. Nature 399: 362–366.

Hu, P. J., J. Xu, and G. Ruvkun, 2006 Two membrane-associated tyrosine phosphatase homologs potentiate C. elegans AKT-1/PKB signaling. PLoS Genet. 2: e99.

Hwangbo, D. S., B. Gershman, M. P. Tu, M. Palmer, and M. Tatar, 2004 Drosophila dFOXO controls lifespan and regulates insulin signalling in brain and fat body. Nature 429: 562–566.

Ishihara, T., Y. Iino, A. Mohri, I. Mori, K. Gengyo-Ando *et al.*, 2002 HEN-1, a secretory protein with an LDL receptor motif, regulates sensory integration and learning in Caenorhabditis elegans. Cell 109: 639–649.

Johnson, T. E., 1990 Increased life-span of age-1 mutants in Caenorhabditis elegans and lower Gompertz rate of aging. Science 249: 908–912.

Junger, M. A., F. Rintelen, H. Stocker, J. D. Wasserman, M. Vegh *et al.*, 2003 The Drosophila forkhead transcription factor FOXO mediates the reduction in cell number associated with reduced insulin signaling. J. Biol. 2: 20.

Kamath, R. S., A. G. Fraser, Y. Dong, G. Poulin, R. Durbin *et al.*, 2003 Systematic functional analysis of the Caenorhabditis elegans genome using RNAi. Nature 421: 231–237.

Kamath, R. S., M. Martinez-Campos, P. Zipperlen, A. G. Fraser, and J. Ahringer, 2001 Effectiveness of specific RNA-mediated interference through ingested double-stranded RNA in Caenorhabditis elegans. Genome Biol. **2:** RESEARCH0002.

Kanaoka, Y., and Y. Urade, 2003 Hematopoietic prostaglandin D synthase. Prostaglandins Leukot. Essent. Fatty Acids 69: 163–167.

Kanehisa, M., and S. Goto, 2000 KEGG: Kyoto Encyclopedia of Genes and Genomes. Nucleic Acids Res. 28: 27–30.

Kenyon, C. J., 2010 The genetics of ageing. Nature 464: 504–512.

Kenyon, C., J. Chang, E. Gensch, A. Rudner, and R. Tabtiang, 1993 A C. elegans mutant that lives twice as long as wild type. Nature 366: 461–464.

Kimura, K. D., H. A. Tissenbaum, Y. Liu, and G. Ruvkun, 1997 daf-2, an insulin receptor-like gene that regulates longevity and diapause in Caenorhabditis elegans. Science 277: 942–946.

Kitamura, T., J. Nakae, Y. Kitamura, Y. Kido, W. H. Biggs, 3rd *et al.*, 2002 The forkhead transcription factor Foxo1 links insulin signaling to Pdx1 regulation of pancreatic beta cell growth. J. Clin. Invest. 110: 1839–1847.

Kwon, E. S., S. D. Narasimhan, K. Yen, and H. A. Tissenbaum, 2010 A new DAF-16 isoform regulates longevity. Nature 466: 498–502.

Langmead, B., 2010 Aligning short sequencing reads with Bowtie. Curr. Protoc. Bioinformatics Chapter 11: Unit 11.7.

Langmead, B., C. Trapnell, M. Pop, and S. L. Salzberg, 2009 Ultrafast and memory-efficient alignment of short DNA sequences to the human genome. Genome Biol. 10: R25.

Lee, R. Y., J. Hench, and G. Ruvkun, 2001 Regulation of C. elegans DAF-16 and its human ortholog FKHRL1 by the daf-2 insulin-like signaling pathway. Curr. Biol. 11: 1950–1957.

Lee, S. S., S. Kennedy, A. C. Tolonen, and G. Ruvkun, 2003 DAF-16 target genes that control C. elegans life-span and metabolism. Science 300: 644–647.

Li, Y., W. J. Wang, H. Cao, J. Lu, C. Wu *et al.*, 2009 Genetic association of FOXO1A and FOXO3A with longevity trait in Han Chinese populations. Hum. Mol. Genet. 18: 4897–4904.

Lin, K., J. B. Dorman, A. Rodan, and C. Kenyon, 1997 daf-16: An HNF-3/forkhead family member that can function to double the life-span of Caenorhabditis elegans. Science 278: 1319–1322.

Lin, K., H. Hsin, N. Libina, and C. Kenyon, 2001 Regulation of the Caenorhabditis elegans longevity protein DAF-16 by insulin/IGF-1 and germline signaling. Nat. Genet. 28: 139–145.

Lunetta, K. L., R. B. D'Agostino, Sr, D. Karasik, E. J. Benjamin, C. Y. Guo *et al.*, 2007 Genetic correlates of longevity and selected age-related phenotypes: a genome-wide association study in the Framingham Study. BMC Med. Genet. 8(Suppl 1): S13.

Ma, Y., A. Creanga, L. Lum, and P. A. Beachy, 2006 Prevalence of off-target effects in Drosophila RNA interference screens. Nature 443: 359–363.

McColl, G., A. N. Rogers, S. Alavez, A. E. Hubbard, S. Melov *et al.*, 2010 Insulin-like signaling determines survival during stress via posttranscriptional mechanisms in C. elegans. Cell Metab. 12: 260–272.

McElwee, J., K. Bubb, and J. H. Thomas, 2003 Transcriptional outputs of the Caenorhabditis elegans forkhead protein DAF-16. Aging Cell 2: 111–121.

Murakami, S., and T. E. Johnson, 1996 A genetic pathway conferring life extension and resistance to UV stress in Caenorhabditis elegans. Genetics 143: 1207–1218.

Murphy, C. T., and P. J. Hu, 2013 Insulin/insulin-like growth factor signaling in C. elegans. WormBook 1–43.

Murphy, C. T., S. A. McCarroll, C. I. Bargmann, A. Fraser, R. S. Kamath *et al.*, 2003 Genes that act downstream of DAF-16 to influence the lifespan of Caenorhabditis elegans. Nature 424: 277–283.

Murphy, C. T., S. J. Lee, and C. Kenyon, 2007 Tissue entrainment by feedback regulation of insulin gene expression in the endoderm of Caenorhabditis elegans. Proc. Natl. Acad. Sci. USA 104: 19046–19050.

Nakae, J., W. H. Biggs, 3rd, T. Kitamura, W. K. Cavenee, C. V. Wright *et al.*, 2002 Regulation of insulin action and pancreatic beta-cell function by mutated alleles of the gene encoding forkhead transcription factor Foxo1. Nat. Genet. 32: 245–253.

Nolan, T., R. E. Hands, and S. A. Bustin, 2006 Quantification of mRNA using real-time RT-PCR. Nat. Protoc. 1: 1559–1582.

O'Rourke, E. J., and G. Ruvkun, 2013 MXL-3 and HLH-30 transcriptionally link lipolysis and autophagy to nutrient availability. Nat. Cell Biol. 15: 668–676.

Ogg, S., S. Paradis, S. Gottlieb, G. I. Patterson, L. Lee *et al.*, 1997 The Fork head transcription factor DAF-16 transduces insulin-like metabolic and longevity signals in C. elegans. Nature 389: 994–999.

Paik, J. H., R. Kollipara, G. Chu, H. Ji, Y. Xiao *et al.*, 2007 FoxOs are lineage-restricted redundant tumor suppressors and regulate endothelial cell homeostasis. Cell 128: 309–323.

Paradis, S., and G. Ruvkun, 1998 Caenorhabditis elegans Akt/PKB transduces insulin receptor-like signals from AGE-1 PI3 kinase to the DAF-16 transcription factor. Genes Dev. 12: 2488–2498.

Pawlikowska, L., D. Hu, S. Huntsman, A. Sung, C. Chu *et al.*, 2009 Association of common genetic variation in the insulin/IGF1 signaling pathway with human longevity. Aging Cell 8: 460–472.

Rached, M. T., A. Kode, L. Xu, Y. Yoshikawa, J. H. Paik *et al.*, 2010 FoxO1 is a positive regulator of bone formation by favoring protein synthesis and resistance to oxidative stress in osteoblasts. Cell Metab. 11: 147–160.

Riddle, D. L., 1988 The dauer larva, pp. 393–412 in *The Nematode Caenorhabditis elegans*, edited by W. B. Wood. Cold Spring Harbor Laboratory Press, Plainview, NJ.

Riddle, D. L., M. M. Swanson, and P. S. Albert, 1981 Interacting genes in nematode dauer larva formation. Nature 290: 668–671.

Riesen, M., I. Feyst, N. Rattanavirotkul, M. Ezcurra, J. M. Tullet *et al.*, 2014 MDL-1, a growth- and tumor-suppressor, slows aging and prevents germline hyperplasia and hypertrophy in C. elegans. Aging (Albany, N.Y.) 6: 98–117.

Robinson, J. T., H. Thorvaldsdottir, W. Winckler, M. Guttman, E. S. Lander *et al.*, 2011 Integrative genomics viewer. Nat. Biotechnol. 29: 24–26.

Sartor, M. A., G. D. Leikauf, and M. Medvedovic, 2009 LRpath: a logistic regression approach for identifying enriched biological groups in gene expression data. Bioinformatics 25: 211–217.

Schuster, E., J. J. McElwee, J. M. Tullet, R. Doonan, F. Matthijssens *et al.*, 2010 DamID in C. elegans reveals longevity-associated targets of DAF-16/FoxO. Mol. Syst. Biol. 6: 399.

Shimokawa, I., T. Komatsu, N. Hayashi, S. E. Kim, T. Kawata *et al.*, 2015 The life-extending effect of dietary restriction requires Foxo3 in mice. Aging Cell **14:** 707–709.

Slack, C., M. E. Giannakou, A. Foley, M. Goss, and L. Partridge, 2011 dFOXO-independent effects of reduced insulin-like signaling in Drosophila. Aging Cell 10: 735–748.

Suh, Y., G. Atzmon, M. O. Cho, D. Hwang, B. Liu *et al.*, 2008 Functionally significant insulin-like growth factor I receptor mutations in centenarians. Proc. Natl. Acad. Sci. USA 105: 3438–3442.

Supek, F., M. Bosnjak, N. Skunca, and T. Smuc, 2011 REVIGO summarizes and visualizes long lists of gene ontology terms. PLoS One 6: e21800.

Sykes, S. M., S. W. Lane, L. Bullinger, D. Kalaitzidis, R. Yusuf *et al.*, 2011 AKT/FOXO signaling enforces reversible differentiation blockade in myeloid leukemias. Cell 146: 697–708.

Tabara, H., M. Sarkissian, W. G. Kelly, J. Fleenor, A. Grishok *et al.*, 1999 The rde-1 gene, RNA interference, and transposon silencing in C. elegans. Cell 99: 123–132.

Tabara, H., E. Yigit, H. Siomi, and C. C. Mello, 2002 The dsRNA binding protein RDE-4 interacts with RDE-1, DCR-1, and a DExH-box helicase to direct RNAi in C. elegans. Cell 109: 861–871.

Tazearslan, C., J. Huang, N. Barzilai, and Y. Suh, 2011 Impaired IGF1R signaling in cells expressing longevity-associated human IGF1R alleles. Aging Cell 10: 551–554.

Thompson, O., M. Edgley, P. Strasbourger, S. Flibotte, B. Ewing *et al.*, 2013 The million mutation project: a new approach to genetics in Caenorhabditis elegans. Genome Res. 23: 1749–1762.

Thorvaldsdottir, H., J. T. Robinson, and J. P. Mesirov, 2013 Integrative Genomics Viewer (IGV): high-performance genomics data visualization and exploration. Brief. Bioinform. 14: 178–192.

Trapnell, C., L. Pachter, and S. L. Salzberg, 2009 TopHat: discovering splice junctions with RNA-Seq. Bioinformatics 25: 1105–1111.

Trapnell, C., A. Roberts, L. Goff, G. Pertea, D. Kim *et al.*, 2012 Differential gene and transcript expression analysis of RNA-seq experiments with TopHat and Cufflinks. Nat. Protoc. 7: 562–578.

Trapnell, C., D. G. Hendrickson, M. Sauvageau, L. Goff, J. L. Rinn *et al.*, 2013 Differential analysis of gene regulation at transcript resolution with RNA-seq. Nat. Biotechnol. 31: 46–53.

Tsuchiya, K., J. Tanaka, Y. Shuiqing, C. L. Welch, R. A. DePinho *et al.*, 2012 FoxOs integrate pleiotropic actions of insulin in vascular endothelium to protect mice from atherosclerosis. Cell Metab. 15: 372–381.

Tsuchiya, K., M. Westerterp, A. J. Murphy, V. Subramanian, A. W. Ferrante, Jr. *et al.*, 2013 Expanded granulocyte/monocyte compartment in myeloid-specific triple FoxO knockout increases oxidative stress and accelerates atherosclerosis in mice. Circ. Res. 112: 992–1003.

Tullet, J. M., C. Araiz, M. J. Sanders, C. Au, A. Benedetto *et al.*, 2014 DAF-16/FoxO directly regulates an atypical AMP-activated protein kinase gamma isoform to mediate the effects of insulin/IGF-1 signaling on aging in Caenorhabditis elegans. PLoS Genet. 10: e1004109.

van der Horst, A., and B. M. Burgering, 2007 Stressing the role of FoxO proteins in lifespan and disease. Nat. Rev. Mol. Cell Biol. 8: 440–450.

Vowels, J. J., and J. H. Thomas, 1992 Genetic analysis of chemosensory control of dauer formation in Caenorhabditis elegans. Genetics 130: 105–123.

Willcox, B. J., T. A. Donlon, Q. He, R. Chen, J. S. Grove *et al.*, 2008 FOXO3A genotype is strongly associated with human longevity. Proc. Natl. Acad. Sci. USA 105: 13987–13992.

Yamamoto, R., and M. Tatar, 2011 Insulin receptor substrate chico acts with the transcription factor FOXO to extend Drosophila lifespan. Aging Cell 10: 729–732.

Communicating editor: D. Greenstein

GENETICS

Supporting Information
www.genetics.org/lookup/suppl/doi:10.1534/genetics.115.177998/-/DC1

Longevity Genes Revealed by Integrative Analysis of Isoform-Specific *daf-16/FoxO* Mutants of *Caenorhabditis elegans*

Albert Tzong-Yang Chen, Chunfang Guo, Omar A. Itani, Breane G. Budaitis, Travis W. Williams, Christopher E. Hopkins, Richard C. McEachin, Manjusha Pande, Ana R. Grant, Sawako Yoshina, Shohei Mitani, and Patrick J. Hu

DOI: 10.1534/genetics.115.177998

Supporting Information: Longevity genes revealed by integrative analysis of isoform-specific *daf-16/FoxO* mutants of *Caenorhabditis elegans*

Albert Tzong-Yang Chen, Chunfang Guo, Omar A. Itani, Breane G. Budaitis, Travis W. Williams, Christopher E. Hopkins, Richard C. McEachin, Manjusha Pande, Ana R. Grant, Sawako Yoshina, Shohei Mitani, and Patrick J. Hu

* = in a separate file

SUPPLEMENTAL FIGURES

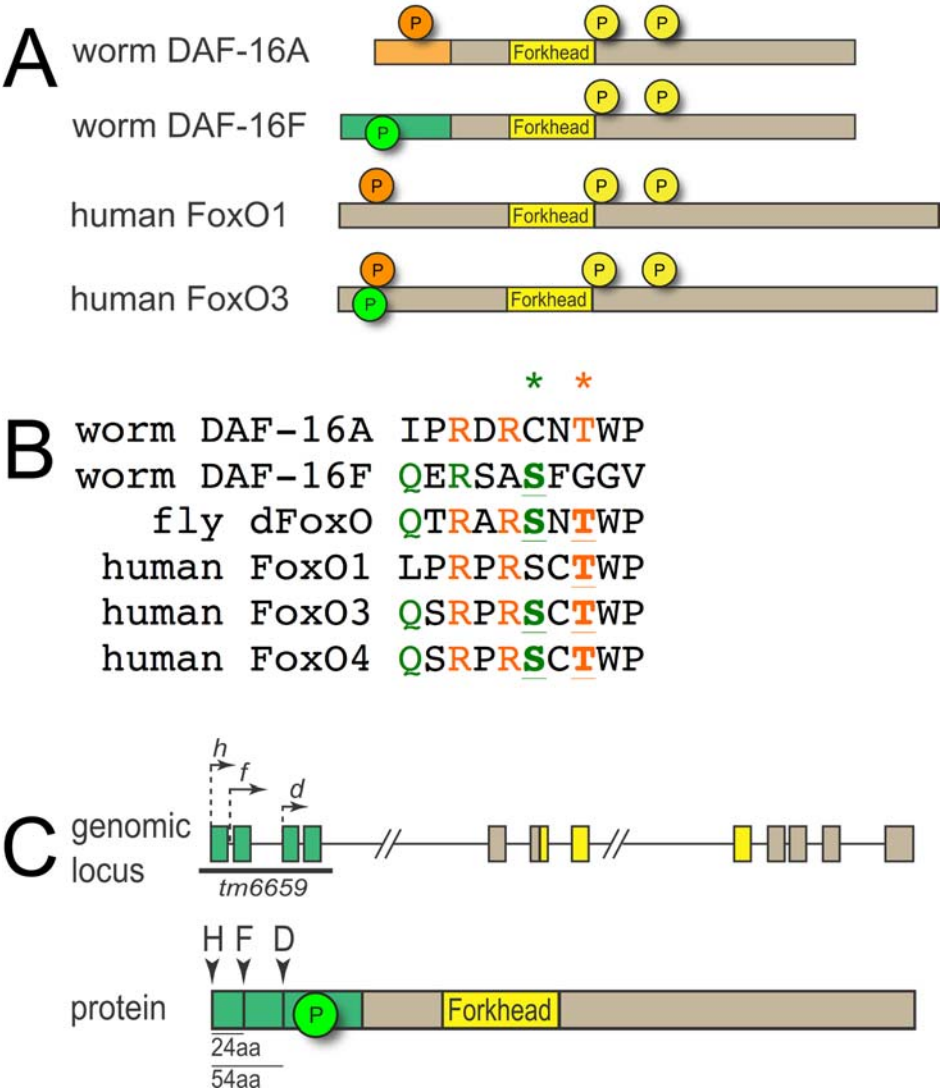

Figure S1 DAF-16/FoxO protein isoforms. (A) Protein schematic comparing *C. elegans* DAF-16A and DAF-16F isoforms with human FoxO1 and FoxO3 proteins. The identical C-termini of DAF-16A and DAF-16F share two highly conserved RxRxxS/T Akt-family consensus phosphorylation motifs (yellow) with human FoxO. The N-terminus of DAF-16A includes an RxRxxS/T phosphorylation motif (orange) conserved in human FoxO1 and FoxO3, while the unique N-terminus of DAF-16F harbors a QxRxxS motif (green) conserved in FoxO3. (B) N-terminal phosphorylation motifs in *C. elegans*, *Drosophila melanogaster,* and human FoxO proteins. Asterisks indicate conserved phosphoacceptor sites. Residues known to be phosphorylated *in vivo* (DAF-16F) or in intact cells (dFoxO, FoxO3, and FoxO4) are emboldened and underlined. (C) Distinction between *daf-16d*, *daf-16f*, and *daf-16h*, collectively referred to as *daf-16f* in this study. *daf-16d/f/h* transcripts (arrows) differ slightly in their 5' ends. DAF-16D/F/H proteins are translated from distinct translational start sites (arrowheads). *daf-16f(tm6659)* eliminates all three isoforms, and the *daf-16f* RNAi construct is predicted to knock down all three isoforms.

A. *daf-16d* cDNA sequence - first 3 exons, including 5'UTR

GGTTTAATTACCCAAGTTTGAG*TTTTCAG*CTCGATTCGCCGCTACCATCTGACATCACACTGCACAATC
*TCGAACCGGCAAGGCCTGATTCCGGA*ATGAGTTTTTCCACTGATTTTGAC|GATGATTTCTTCAATCTC
GACCTCCATCAACAAGAGCGTTCGGCTTCTTTTGGCGGAGTAACCCAGTATTCTCAACAATTTCTTCGC
GAAGAATGCTCGTTCTCTCCGTATTTCCACACATCTTTAGAGACTGTTGACAGCGGAAGAACTAG|CCT
ATACGGGAGCAATGAGCAATGTGGACAGCTCGGCGGAGCATCTTCAAACGGGTCGACAGCAATGCTTCA
TACTCCAGATGGAAGCAATTCTCATCAGACATCGTTTCCTTCGGA

B. *daf-16f* cDNA sequence - first 4 exons, including 5'UTR

GGTTTAATTACCCAAGTTTGAG*CAAAAGTCTTCATTACATTGCTCGAAGTGCCGAAATTTTCTGCAAAA
ATTCTCACAGGAC*ATGCAAGCGTGGAACTGTCGTGAG|CTCGATTCGCCGCTACCATCTGACATCACAC
TGCACAATCTCGAACCGGCAAGGCCTGATTCCGGAATGAGTTTTTCCACTGATTTTGAC|GATGATTTC
TTCAATCTCGACCTCCATCAACAAGAGCGTTCGGCTTCTTTTGGCGGAGTAACCCAGTATTCTCAACAA
TTTCTTCGCGAAGAATGCTCGTTCTCTCCGTATTTCCACACATCTTTAGAGACTGTTGACAGCGGAAGA
ACTAG|CCTATACGGGAGCAATGAGCAATGTGGACAGCTCGGCGGAGCATCTTCAAACGGGTCGACAGC
AATGCTTCATACTCCAGATGGAAGCAATTCTCATCAGACATCGTTTCCTTCGGA

Figure S2 *daf-16f* N-terminal cDNA sequence

Legend

Green: Coding sequences unique to *daf-16d* and *daf-16f*. Start codons are underlined.
Blue: 7 nucleotides included in two RACE clones due to alternative trans-splicing
Bold: *C. elegans* SL1 trans-spliced leader
Italics: 5'UTR
| exon-exon junction

No *daf-16h* transcripts were detected by 5' RACE.

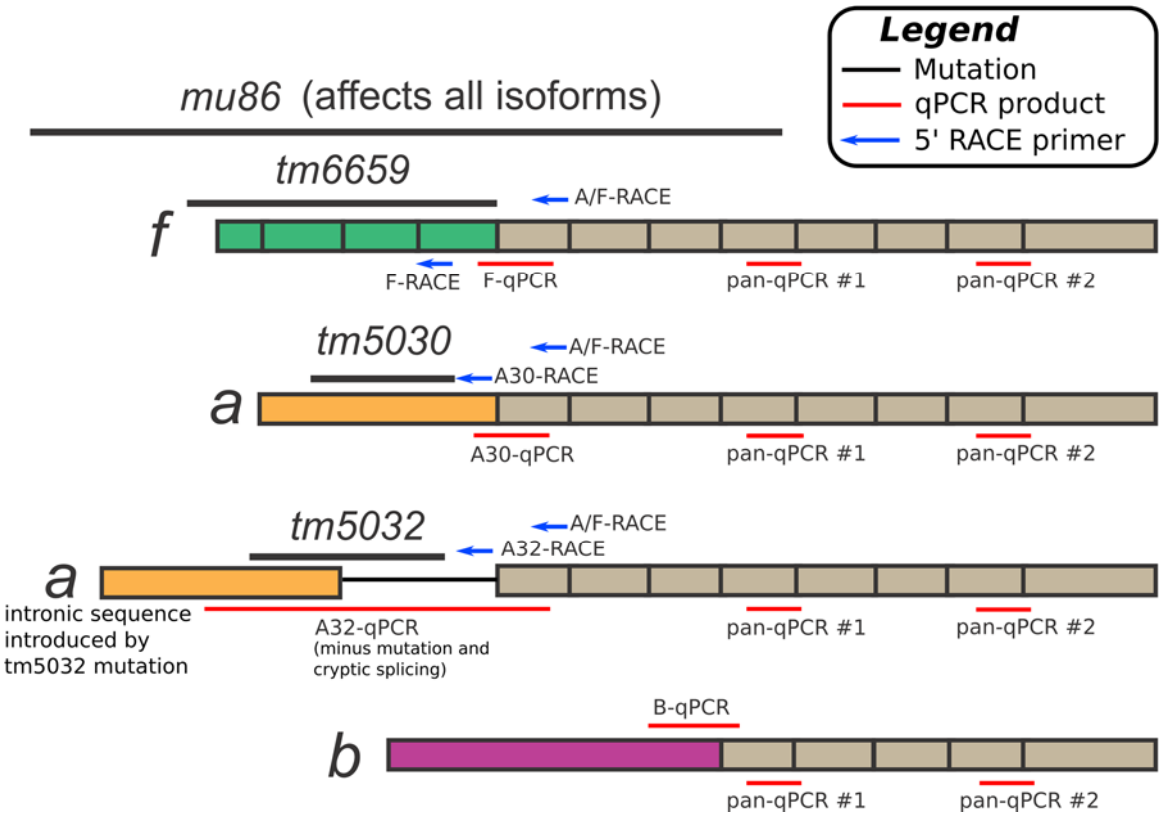

Figure S3 Overview of strategy for characterizing *daf-16/FoxO* transcripts in isoform-specific mutants. Spliced transcripts are shown, and exons are separated by black lines. Note that *daf-16a(tm5032)* disrupts a 5′ splice site and therefore intronic sequence is included.

For 5′ RACE, a semi-synchronized population of young adults was harvested for RNA. RNA was purified and analyzed as described in Methods. The A/F-RACE primer was used for first-strand cDNA synthesis. PCR amplification was performed using either the A30-RACE primer, A32-RACE primer, or the F-RACE primer, in combination with the Abridged Anchor Primer from the Invitrogen RACE kit. For *daf-16(tm5032)*, a different primer A32-RACE was used. RACE sequences are presented in Figures S2 and S4.

qPCR results are presented in Fig. S6 and Table S1.

A. *daf-16a(tm5030)* cDNA sequence - first 3 exons, including 5'UTR

```
wild-type GGTTTAATTACCCAAGTTTGAGAGAACTCACTGATCTTTCAAGCCGAAGCAATCAAGACC
   tm5030 GGTTTAATTACCCAAGTTTGAGAGAACTCACTGATCTTTCAAGCCGAAGCAATCAAGACC

wild-type TCAAAGCCAATCAACTCTACTCACTTTTCTTCAGAACCTTAACTTTTTGTGTCACTTTCC
   tm5030 TCAAAGCCAATCAACTCTACTCACTTTTCTTCAGAACCTTAACTTTTTGTGTCACTTTCC

wild-type CCAAAAACCGTTCAAGCTGCTGCCTTCACTCTCATCCCCTCCTCTTACTCCTTCTTTCTC
   tm5030 CCAAAAACCGTTCAAGCTGCTGCCTTCACTCTCATCCCCTCCTCTTACTCCTTCTTTCTC

wild-type GTCCGCTACTACTGTATCTTCTGGACATCTACCTGTATACACACCAGTGGCCAGTCATCT
   tm5030 GTCCGCTACTACTGTATCTTCTGGACATCTACCTGTATACACACCAGTGGCCAGTCATCT

wild-type GCCATTACAATTTCATCAATTGACACTTCTTCAACAACAACCGCCGTCCTCATTCACTCC
   tm5030 GCCATTACAATTTCATCAATTGACACTTCTTCAACAACAACCGCCGTCCTCATTCACTCC

wild-type CGATTCTTCCTCATCCTCAACATCGTCGTCTTTGGCTGAAATTCCCGAAGACGTTATGAT
   tm5030 CGATTCTTCCTCATCCTCAACATCGTCGTCTTTGGCTGAAATTCCCGAAGACGTTATGAT

wild-type GGAGATGCTGGTAGATCAGGGAACTGATGCATCGTCATCCGCCTCCACGTCCACCTCATC
   tm5030 GGAGATGCTGGTAGAT-------------------------------------------

wild-type TGTTTCGAGATTCGGAGCGGACACGTTCATGAATACACCGGATGATGTGATGATGAATGA
   tm5030 ------------------------------------------------------------

wild-type TGATATGGAACCGATTCCTCGTGATCGGTGCAATACGTGGCCAATGCGTAGGCCGCAACT
   tm5030 ------------------------------------------------------------

wild-type CGAACCACCACTCAACTCGAGTCCCATTATTCATGAACAAATTCCTGAAGAAGATGCTGA
   tm5030 ------------------------------TTCATGAACAAATTCCTGAAGAAGATGCTGA

wild-type |CCTATACGGGAGCAATGAGCAATGTGGACAGCTCGGCGGAGCATCTTCAAACGGGTCGA
   tm5030 |CCTATACGGGAGCAATGAGCAATGTGGACAGCTCGGCGGAGCATCTTCAAACGGGTCGA

wild-type CAGCAATGCTTCATACTCCAGATGGAAGCAATTCTCATCAGACATCGTTTCCTTCGGA|
   tm5030 CAGCAATGCTTCATACTCCAGATGGAAGCAATTCTCATCAGACATCGTTTCCTTCGGA|

wild-type TTTACGAATGTCCGAATCGCCAGACGATACCGTATCGGGAAAAAAGACAACGACCAGACG
   tm5030 TTTACGAATGTCCGAATCGCCAGACGATACCGTATCGGGAAAAAAGACAACGACCAGACG

wild-type GAACGCTTGGGGAAATATGTCATATGCTGAACTTATCACTACAGCCATTATGGCTAGTCC
   tm5030 GAACGCTTGGGGAAATATGTCATATGCTGAACTTATCACTACAGCCATTATGGCTAGTCC

wild-type AGAGAAACGGTTAACTCTTGCACAAG|...
   tm5030 AGAGAAACGGTTAACTCTTGCACAAG|...
                     STOP
```

Figure S4 Effects of *daf-16a* mutations on daf-*16a* N-terminal cDNA sequence (continued on next page)

Legend

Orange: Unique *daf-16a* N-terminal exon. Start codon is underlined.
Red: early stop codon in *daf-16a(tm5030)* and *daf-16a(tm5032)* transcripts
Blue: 6 nucleotides included in R13H8.1c but not R13H8.1b by alternative splicing that do not affect the reading frame. R13H8.1c and R13H8.1b are both *daf-16a* transcripts.
Bold: *C. elegans* SL1 trans-spliced leader
Italics: 5'UTR
| exon-exon junction

B. *daf-16a(tm5032)* cDNA sequence - first exon and intron

```
wild-type GGTTTAATTACCCAAGTTTGAGAGAACTCACTGATCTTTCAAGCCGAAGCAATCAAGACC
tm5032 #1 GGTTTAATTACCCAAGTTTGAGAGAACTCACTGATCTTTCAAGCCGAAGCAATCAAGACC
tm5032 #2 GGTTTAATTACCCAAGTTTGAGAGAACTCACTGATCTTTCAAGCCGAAGCAATCAAGACC

wild-type TCAAAGCCAATCAACTCTACTCACTTTTCTTCAGAACCTTAACTTTTTGTGTCACTTTCC
tm5032 #1 TCAAAGCCAATCAACTCTACTCACTTTTCTTCAGAACCTTAACTTTTTGTGTCACTTTCC
tm5032 #2 TCAAAGCCAATCAACTCTACTCACTTTTCTTCAGAACCTTAACTTTTTGTGTCACTTTCC

wild-type CCAAAAACCGTTCAAGCTGCTGCCTTCACTCTCATCCCCTCCTCTTACTCCTTCTTTCTC
tm5032 #1 CCAAAAACCGTTCAAGCTGCTGCCTTCACTCTCATCCCCTCCTCTTACTCCTTCTTTCTC
tm5032 #2 CCAAAAACCGTTCAAGCTGCTGCCTTCACTCTCATCCCCTCCTCTTACTCCTTCTTTCTC

wild-type GTCCGCTACTACTGTATCTTCTGGACATCTACCTGTATACACACCAGTGGCCAGTCATCT
tm5032 #1 GTCCGCTACTACTGTATCTTCTGGACATCTACCTGTATACACACCAGTGGCCAGTCATCT
tm5032 #2 GTCCGCTACTACTGTATCTTCTGGACATCTACCTGTATACACACCAGTGGCCAGTCATCT

wild-type GCCATTACAATTTCATCAATTGACACTTCTTCAACAACAACCGCCGTCCTCATTCACTCC
tm5032 #1 GCCATTACAATTTCATCAATTGACACTTCTTCAACAACAACCGCCGTCCTCATTCACTCC
tm5032 #2 GCCATTACAATTTCATCAATTGACACTTCTTCAACAACAACCGCCGTCCTCATTCACTCC

wild-type CGATTCTTCCTCATCCTCAACATCGTCGTCTTTGGCTGAAATTCCCGAAGACGTTATGAT
tm5032 #1 CGATTCTTCCTCATCCTCAACATCGTCGTCTTTGGCTGAAATTCCCGAAGACGTTATGAT
tm5032 #2 CGATTCTTCCTCATCCTCAACATCGTCGTCTTTGGCTGAAATTCCCGAAGACGTTATGAT

wild-type GGAGATGCTGGTAGATCAGGGAACTGATGCATCGTCATCCGCCTCCACGTCCACCTCATC
tm5032 #1 GGAGATGCTGGTAGATCAGGGAACTGATGCATCGTCATCCGCCTCCACGTCCACCTCATC
tm5032 #2 GGAGATGCTGGTAGATCAGGGAACTGATGCATCGTCATCCGCCTCCACGTCCACCTCATC

wild-type TGTTTCGAGATTCGGAGCGGACACGTTCATGAATACACCGGATGATGTGATGATGAATGA
tm5032 #1 TGTTTCGAGATTCGGAGCGGACACGTTCATGAATACACCGGATGATGTGATGATGAATGA
tm5032 #2 TGTTTCGAGATTCGGAGCGGACACGTTCATGAATACACCGGATGATGTGATGATGAATGA

wild-type TGATATGGAACCGATTCCTCGTGATCGGTGCAATACGTGGCCAATGCGTAGGCCGCAACT
tm5032 #1 TGATATGGAACCGATTCCTCGTGATCGGTGCAATACGTGGCC------------------
tm5032 #2 TGATATGGAACCGATTCCTCGTGATCGGTGCAATACGTGGCC------------------

wild-type CGAACCACCACTCAACTCGAGTCCCATTATTCATGAACAAATTCCTGAAGAAGATGCTGA
tm5032 #1 ------------------------------------------------------------
tm5032 #2 ------------------------------------------------------------

wild-type ------------------------------------------------------------
tm5032 #1 ttttgtatttttggagcataa*-------------------------------------
tm5032 #2 ttttgtatttttggagcataa*gtaatacgactgatatgaacctgaaaaaccaccaatta
                               STOP

wild-type -------------------------------------------|CCTATACGGGAGCA...
tm5032 #1 ------------------------------------------CCTATACGGGAGCA...
tm5032 #2 tatctaattttcccgaacattgtctaatatttctattttcag-CCTATACGGGAGCA...
```

Figure S4 (continued)

<u>Additional legend- specific to *daf-16a(tm5032)*</u>

lower-case: intronic sequence introduced by *tm5032* mutation

tm5032 #1 *vs.* #2: Two products detected by cDNA sequencing. #1 is the major product, formed by cryptic splice site activation. * denotes cryptic splice site.

C. *daf-16a(tm5030)* and *daf-16a(tm5032)* genomic sequence (nt 6064-6837 of cosmid R13H8).

```
wild-type ...atccaattccagAGAACTCACTGATCTTTCAAGCCGAAGCAATCAAGACCTCAAAGC
   tm5030 ...atccaattccagAGAACTCACTGATCTTTCAAGCCGAAGCAATCAAGACCTCAAAGC
   tm5032 ...atccaattccagAGAACTCACTGATCTTTCAAGCCGAAGCAATCAAGACCTCAAAGC

wild-type CAATCAACTCTACTCACTTTTCTTCAGAACCTTAACTTTTTGTGTCACTTTCCCCAAAAA
   tm5030 CAATCAACTCTACTCACTTTTCTTCAGAACCTTAACTTTTTGTGTCACTTTCCCCAAAAA
   tm5032 CAATCAACTCTACTCACTTTTCTTCAGAACCTTAACTTTTTGTGTCACTTTCCCCAAAAA

wild-type CCGTTCAAGCTGCTGCCTTCACTCTCATCCCCTCCTCTTACTCCTTCTTTCTCGTCCGCT
   tm5030 CCGTTCAAGCTGCTGCCTTCACTCTCATCCCCTCCTCTTACTCCTTCTTTCTCGTCCGCT
   tm5032 CCGTTCAAGCTGCTGCCTTCACTCTCATCCCCTCCTCTTACTCCTTCTTTCTCGTCCGCT

wild-type ACTACTGTATCTTCTGGACATCTACCTGTATACACACCAGTGGCCAGTCATCTGCCATTA
   tm5030 ACTACTGTATCTTCTGGACATCTACCTGTATACACACCAGTGGCCAGTCATCTGCCATTA
   tm5032 ACTACTGTATCTTCTGGACATCTACCTGTATACACACCAGTGGCCAGTCATCTGCCATTA

wild-type CAATTTCATCAATTGACACTTCTTCAACAACAACCGCCGTCCTCATTCACTCCCGATTCT
   tm5030 CAATTTCATCAATTGACACTTCTTCAACAACAACCGCCGTCCTCATTCACTCCCGATTCT
   tm5032 CAATTTCATCAATTGACACTTCTTCAACAACAACCGCCGTCCTCATTCACTCCCGATTCT

wild-type TCCTCATCCTCAACATCGTCGTCTTTGGCTGAAATTCCCGAAGACGTTATGATGGAGATG
   tm5030 TCCTCATCCTCAACATCGTCGTCTTTGGCTGAAATTCCCGAAGACGTTATGATGGAGATG
   tm5032 TCCTCATCCTCAACATCGTCGTCTTTGGCTGAAATTCCCGAAGACGTTATGATGGAGATG

wild-type CTGGTAGATCAGGGAACTGATGCATCGTCATCCGCCTCCACGTCCACCTCATCTGTTTCG
   tm5030 CTGGTAGAT-----------------------------------------------------
   tm5032 CTGGTAGATCAGGGAACTGATGCATCGTCATCCGCCTCCACGTCCACCTCATCTGTTTCG

wild-type AGATTCGGAGCGGACACGTTCATGAATACACCGGATGATGTGATGATGAATGATGATATG
   tm5030 ------------------------------------------------------------
   tm5032 AGATTCGGAGCGGACACGTTCATGAATACACCGGATGATGTGATGATGAATGATGATATG

wild-type GAACCGATTCCTCGTGATCGGTGCAATACGTGGCCAATGCGTAGGCCGCAACTCGAACCA
   tm5030 ------------------------------------------------------------
   tm5032 GAACCGATTCCTCGTGATCGGTGCAATACGTGGCC--------------------------

wild-type CCACTCAACTCGAGTCCCATTATTCATGAACAAATTCCTGAAGAAGATGCTGagtatgtg
   tm5030 ----------------------TTCATGAACAAATTCCTGAAGAAGATGCTGagtatgtg
   tm5032 ------------------------------------------------------------

wild-type ttgaacaataaaatgttttagtagataaaatgccatttgaaaaaactaaaaatgatgtag
   tm5030 ttgaacaataaaatgttttagtagataaaatgccatttgaaaaaactaaaaatgatgtag
   tm5032 ------------------------------------------------------------

wild-type atcatatctatttgctagaaaataattcaggaaaaatttgaaaaagaatattacaaagtc
   tm5030 atcatatctatttgctagaaaataattcaggaaaaatttgaaaaagaatattacaaagtc
   tm5032 ------------------------------------------------------------

wild-type gcgaaatttttattttgtatttttggagcataagtaatacgactgatatgaacct...
   tm5030 gcgaaatttttattttgtatttttggagcataagtaatacgactgatatgaacct...
   tm5032 --------------ttttgtatttttggagcataagtaatacgactgatatgaacct...
```

Figure S4 (continued). Lower and upper case indicate intronic and exonic sequence, respectively. Start codon is underlined and emboldened.

A. Predicted DAF-16A protein encoded by *daf-16a(tm5030)*

```
                                                                  ↓
wild-type MMEMLVDQGTDASSSASTSTSSVSRFGADTFMNTPDDVMMNDDMEPIPRDRCNTW
 identity ||||||
   tm5030 MMEMLVDFMNKFLKKMLTYTGAMSNVDSSAEHLQTGRQQCFILQMEAILIRHRFL

wild-type PMRRPQLEPPLNSSPIIHEQIPEEDADLYGSNEQCGQLGGASSNGSTAMLHTPDG
 identity
   tm5030 RIYECPNRQTIPYREKRQRPDGTLGEICHMLNLSLQPLWLVQRNG*---------

wild-type SNSHQTSFPSDFRMSESPDDTVSGKKTTTRRNAWGNMSYAELITTAIMASPE...
 identity
   tm5030 ----------------------------------------------------------
```

B. Predicted DAF-16A protein encoded by *daf-16a(tm5032)*

```
                                                                  ↓
wild-type MMEMLVDQGTDASSSASTSTSSVSRFGADTFMNTPDDVMMNDDMEPIPRDRCNTW
 identity ||||||||||||||||||||||||||||||||||||||||||||||||||||||||
   tm5032 MMEMLVDQGTDASSSASTSTSSVSRFGADTFMNTPDDVMMNDDMEPIPRDRCNTW

wild-type PMRRPQLEPPLNSSPIIHEQIPEEDADLYGSNEQCGQLGGASSNGSTAMLHTPDG
 identity |||
   tm5032 PMRFCILEHK*-------------------------------------------

wild-type SNSHQTSFPSDFRMSESPDDTVSGKKTTTRRNAWGNMSYAELITTAIMASPE...
 identity
   tm5032 ----------------------------------------------------------
```

Figure S5 Predicted DAF-16A proteins encoded by *daf-16a* mutants

For wild-type DAF-16A, 162 out of 510 amino acids are shown. Predicted mutant DAF-16A sequences are aligned to wild-type. Note that R13H8.1b and R13H8.1c are two nearly identical transcripts that both encode DAF-16A.

Legend

| = identity with wild-type sequence

Underline: start of Forkhead domain

Bold: RxRxxT AKT family phosphorylation motif

↓ = phosphothreonine

* = early stop

Blue: amino acids included in the protein products of R13H8.1c but not R13H8.1b due to inclusion of 6 nucleotides that do not affect the reading frame (see figure S4). In wild-type, the three indicated amino acids are present in R13H8.1c, but are replaced by a single glutamic acid residue in R13H8.1b. In *daf-16a(tm5030)*, the three indicated amino acids are present in R13H8.1c, but are replaced by a single lysine residue in R13H8.1b.

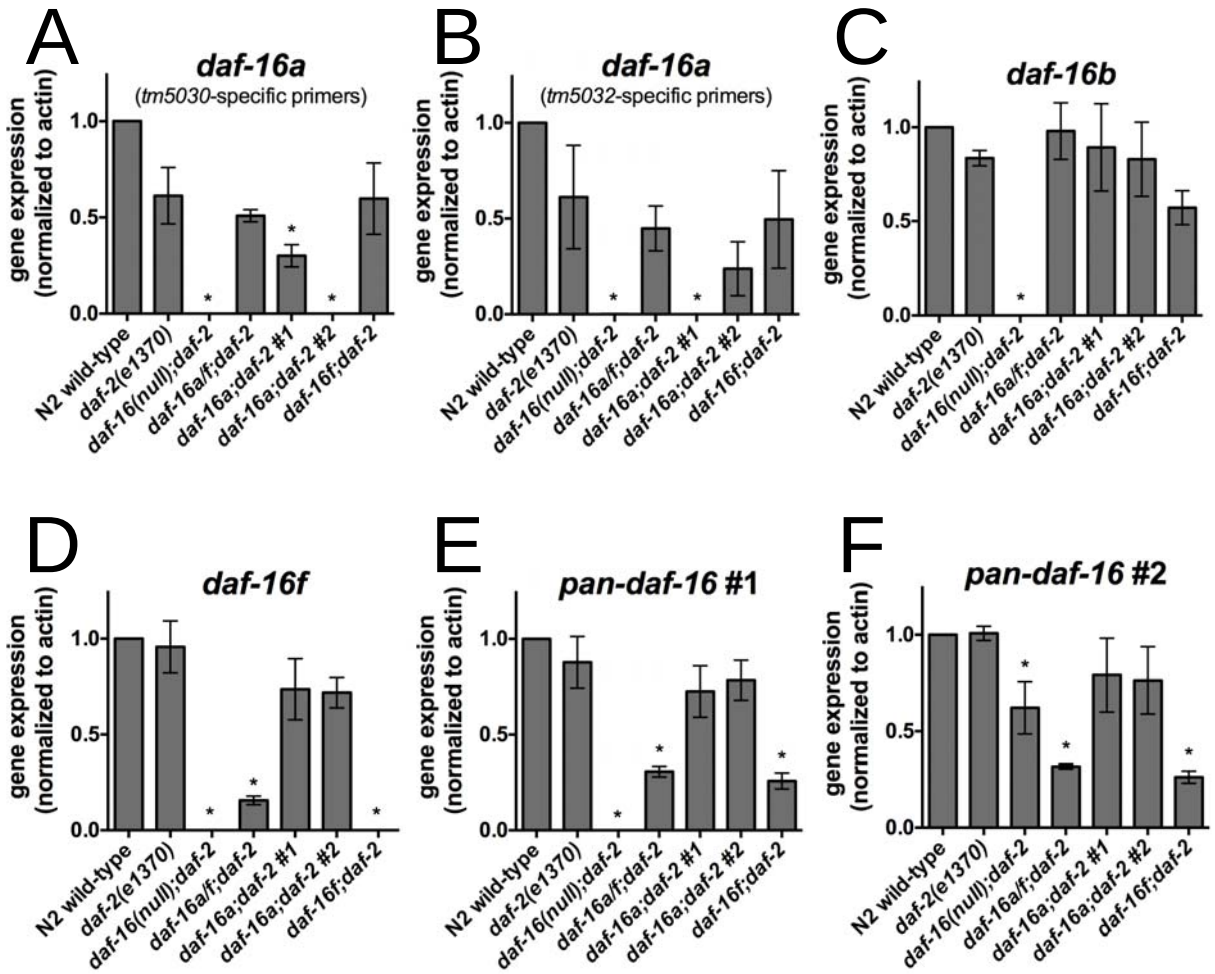

Figure S6 qPCR measurements of *daf-16/FoxO* transcripts in isoform-specific mutants. Mean values are presented from three biological replicates, error bars represent standard deviation and asterisks indicate samples that display statistically significant changes ($p < 0.05$ by paired ratio *t*-test). Data and statistics are summarized in Table S1. Note that *pan-daf-16* #1 primers anneal within the deletion of the *daf-16(mu86)* null allele, and *pan-daf-16* #2 primers anneal outside of the deletion. Likewise, *tm5030*-specific primers anneal within the *tm5032* deletion and vice versa. See Fig. S3 for a visual representation.

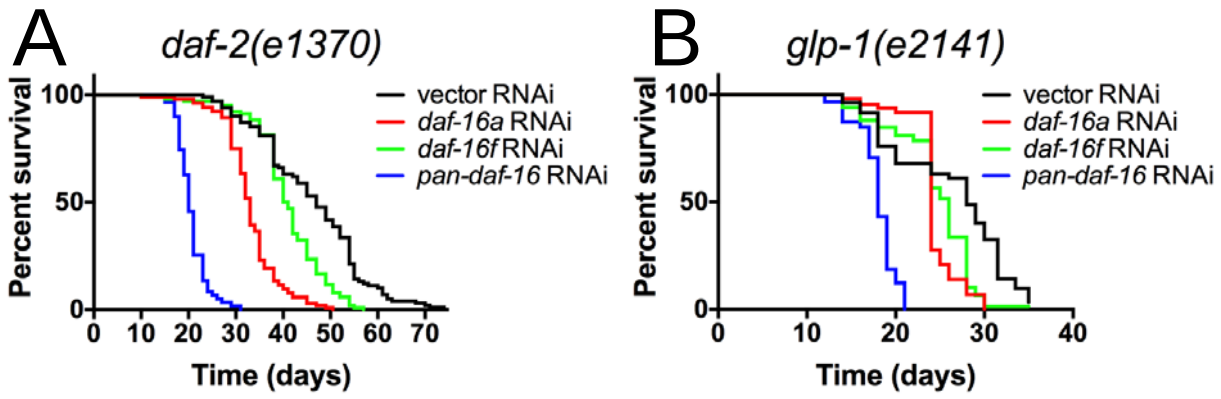

Figure S7 Effect of isoform-specific RNAi in (A) *daf-2(e1370)* and (B) *glp-1(e2141)* animals. Compare to Figures 3E-F and 4C-D.

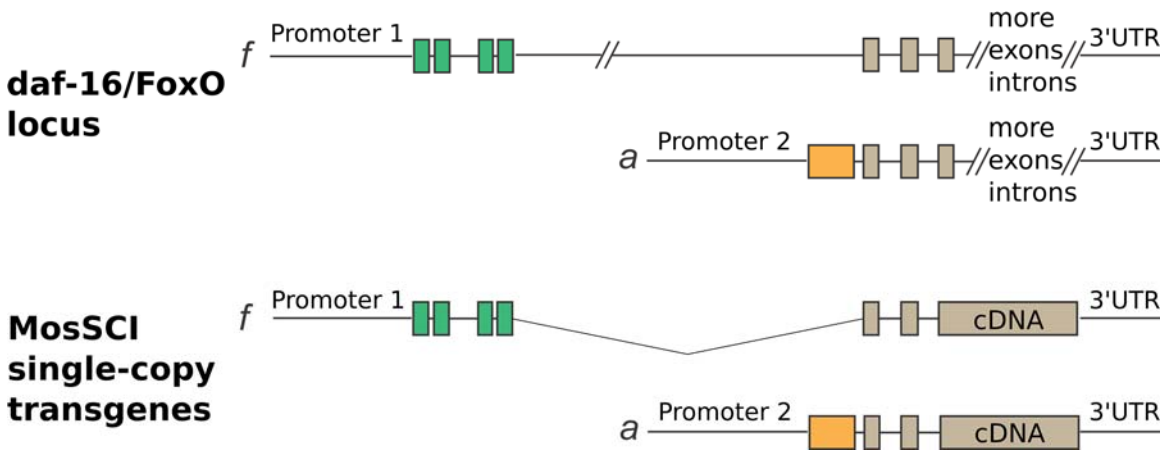

Figure S8 Diagram of single-copy *daf-16a* and *daf-16f* transgenes.
daf-16a and *daf-16f* transgenes are both integrated on chromosome II at the *ttTi5605* locus. Promoter 1 is 3kb while Promoter 2 is 4kb. The complete 1.7kb 3′UTR was incorporated. Note that a *C. briggsae unc-119* sequence is incorporated 5′ upstream of both transgenes for strain generation and selection.

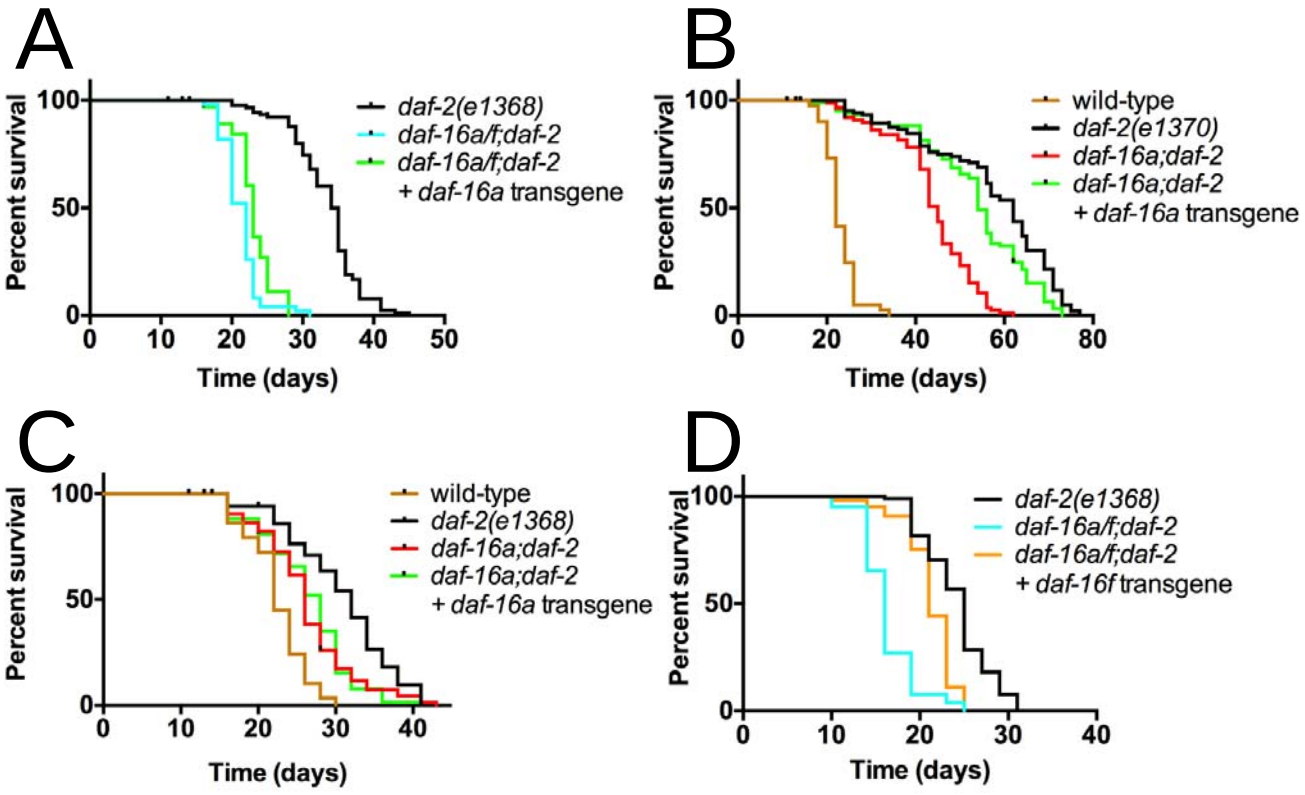

Figure S9 Rescue of life span phenotypes by single-copy transgenes in the *daf-2(e1368)* background. (A) The *daf-16a* single-copy transgene does not fully recapitulate endogenous *daf-16a* function in the *daf-2(e1368)* background. (B) The *daf-16f* single-copy transgene extends the life span of *daf-16a/f;daf-2(e1368)* animals.

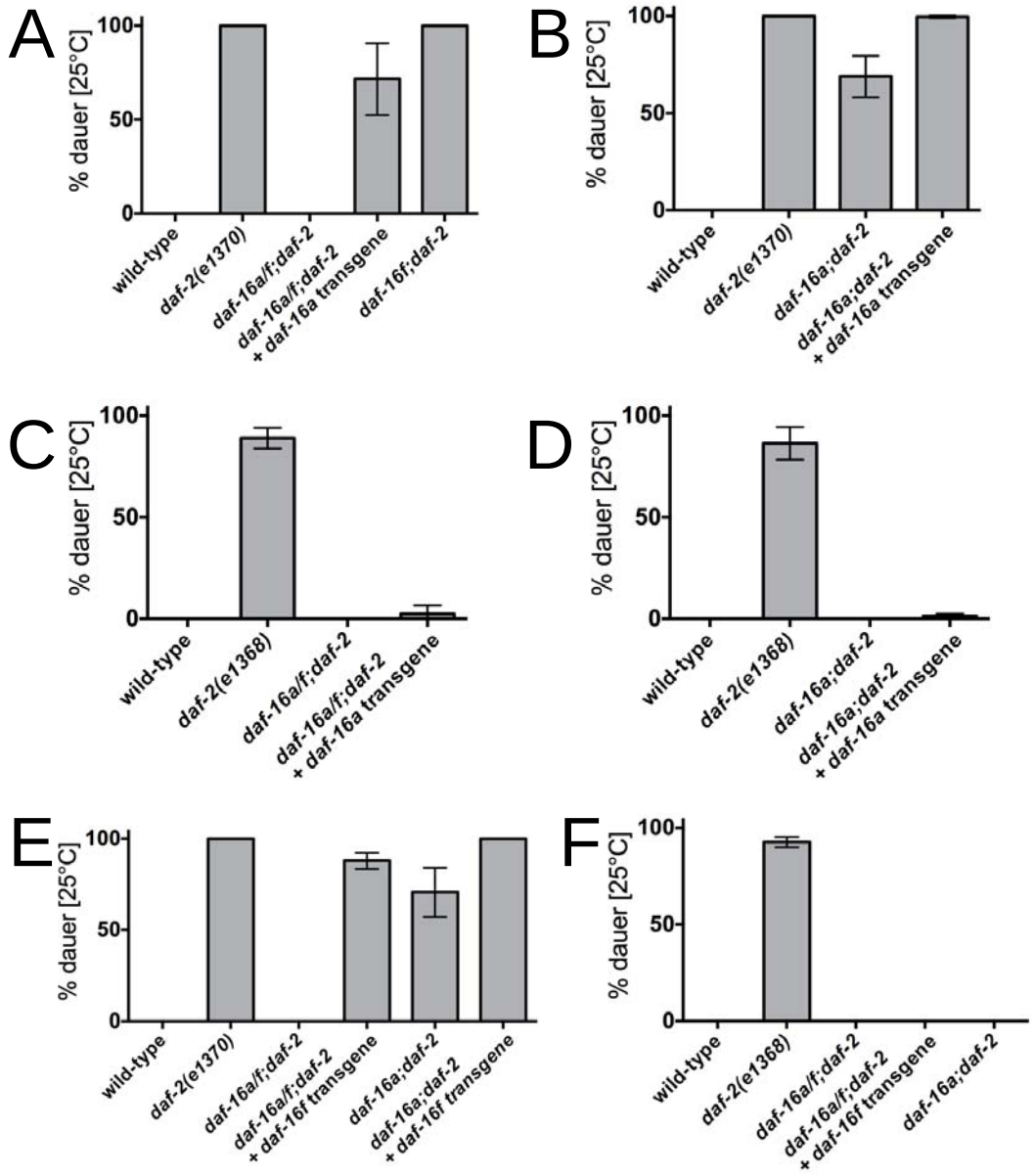

Figure S10 Rescue of dauer phenotypes by single-copy transgenes. (A) *daf-16a*-rescued *daf-16a/f;daf-2(e1370)* animals do not exhibit the same phenotype as *daf-16f;daf-2*. (B) The *daf-16a* transgene rescues dauer arrest in *daf-16a;daf-2(e1370)* double mutant animals. (C-D) The *daf-16a* transgene does not rescue *daf-16a* mutant dauer arrest in the *daf-2(e1368)* background. (E-F) *daf-16f*-rescued *daf-16a/f;daf-2* animals exhibit the same phenotypes as *daf-16a;daf-2*, suggesting that the *daf-16f* single-copy transgene has the same activity as *daf-16f* expressed from the genomic locus. Note: the *daf-16a;daf-2(e1368)* in D and F are the same, as they were performed in the same biological replicates, and are shown twice for relevant comparisons. See Table S11 for data and statistics. For all panels, the average and SD of three biological replicates are plotted.

(A)

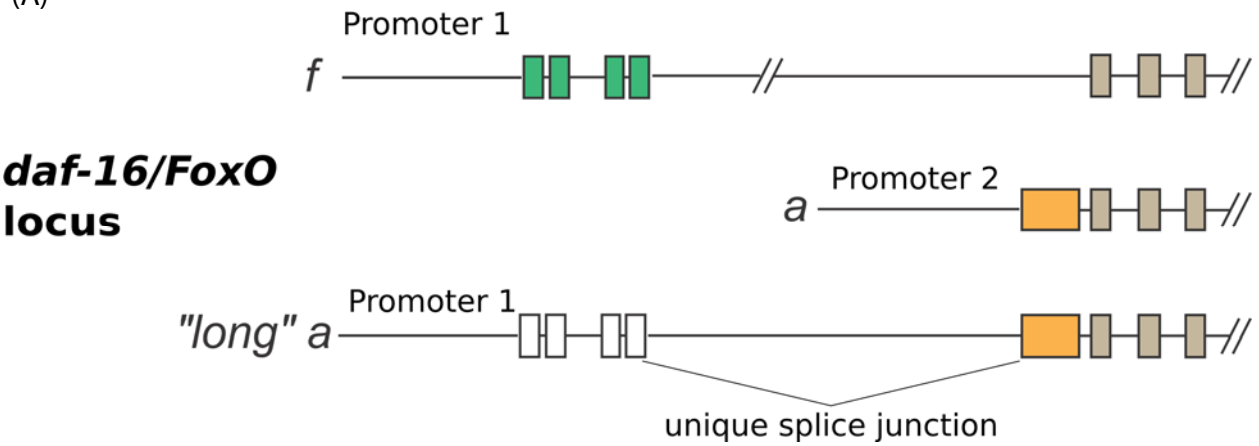

(B)

CCGCTACCATCTGACATCACACTGCACAATCTCGAACCGGCAAGGCCTGATTCCGGAATGAGTTTTTCC
ACTGATTTTGACGATGATTTCTTCAATCTCGACCTCCATCAACAAGAGCGTTCGGCTTCTTTTGGCGGA
GTAACCCAGTATTCTCAACAATTTCTTCG**CGAAAAATGCTCGTTCTCTCCGTATTTCCACACATCTTTA**
GAGACTGTTGACAGCGGAAGAACTAGAGAACTCACTGATCTTTCAAGCCGAAGCAATCAAGACCTCAAA
GCCAATCAACTCTACTCACTTTTCTTCAGAACCTTAACTTTTTGTGTCACTTTCCCCAAAAACCGTTCA
AGCTGCTGCCTTCACTCTCATCCCCTCCTCTTACTCCTTCTTTCTCGTCCGCTACTACTGTATCTTCTG
GACATCTACCTGTATACACACCAGTGGCCAGTCATCTGCCATTACAATTTCATCAATTGACACTTCTTC
AACAACAACCGCCGTCCTCATTCACTCCCGATTCTTCCTCATCCTCAACATCGTCGTCTGCGATC

Figure S11 cDNA sequencing and RNA-seq reads confirm splice junction unique to *daf-16a* transcripts originating from *daf-16f* promoter. (A) Schematic showing *daf-16* transcripts. Note that RNA-seq quantification suggests the "long" *daf-16a* transcript driven by the *daf-16f* promoter is found at 200X lower concentration than *daf-16a* and 500X lower than *daf-16f*, strongly suggesting that this transcript is trans-spliced to yield the canonical *daf-16a* transcript. Thus, the upstream sequence constitutes outrons. (B) cDNA sequence amplified from wild-type RNA. Bolded sequence indicates sequence confirmed by RNA-seq reads. Green indicates *daf-16a* outrons that correspond to *daf-16f* exons. Orange corresponds to the *daf-16a* 5'UTR.

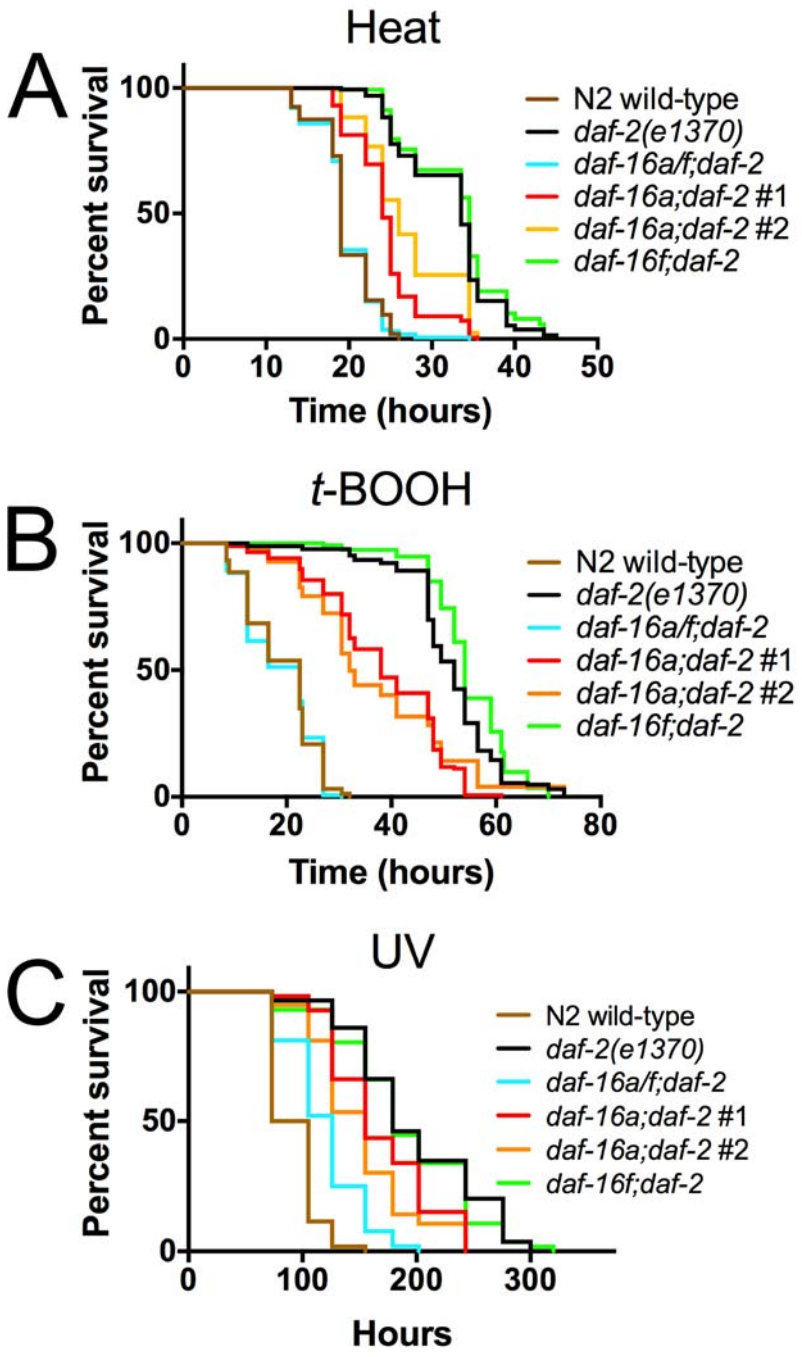

Figure S12 Thermotolerance, oxidative stress resistance, and UV stress resistance of *daf-16* isoform-specific mutants in the *daf-2(e1370)* background. Survival data for animals exposed to 33°C (A), 7.5mM *t*-BOOH (B), or 1200 J/m^2 UV (C) are shown. See Methods for details. For thermotolerance and oxidative stress assays, patterns and absolute values of survival were very similar for all 3 replicates, and therefore combined data for all replicates are presented. For UV stress resistance, one representative trial is shown, but note that *daf-16f* mutation reduced UV resistance in 1 of 3 trials. See Table S12 for data and statistics.

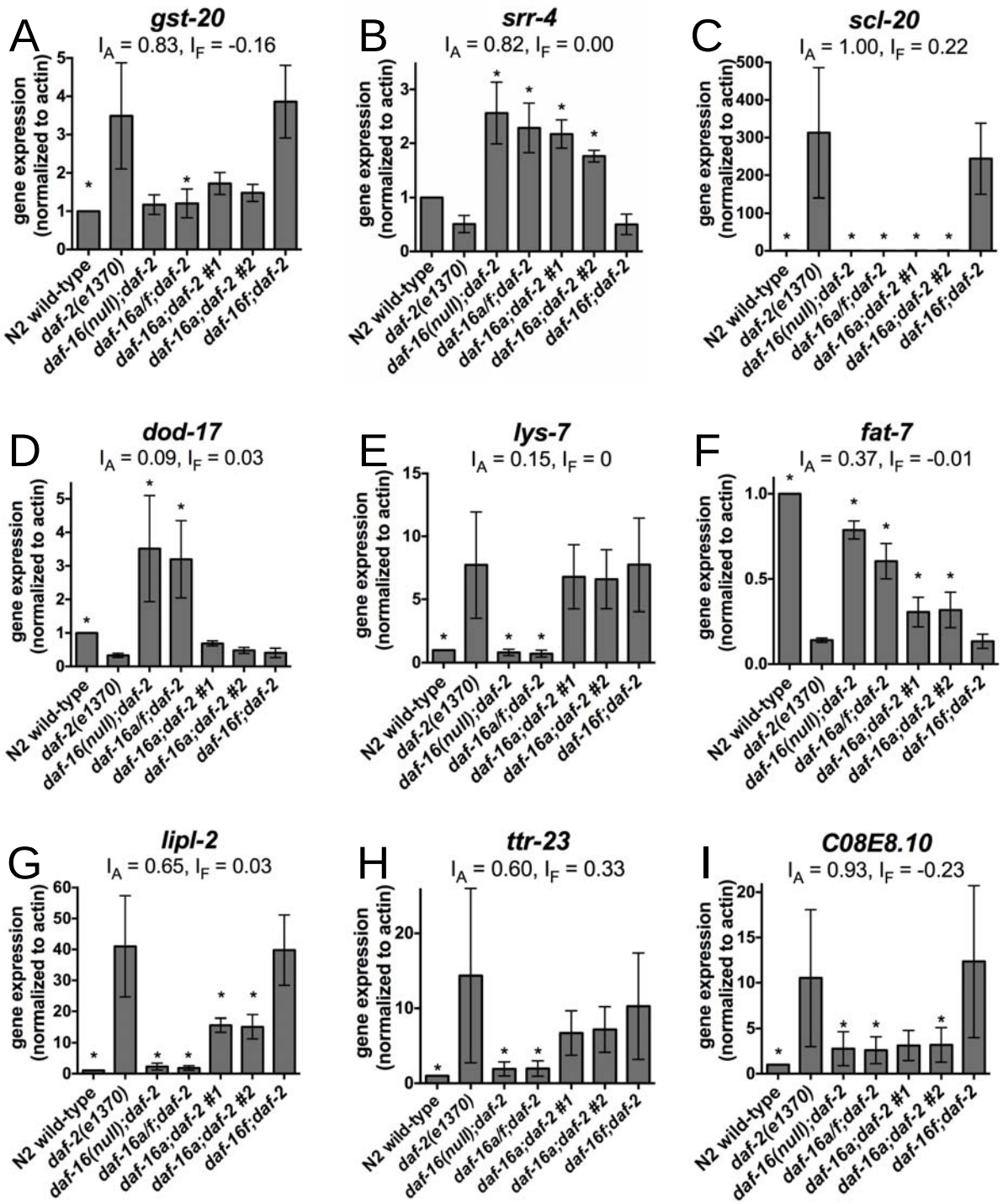

Figure S13 qPCR validation of additional DAF-16A/F target genes not presented in Fig. 6. Mean and standard deviation are plotted for three biological replicates of young adults. Asterisks denote statistically significant changes compared to *daf-2(e1370)* control ($p < 0.05$, paired ratio *t*-test). Data and statistics are presented in Table S14.

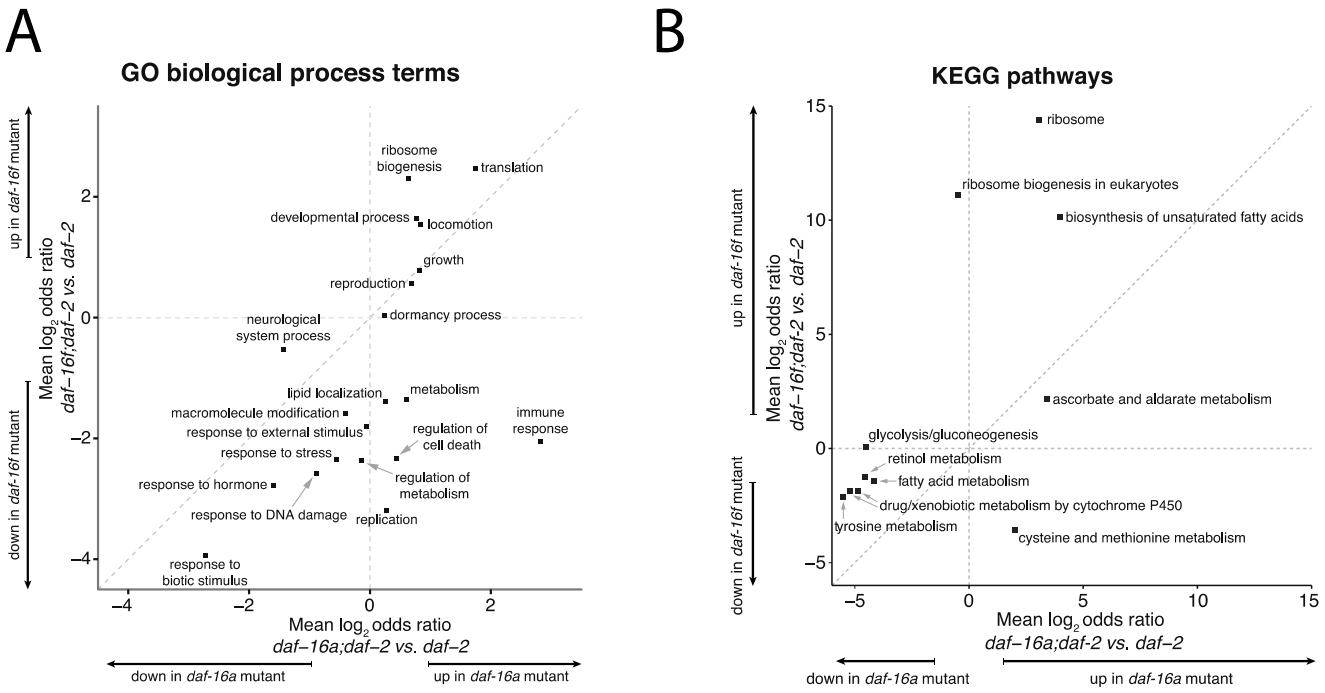

Figure S14 Functional enrichment testing of DAF-16A/F target genes. Log_2 odds ratios for enriched and depleted functions in isoform-specific *daf-16/FoxO* mutants are plotted for (A) GO biological process terms and (B) KEGG pathways. Up-regulated functions have positive ratios, and down-regulated functions have negative ratios. Terms were clustered using REVIGO, and cluster representatives are shown at the centroid of each cluster.

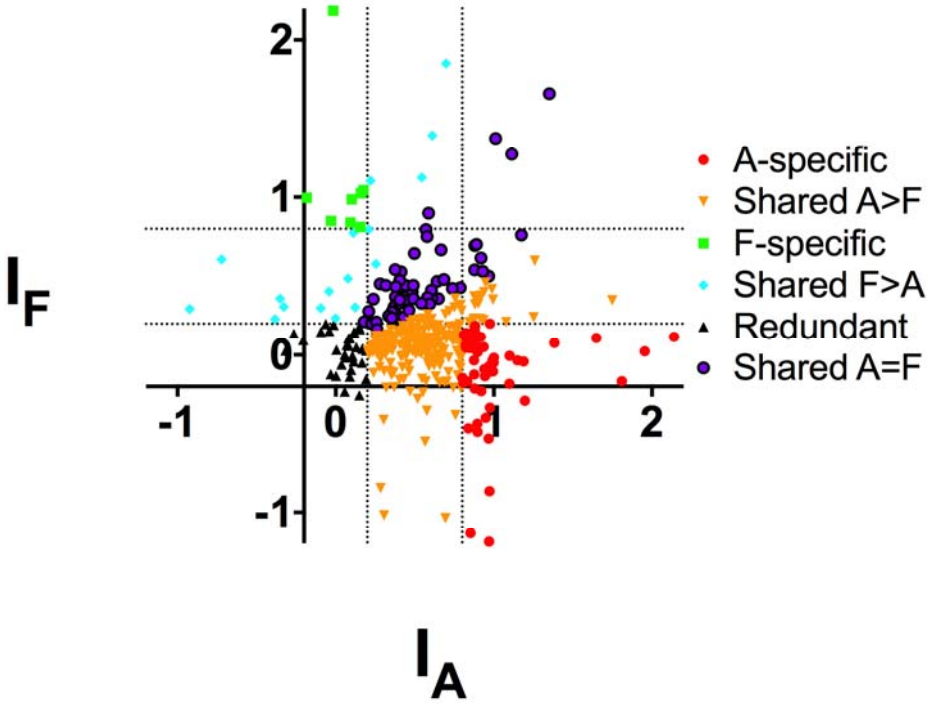

Figure S15 Expanded scatterplot showing more genes from Fig. 5F. Three genes with extreme indices (>2.2 or <-1.2) are omitted for presentation purposes.

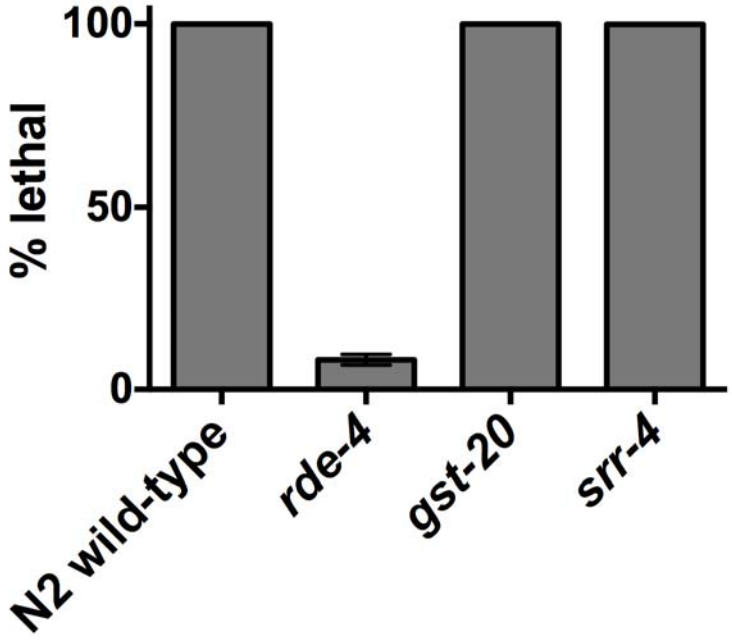

Figure S16 Rde (RNAi-defective) assays for strains with life span phenotypes.

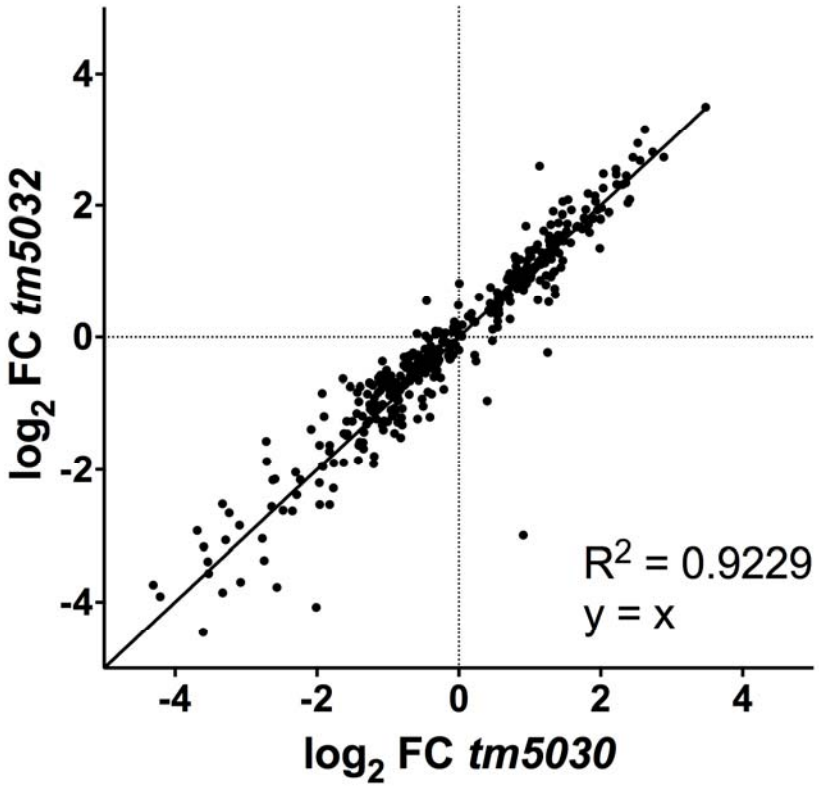

Figure S17 Comparison of effects of two *daf-16a* alleles on expression of DAF-16A/F target genes. Log_2 fold-change (FC) is shown for *daf-2(e1370) vs. daf-16a(tm5030);daf-2* on the X-axis, and log_2 FC is shown for *daf-2(e1370) vs. daf-16a(tm5032);daf-2* on the Y-axis.

SUPPLEMENTAL TABLES

Table S1 *daf-16/FoxO* isoform-specific qPCR data and statistics for Fig. S6.

	Independent cohorts						Statistical Analysis			
	1		2		3		Summary		P value (paired ratio t-test)	Fold change
	Mean	SD	Mean	SD	Mean	SD	Mean	SD		
***daf-16a(tm5030*-specific)**										
daf-2(e1370)	0.44	0.09	0.71	0.11	0.68	0.13	0.61	0.15	control	control
daf-16(mu86);daf-2	0.00	0.00	0.00	0.00	0.00	0.00	0.00	0.00	0.0762	0.00
daf-16(mg54);daf-2	0.47	0.10	0.52	0.04	0.53	0.10	0.51	0.03	0.0029	0.83
daf-16(tm5030);daf-2	0.25	0.05	0.36	0.06	0.30	0.04	0.30	0.06	0.2873	0.49
daf-16(tm5032);daf-2	0.00	0.00	0.00	0.00	0.00	0.00	0.00	0.00	0.0106	0.00
daf-16(tm6659);daf-2	0.38	0.06	0.69	0.17	0.71	0.08	0.60	0.18	0.0015	0.98
N2 wild-type	1.00	0.19	1.00	0.16	1.00	0.16	1.00	0.00	0.5286	1.63
***daf-16a(tm5032*-specific)**										
daf-2(e1370)	0.32	0.08	0.85	0.91	0.66	0.24	0.61	0.27	control	control
daf-16(mu86);daf-2	0.00	0.00	0.00	0.05	0.00	0.00	0.00	0.00	0.0459	0.00
daf-16(mg54);daf-2	0.34	0.13	0.57	0.04	0.43	0.16	0.45	0.12	0.2537	0.73
daf-16(tm5030);daf-2	0.00	0.00	0.00	0.09	0.00	0.00	0.00	0.00	0.0039	0.00
daf-16(tm5032);daf-2	0.16	0.02	0.40	0.09	0.15	0.07	0.24	0.14	0.0586	0.39
daf-16(tm6659);daf-2	0.26	0.03	0.77	0.54	0.45	0.16	0.50	0.25	0.1107	0.81
N2 wild-type	1.00	0.21	1.00	0.18	1.00	0.36	1.00	0.00	0.1926	1.63
daf-16b										
daf-2(e1370)	0.81	0.20	0.88	0.05	0.82	0.07	0.84	0.04	control	control
daf-16(mu86);daf-2	0.00	0.00	0.00	0.00	0.00	0.00	0.00	0.00	0.0017	0.00
daf-16(mg54);daf-2	1.15	0.22	0.86	0.08	0.93	0.07	0.98	0.15	0.3017	1.17
daf-16(tm5030);daf-2	1.06	0.11	0.99	0.08	0.63	0.13	0.89	0.23	0.8191	1.07
daf-16(tm5032);daf-2	0.97	0.19	0.92	0.08	0.60	0.15	0.83	0.20	0.8654	0.99
daf-16(tm6659);daf-2	0.67	0.10	0.49	0.02	0.55	0.14	0.57	0.09	0.0790	0.68
N2 wild-type	1.00	0.22	1.00	0.05	1.00	0.13	1.00	0.00	0.0233	1.20
daf-16f										
daf-2(e1370)	0.80	0.06	1.03	0.06	1.04	0.12	0.96	0.14	control	control
daf-16(mu86);daf-2	0.00	0.00	0.00	0.00	0.00	0.00	0.00	0.00	0.0036	0.00
daf-16(mg54);daf-2	0.16	0.01	0.17	0.01	0.13	0.01	0.16	0.02	0.0063	0.16
daf-16(tm5030);daf-2	0.65	0.04	0.92	0.05	0.64	0.06	0.74	0.16	0.1419	0.77
daf-16(tm5032);daf-2	0.73	0.05	0.79	0.06	0.63	0.09	0.72	0.08	0.1386	0.75
daf-16(tm6659);daf-2	0.00	0.00	0.00	0.00	0.00	0.00	0.00	0.00	<0.0001	0.00
N2 wild-type	1.00	0.19	1.00	0.09	1.00	0.17	1.00	0.00	0.6128	1.04
pan-daf-16 #1										
daf-2(e1370)	0.72	0.03	0.95	0.05	0.96	0.07	0.88	0.14	control	control
daf-16(mu86);daf-2	0.00	0.00	0.00	0.00	0.00	0.00	0.00	0.00	0.0159	0.00
daf-16(mg54);daf-2	0.31	0.02	0.33	0.02	0.28	0.02	0.31	0.03	0.0120	0.35
daf-16(tm5030);daf-2	0.68	0.04	0.88	0.04	0.62	0.04	0.72	0.13	0.2511	0.83
daf-16(tm5032);daf-2	0.78	0.05	0.89	0.07	0.68	0.07	0.78	0.11	0.4710	0.89
daf-16(tm6659);daf-2	0.23	0.03	0.23	0.02	0.31	0.01	0.26	0.04	0.0054	0.29
N2 wild-type	1.00	0.12	1.00	0.20	1.00	0.11	1.00	0.00	0.2767	1.14
pan-daf-16 #2										
daf-2(e1370)	0.63	0.09	0.99	0.03	1.05	0.05	0.89	0.22	control	control
daf-16(mu86);daf-2	0.76	0.07	0.54	0.03	0.78	0.04	0.69	0.13	0.0377	0.78
daf-16(mg54);daf-2	0.30	0.03	0.33	0.01	0.30	0.02	0.31	0.01	0.0014	0.35
daf-16(tm5030);daf-2	0.62	0.11	0.90	0.05	0.57	0.12	0.70	0.18	0.2679	0.79
daf-16(tm5032);daf-2	0.66	0.10	0.86	0.08	0.56	0.16	0.69	0.15	0.2132	0.78
daf-16(tm6659);daf-2	0.22	0.03	0.24	0.01	0.30	0.07	0.26	0.04	0.0012	0.29
N2 wild-type	1.00	0.14	1.00	0.11	1.00	0.07	1.00	0.00	0.7706	1.12

Table S2 Summary of dauer data and statistics plotted in Fig. 2. Column statistics are calculated from multiple replicates listed in Tables S3 and S4.

		dauer				adult		non-dauer larvae		
# replicates	**genotype**	***p*-value** *vs* control (unpaired *t*-test with Welch's)	**statistically significant**	**mean**	**SD**	**mean**	**SD**	**mean**	**SD**	**N**
3	*daf-2(e1368)*	control	control	92.8	3.1	0.8	1.4	6.4	3.7	807
3	*daf-16(mu86);daf-2*	0.0004	yes	0.0	0.0	100.0	0.0	0.0	0.0	965
6	*daf-16(mg54);daf-2*	0.0004	yes	0.0	0.0	100.0	0.0	0.0	0.0	2318
3	*daf-16(tm5030);daf-2*	0.0004	yes	0.0	0.0	100.0	0.0	0.0	0.0	1280
3	*daf-16(tm5032);daf-2*	0.0004	yes	0.0	0.0	100.0	0.0	0.0	0.0	1338
5	*daf-16(tm6659);daf-2*	0.4342	no	95.3	5.6	1.5	2.6	3.2	3.5	1403
4	N2 wild-type	0.0004	yes	0.0	0.0	100.0	0.0	0.0	0.0	950
2	wild-type sib of *daf-16(tm6659);daf-2*	0.0004	yes	0.0	0.0	100.0	0.0	0.0	0.0	793
2	*daf-16(tm6659)* sib of *daf-16(tm6659);daf-2*	0.0004	yes	0.0	0.0	100.0	0.0	0.0	0.0	448
3	*daf-2* sib of *daf-16(tm6659);daf-2*	0.6300	no	95.1	6.7	4.6	6.2	0.3	0.6	844

		dauer				adult		non-dauer larvae		
# replicates	**genotype**	***p*-value** *vs* control (unpaired *t*-test with Welch's)	**statistically significant**	**mean**	**SD**	**mean**	**SD**	**mean**	**SD**	**N**
6	*daf-2(e1370)*	control	control	100.0	0.0	0.0	0.0	0.0	0.0	1584
5	*daf-16(mu86);daf-2*	***	yes	0.0	0.0	100.0	0.0	0.0	0.0	1469
6	*daf-16(mg54);daf-2*	***	yes	0.0	0.0	100.0	0.0	0.0	0.0	1655
6	*daf-16(tm5030);daf-2* #	0.0204	yes	78.6	15.7	0.1	0.2	21.4	15.7	1339
5	*daf-16(tm5032);daf-2* #	0.0408	yes	76.5	17.6	0.0	0.0	23.5	17.6	1047
3	*daf-16(tm6659);daf-2*	0.4226	no	99.7	0.5	0.0	0.0	0.3	0.5	648
3	N2 wild-type	***	yes	0.0	0.0	100.0	0.0	0.0	0.0	752
2	wild-type sib of *daf-16(tm6659);daf-2*	***	yes	0.0	0.0	100.0	0.0	0.0	0.0	699
1	*daf-16(tm6659)* sib of *daf-16(tm6659);daf-2*	***	yes	0.0	0.0	100.0	0.0	0.0	0.0	289
2	*daf-2* sib of *daf-16(tm6659);daf-2*	^	no	100.0	0.0	0.0	0.0	0.0	0.0	396

*** *p*-value cannot be calculated because SD = 0, but effectively $p < 0.0001$

^ *p*-value cannot be calculated because SD = 0, but effectively $p = 1$

daf-16(tm5030);daf-2(e1370) and *daf-2(tm5032);daf-2(e1370)* non-dauer larvae developed into sterile adults after an additional 48 hours at 25°C

Table S3 ***daf-2(e1368)*** **dauer arrest raw data**. Column statistics are calculated from measurements from three plates per genotype for each replicate.

		dauer			adult		non-dauer larvae		
Replicate	**genotype**	***p*-value** (unpaired, two-tailed *t*-test with Welch's)	**mean**	**SD**	**mean**	**SD**	**mean**	**SD**	**N**
Replicate 1	*daf-2(e1368)*	control	95.1	2.5	0.0	0.0	4.9	2.5	175
Both A and F	*daf-16(mu86);daf-2*	0.0002	0.0	0.0	100.0	0.0	0.0	0.0	244
	daf-16(mg54);daf-2	0.0002	0.0	0.0	100.0	0.0	0.0	0.0	450
	daf-16(tm5030);daf-2	0.0002	0.0	0.0	100.0	0.0	0.0	0.0	314
	daf-16(tm5032);daf-2	0.0002	0.0	0.0	100.0	0.0	0.0	0.0	370
	daf-16(tm6659);daf-2	0.3347	97.4	2.7	0.0	0.0	2.6	2.7	184
	N2 wild-type	0.0002	0.0	0.0	100.0	0.0	0.0	0.0	391
Replicate 2	*daf-2(e1368)*	control	89.3	4.1	0.0	0.0	10.7	4.1	289
Both A and F	*daf-16(mu86);daf-2*	0.0007	0.0	0.0	100.0	0.0	0.0	0.0	425
	daf-16(mg54);daf-2	0.0007	0.0	0.0	100.0	0.0	0.0	0.0	397
	daf-16(tm5030);daf-2	0.0007	0.0	0.0	100.0	0.0	0.0	0.0	318
	daf-16(tm5032);daf-2	0.0007	0.0	0.0	100.0	0.0	0.0	0.0	350
	daf-16(tm6659);daf-2	0.1255	95.0	2.2	0.0	0.0	5.0	2.2	287
	N2 wild-type	0.0007	0.0	0.0	100.0	0.0	0.0	0.0	372
Replicate 3	*daf-2(e1368)*	control	93.9	1.7	2.5	0.9	3.7	2.4	343
A only	*daf-16(mu86);daf-2*	0.0001	0.0	0.0	100.0	0.0	0.0	0.0	296
	daf-16(mg54);daf-2	0.0001	0.0	0.0	100.0	0.0	0.0	0.0	464
	daf-16(tm5030);daf-2	0.0001	0.0	0.0	100.0	0.0	0.0	0.0	648
	daf-16(tm5032);daf-2	0.0001	0.0	0.0	100.0	0.0	0.0	0.0	618
Replicate 4	*daf-2(e1368)* sib of *daf-16(tm6659);daf-2*	control	100.0	0.0	0.0	0.0	0.0	0.0	207
F only	*daf-16(mg54);daf-2*	***	0.0	0.0	100.0	0.0	0.0	0.0	282
	daf-16(tm6659);daf-2	0.4226	99.6	0.8	0.4	0.8	0.0	0.0	252
	daf-16(tm6659) sib of *daf-16(tm6659);daf-2*	***	0.0	0.0	100.0	0.0	0.0	0.0	300
	N2 wild-type	***	0.0	0.0	100.0	0.0	0.0	0.0	98
Replicate 5	*daf-2(e1368)* sib of *daf-16(tm6659);daf-2*	control	97.8	2.9	2.2	2.9	0.0	0.0	224
F only	*daf-16(mg54);daf-2*	0.0003	0.0	0.0	100.0	0.0	0.0	0.0	229
	daf-16(tm6659);daf-2	0.5633	98.9	0.9	1.1	0.9	0.0	0.0	222
	wild-type sib of *daf-16(tm6659);daf-2*	0.0003	0.0	0.0	100.0	0.0	0.0	0.0	354
	N2 wild-type	0.0003	0.0	0.0	100.0	0.0	0.0	0.0	89
Replicate 6	*daf-2(e1368)* sib of *daf-16(tm6659);daf-2*	control	87.4	2.8	11.6	3.2	1.0	0.5	413
F only	*daf-16(mg54);daf-2*	0.0003	0.0	0.0	100.0	0.0	0.0	0.0	496
	daf-16(tm6659);daf-2	0.5099	85.8	2.7	6.0	1.5	8.2	3.9	458
	wild-type sib of *daf-16(tm6659);daf-2*	0.0003	0.0	0.0	100.0	0.0	0.0	0.0	439
	daf-16(tm6659) sib of *daf-16(tm6659);daf-2*	0.0003	0.0	0.0	100.0	0.0	0.0	0.0	418

*** *p*-value cannot be calculated because SD = 0, but effectively $p < 0.0001$

Table S4 ***daf-2(e1370)*** **dauer arrest raw data.** Column statistics are calculated from measurements from three plates per genotype for each replicate.

		dauer			adult		non-dauer larvae		
Replicate	**genotype**	***p*-value** *vs* control (two-tailed, unpaired *t*-test with Welch's)	**mean**	**SD**	**mean**	**SD**	**mean**	**SD**	**N**
Replicate 1	*daf-2(e1370)*	control	100.0	0.0	0.0	0.0	0.0	0.0	321
Both A and F	*daf-16(mu86);daf-2*	***	0.0	0.0	100.0	0.0	0.0	0.0	419
	daf-16(mg54);daf-2	***	0.0	0.0	100.0	0.0	0.0	0.0	465
	daf-16(tm5030);daf-2 #	0.0102	65.4	6.1	0.0	0.0	34.6	6.1	446
	daf-16(tm5032);daf-2 #	0.0032	46.5	5.3	0.0	0.0	53.5	5.3	270
	daf-16(tm6659);daf-2	^	100.0	0.0	0.0	0.0	0.0	0.0	265
	N2 wild-type	***	0.0	0.0	100.0	0.0	0.0	0.0	527
Replicate 2	*daf-2(e1370)*	control	100.0	0.0	0.0	0.0	0.0	0.0	176
Both A and F	*daf-16(mu86);daf-2*	***	0.0	0.0	100.0	0.0	0.0	0.0	173
	daf-16(mg54);daf-2	***	0.0	0.0	100.0	0.0	0.0	0.0	133
	daf-16(tm5030);daf-2 #	0.1884	94.3	5.0	0.0	0.0	5.7	5.0	194
	daf-16(tm5032);daf-2 #	0.1441	93.2	5.1	0.0	0.0	6.8	5.1	186
	daf-16(tm6659);daf-2	^	100.0	0.0	0.0	0.0	0.0	0.0	150
	N2 wild-type	***	0.0	0.0	100.0	0.0	0.0	0.0	120
	wild-type sib of *daf-16(tm6659);daf-2*	***	0.0	0.0	100.0	0.0	0.0	0.0	351
	daf-2 sib of *daf-16(tm6659);daf-2*	^	100.0	0.0	0.0	0.0	0.0	0.0	160
Replicate 3	*daf-2(e1370)*	control	100.0	0.0	0.0	0.0	0.0	0.0	267
Both A and F	*daf-16(mg54);daf-2*	***	0.0	0.0	100.0	0.0	0.0	0.0	171
	daf-16(tm5030);daf-2 #	0.2697	97.3	3.1	0.0	0.0	2.7	3.1	135
	daf-16(tm6659);daf-2	0.1840	99.1	0.8	0.0	0.0	0.9	0.8	233
	N2 wild-type	***	0.0	0.0	100.0	0.0	0.0	0.0	105
	wild-type sib of *daf-16(tm6659);daf-2*	***	0.0	0.0	100.0	0.0	0.0	0.0	348
	daf-16(tm6659) sib of *daf-16(tm6659);daf-2*	***	0.0	0.0	100.0	0.0	0.0	0.0	289
	daf-2 sib of *daf-16(tm6659);daf-2*	^	100.0	0.0	0.0	0.0	0.0	0.0	236
Replicate 4	*daf-2(e1370)*		100.0	0.0	0.0	0.0	0.0	0.0	209
A only	*daf-16(mu86);daf-2*	***	0.0	0.0	100.0	0.0	0.0	0.0	168
	daf-16(mg54);daf-2	***	0.0	0.0	100.0	0.0	0.0	0.0	137
	daf-16(tm5030);daf-2 #	0.0240	59.3	11.1	0.0	0.0	40.7	11.1	87
	daf-16(tm5032);daf-2 #	0.0375	79.5	7.0	0.0	0.0	20.5	7.0	97
Replicate 5	*daf-2(e1370)*	control	100.0	0.0	0.0	0.0	0.0	0.0	286
A ony	*daf-16(mu86);daf-2*	***	0.0	0.0	100.0	0.0	0.0	0.0	264
	daf-16(mg54);daf-2	***	0.0	0.0	100.0	0.0	0.0	0.0	297
	daf-16(tm5030);daf-2 #	0.0130	71.2	5.7	0.0	0.0	28.8	5.7	167
	daf-16(tm5032);daf-2 #	0.0202	82.2	4.4	0.0	0.0	17.8	4.4	185
Replicate 6	*daf-2(e1370)*	control	100.0	0.0	0.0	0.0	0.0	0.0	325
A ony	*daf-16(mu86);daf-2*	***	0.0	0.0	100.0	0.0	0.0	0.0	445
	daf-16(mg54);daf-2	***	0.0	0.0	100.0	0.0	0.0	0.0	488
	daf-16(tm5030);daf-2 #	0.0556	84.0	6.8	0.4	0.6	15.7	6.3	310
	daf-16(tm5032);daf-2 #	<0.0001	81.2	0.1	0.0	0.0	18.8	0.1	309

*** *p*-value cannot be calculated because SD = 0, but effectively $p < 0.0001$

^ *p*-value cannot be calculated because SD = 0, but effectively $p = 1$

daf-16(tm5030);daf-2(e1370) and *daf-2(tm5032);daf-2(e1370)* non-dauer larvae developed into sterile adults after an additional 48 hours at 25°C

Tables S5-S10

Available for download as Excel files at www.genetics.org/lookup/suppl/doi:10.1534/genetics.115.177998/-/DC1

Table S5 *daf-2(e1368)* life span data and statistics for each replicate of Fig. 3A-B
Table S6 *daf-2(e1370)* life span data and statistics for each replicate of Fig. 3C-D
Table S7 Mutant-RNAi combination life span data and statistics for each replicate of Fig. 3E-F and Figure S7
Table S8 MosSCI single-copy transgene life span data and statistics for Fig. 3G-H and S9.
Table S9 *glp-1(e2141)* life span data and statistics for each replicate of Fig. 4A-B
Table S10 Mutant-RNAi combination life span data and statistics for each replicate of Fig. 4C-E

Table S11 Dauer arrest data and statistics for single-copy transgenes

		dauer				
# replicates	genotype	***p*-value** (unpaired *t*-test with Welch's)	compared to	mean	SD	N
3	*daf-2(e1370)*			100.0	0.0	1069
3	*daf-16(mg54);daf-2*			0.0	0.0	932
3	*daf-16(mg54);knuSi263;daf-2*	0.0229	*daf-16(mg54);daf-2*	71.6	19.1	968
3	*daf-16(tm6659);daf-2*	0.1232	*daf-16(mg54);knuSi263);daf-2*	100.0	0.0	884
3	wild-type			0.0	0.0	362

		dauer				
# replicates	genotype	***p*-value** (unpaired *t*-test with Welch's)	compared to	mean	SD	N
3	*daf-2(e1370)*			100.0	0.0	843
3	*daf-16(tm5030);daf-2*			68.9	10.6	887
3	*daf-16(tm5030);knuSi263;daf-2*	0.0372	*daf-16(tm5030);daf-2*	99.6	0.6	869
3	wild-type			0.0	0.0	445

		dauer				
# replicates	genotype	***p*-value** (unpaired *t*-test with Welch's)	compared to	mean	SD	N
3	*daf-2(e1368)*			89.0	5.1	821
3	*daf-16(mg54);daf-2*			0.0	0.0	924
3	*daf-16(mg54);knuSi263;daf-2*	0.4226	*daf-16(mg54);daf-2*	2.4	4.2	928
3	wild-type			0.0	0.0	395

		dauer				
# replicates	genotype	***p*-value** (unpaired *t*-test with Welch's)	compared to	mean	SD	N
3	*daf-2(e1368)*			86.4	8.1	946
3	*daf-16(tm5030);daf-2*			0.0	0.0	902
3	*daf-16(tm5030);knuSi263;daf-2*	0.1410	*daf-16(tm5030);daf-2*	1.4	1.0	860
3	wild-type			0.0	0.0	454

		dauer				
# replicates	genotype	***p*-value** (unpaired *t*-test with Welch's)	compared to	mean	SD	N
3	*daf-2(e1370)*			100.0	0.0	1079
3	*daf-16(mg54);daf-2*			0.0	0.0	1246
3	*daf-16(mg54);knuSi292;daf-2*	0.0008	*daf-16(mg54);daf-2*	87.9	4.4	747
3	*daf-16(tm5030);daf-2*	0.1483	*daf-16(mg54);knuSi292;daf-2*	70.7	13.5	799
3	*daf-16(tm5030);knuSi292;daf-2*	0.0638	*daf-16(tm5030);daf-2*	100.0	0.0	932
3	wild-type			0.0	0.0	312

		dauer				
# replicates	genotype	***p*-value** (unpaired *t*-test with Welch's)	compared to	mean	SD	N
3	*daf-2(e1368)*			92.6	2.7	934
3	*daf-16(mg54);daf-2*			0.0	0.0	1077
3	*daf-16(mg54);knuSi292;daf-2*	^	*daf-16(mg54);daf-2*	0.0	0.0	1048
3	wild-type			0.0	0.0	398

^ *p*-value cannot be calculated because SD = 0, but effectively $p = 1$

Table S12 Stress resistance data and statistics. Plots shown in Fig. S12.

A. Thermotolerance (33°C)

genotype	deaths (cens.)	mean survival (hours)	SD	median survival (hours)	P value (Log-rank)	P value compared to	% change mean	% change median	P value (Log-rank)	P value compared to	% change mean	% change median
Replicate 1												
daf-2(e1370)	40 (22)	30.1	6.3	35.5								
daf-16(mg54);daf-2	57 (3)	19.5	4.4	19	<0.0001	*daf-2(e1370)*	-35	-46	0.0721	N2 wild-type	NS	NS
daf-16(tm5030);daf-2	58 (3)	24.4	3.1	24	<0.0001	*daf-2(e1370)*	-19	-32	0.5459	*daf-16(tm5032);daf-2*	NS	NS
daf-16(tm5032);daf-2	60 (1)	24.8	4.1	24	<0.0001	*daf-2(e1370)*	-18	-32				
daf-16(tm6659);daf-2	49 (8)	31.2	6.2	35.5	0.9993	*daf-2(e1370)*	NS	NS				
N2 wild-type	57 (3)	18.5	3.4	19	<0.0001	*daf-2(e1370)*	-39	-46				
Replicate 2												
daf-2(e1370)	55 (6)	34.0	5.4	34.5								
daf-16(mg54);daf-2	60 (0)	20.7	2.8	22	<0.0001	*daf-2(e1370)*	-39	-36	0.8421	N2 wild-type		
daf-16(tm5030);daf-2	58 (1)	24.6	5.6	22	<0.0001	*daf-2(e1370)*	-28	-36	0.0001	*daf-16(tm5032);daf-2*	-15	-15
daf-16(tm5032);daf-2	58 (2)	28.9	5.6	26	<0.0001	*daf-2(e1370)*	-15	-25				
daf-16(tm6659);daf-2	50 (1)	35.1	4.6	34.5	0.4300	*daf-2(e1370)*	NS	NS				
N2 wild-type	54 (2)	20.5	2.4	22	<0.0001	*daf-2(e1370)*	-40	-36				
Replicate 3												
daf-2(e1370)	44 (1)	30.2	4.6	33.5								
daf-16(mg54);daf-2	44 (0)	18.0	2.4	19	<0.0001	*daf-2(e1370)*	-40	-43	0.0118	N2 wild-type	-9	0
daf-16(tm5030);daf-2	52 (1)	24.1	3.5	25	<0.0001	*daf-2(e1370)*	-20	-25				
daf-16(tm6659);daf-2	41 (2)	31.5	6.1	33.5	0.1278	*daf-2(e1370)*	NS	NS				
N2 wild-type	45 (0)	19.7	3.7	19	<0.0001	*daf-2(e1370)*	-35	-43				

B. Oxidative stress (*t*-BOOH)

genotype	deaths (cens.)	mean survival (hours)	SD	median survival (hours)	P value (Log-rank)	P value compared to	% change mean	% change median	P value (Log-rank)	P value compared to	% change mean	% change median
Replicate 1												
daf-2(e1370)	58 (1)	53.7	8.2	54								
daf-16(mg54);daf-2	60 (0)	23.3	5.5	27	<0.0001	*daf-2(e1370)*	-57	-50	0.0163	N2 wild-type	+14	+64
daf-16(tm5030);daf-2	59 (1)	41.9	12.2	41	<0.0001	*daf-2(e1370)*	-22	-24	<0.0001	*daf-16(tm5032);daf-2*	+21	+24
daf-16(tm5032);daf-2	60 (0)	34.6	11.3	33	<0.0001	*daf-2(e1370)*	-36	-39				
daf-16(tm6659);daf-2	54 (3)	54.1	7.5	54	0.9578	*daf-2(e1370)*	NS	NS				
N2 wild-type	60 (0)	20.4	6.7	16.5	<0.0001	*daf-2(e1370)*	-62	-69				
Replicate 2												
daf-2(e1370)	59 (0)	49.8	4.9	47								
daf-16(mg54);daf-2	56 (2)	15.8	6.7	12.5	<0.0001	*daf-2(e1370)*	-68	-73	0.0705	N2 wild-type	NS	NS
daf-16(tm5030);daf-2	57 (1)	36.1	9.9	38	<0.0001	*daf-2(e1370)*	-28	-19	0.0001	*daf-16(tm5032);daf-2*	+19	+25
daf-16(tm5032);daf-2	60 (0)	30.3	7.9	30.5	<0.0001	*daf-2(e1370)*	-39	-35				
daf-16(tm6659);daf-2	59 (0)	55.2	7.8	59	<0.0001	*daf-2(e1370)*	+11	+26				
N2 wild-type	57 (2)	18.0	6.7	22.5	<0.0001	*daf-2(e1370)*	-64	-52				
Replicate 3												
daf-2(e1370)	48 (11)	49.9	13.9	48								
daf-16(mg54);daf-2	60 (0)	16.9	5.2	12.5	<0.0001	*daf-2(e1370)*	-66	-74	0.0289	N2 wild-type	-7	-46
daf-16(tm5030);daf-2	46 (10)	35.9	12.0	32	<0.0001	*daf-2(e1370)*	-28	-33				
daf-16(tm6659);daf-2	57 (3)	46.5	16.3	48	0.4865	*daf-2(e1370)*	NS	NS				
N2 wild-type	49 (8)	18.2	5.9	23	<0.0001	*daf-2(e1370)*	-64	-52				

C. UV stress

genotype	deaths (cens.)	mean survival (hours)	SD	median survival (hours)	P value (Log-rank)	P value compared to	% change mean	% change median	P value (Log-rank)	P value compared to	% change mean	% change median
Replicate 1												
daf-2(e1370)	55 (2)	197.1	68.4	202								
daf-16(mg54);daf-2	60 (0)	116.2	39.3	105	<0.0001	*daf-2(e1370)*	-41	-48	<0.0001	N2 wild-type	+23	+28
daf-16(tm5030);daf-2	59 (0)	165.8	60.6	156	0.0069	*daf-2(e1370)*	-16	-23	0.0600	*daf-16(tm5032);daf-2*	NS	NS
daf-16(tm5032);daf-2	55 (1)	158.1	39.6	156	<0.0001	*daf-2(e1370)*	-20	-23				
daf-16(tm6659);daf-2	58 (0)	188.5	70.1	175	0.6215	*daf-2(e1370)*	NS	NS				
N2 wild-type	57 (0)	94.6	21.5	82	<0.0001	*daf-2(e1370)*	-52	-59				
Replicate 2												
daf-2(e1370)	55 (4)	196.7	57.5	179								
daf-16(mg54);daf-2	52 (1)	119.3	32.6	126	<0.0001	*daf-2(e1370)*	-39	-30	<0.0001	N2 wild-type	+31	+42
daf-16(tm5030);daf-2	53 (2)	167.4	44.9	155	0.0010	*daf-2(e1370)*	-15	-13	0.0620	*daf-16(tm5032);daf-2*	NS	NS
daf-16(tm5032);daf-2	57 (1)	150.2	44.0	155	<0.0001	*daf-2(e1370)*	-24	-13				
daf-16(tm6659);daf-2	56 (1)	190.3	58.9	179	0.5871	*daf-2(e1370)*	NS	NS				
N2 wild-type	54 (2)	91.3	20.9	89	<0.0001	*daf-2(e1370)*	-54	-50				
Replicate 3												
daf-2(e1370)	61 (0)	250.2	76.4	248								
daf-16(mg54);daf-2	59 (0)	126.9	36.6	128	<0.0001	*daf-2(e1370)*	-49	-48	<0.0001	N2 wild-type	+46	+38
daf-16(tm5030);daf-2	62 (0)	194.0	74.7	200	<0.0001	*daf-2(e1370)*	-22	-19				
daf-16(tm6659);daf-2	60 (0)	171.0	62.6	175	<0.0001	*daf-2(e1370)*	-32	-29				
N2 wild-type	58 (0)	86.9	36.6	93	<0.0001	*daf-2(e1370)*	-65	-63				

Table S13 Complete list of DAF-16A/F target genes organized by class.

Available for download as an Excel file at www.genetics.org/lookup/suppl/doi:10.1534/genetics.115.177998/-/DC1

Table S14 qPCR data and statistics for Fig. 6 and Fig. S13. Mean and standard error of the mean for each cohort is calculated based on triplicate measurements. Mean and standard deviation overall is calculated based on means of three biological replicates.

	Independent cohorts						Statistical Analysis			
	1		2		3				P value (ratio paired t-test)	Fold change
	Mean	SEM	Mean	SEM	Mean	SEM	Mean	SD		
C08E8.10										
daf-2(e1370)	17.88	1.05	10.93	1.21	2.81	0.10	10.54	7.54	control	control
daf-16(mu86);daf-2	4.82	0.27	2.36	0.17	1.13	0.09	2.77	1.88	0.0207	0.263
daf-16(mg54);daf-2	4.32	0.48	1.83	0.38	1.67	0.07	2.60	1.48	0.0809	0.247
daf-16(tm5030);daf-2	4.89	0.20	2.91	0.56	1.57	0.09	3.12	1.67	0.0480	0.296
daf-16(tm5032);daf-2	5.39	0.33	2.10	0.24	2.08	0.11	3.19	1.90	0.1185	0.303
daf-16(tm6659);daf-2	19.70	1.59	14.12	1.72	3.25	0.08	12.36	8.37	0.0719	1.173
N2 wild-type	1.00	0.17	1.00	0.14	1.00	0.08	1.00	0.00	0.0628	0.095
dod-17										
daf-2(e1370)	0.40	0.20	0.31	0.05	0.28	0.04	0.33	0.06	control	control
daf-16(mu86);daf-2	2.01	0.72	3.36	0.49	5.17	0.65	3.52	1.58	0.0200	10.660
daf-16(mg54);daf-2	2.91	1.01	2.22	0.47	4.47	0.57	3.20	1.15	0.0092	9.699
daf-16(tm5030);daf-2	0.62	0.17	0.67	0.12	0.77	0.07	0.69	0.07	0.9712	2.084
daf-16(tm5032);daf-2	0.42	0.07	0.44	0.11	0.58	0.08	0.48	0.09	0.5286	1.453
daf-16(tm6659);daf-2	0.33	0.07	0.57	0.16	0.32	0.05	0.41	0.14	0.9818	1.232
N2 wild-type	1.00	0.43	1.00	0.14	1.00	0.17	1.00	0.00	0.0053	3.032
far-3										
daf-2(e1370)	2.16	0.21	5.28	0.91	4.20	0.66	3.88	1.58	control	control
daf-16(mu86);daf-2	0.44	0.05	0.35	0.05	0.41	0.07	0.40	0.05	0.0215	0.104
daf-16(mg54);daf-2	0.43	0.06	0.76	0.04	0.54	0.08	0.57	0.17	0.0050	0.148
daf-16(tm5030);daf-2	0.38	0.05	0.82	0.09	0.46	0.00	0.55	0.23	0.0055	0.143
daf-16(tm5032);daf-2	0.59	0.17	1.07	0.09	0.78	0.11	0.81	0.24	0.0056	0.209
daf-16(tm6659);daf-2	2.35	0.27	5.58	0.54	3.68	0.40	3.87	1.62	0.9758	0.997
N2 wild-type	1.00	0.16	1.00	0.18	1.00	0.21	1.00	0.00	0.0407	0.258
fat-7										
daf-2(e1370)	0.13	0.04	0.15	0.01	0.15	0.00	0.14	0.01	control	control
daf-16(mu86);daf-2	0.82	0.22	0.81	0.02	0.73	0.03	0.79	0.05	0.0023	5.597
daf-16(mg54);daf-2	0.63	0.19	0.69	0.01	0.49	0.02	0.60	0.10	0.0075	4.289
daf-16(tm5030);daf-2	0.23	0.07	0.29	0.05	0.40	0.00	0.31	0.09	0.0258	2.174
daf-16(tm5032);daf-2	0.26	0.08	0.26	0.02	0.44	0.03	0.32	0.10	0.0377	2.260
daf-16(tm6659);daf-2	0.09	0.02	0.17	0.02	0.14	0.01	0.13	0.04	0.6365	0.955
N2 wild-type	1.00	0.32	1.00	0.05	1.00	0.06	1.00	0.00	0.0008	7.107
gst-20										
daf-2(e1370)	2.35	0.21	5.03	0.57	3.10	0.27	3.49	1.38	control	control
daf-16(mu86);daf-2	1.39	0.08	1.24	0.09	0.89	0.06	1.17	0.26	0.0591	0.336
daf-16(mg54);daf-2	1.09	0.06	1.62	0.09	0.90	0.04	1.20	0.38	0.0177	0.345
daf-16(tm5030);daf-2	1.65	0.12	2.04	0.20	1.48	0.16	1.72	0.29	0.0549	0.494
daf-16(tm5032);daf-2	1.49	0.08	1.69	0.11	1.25	0.06	1.48	0.22	0.0501	0.424
daf-16(tm6659);daf-2	3.76	0.20	4.86	0.12	2.97	0.29	3.86	0.95	0.5192	1.107
N2 wild-type	1.00	0.09	1.00	0.12	1.00	0.05	1.00	0.00	0.0328	0.287

Table S14 (continued)

	Independent cohorts						Statistical Analysis			
	1		2		3				P value (ratio paired t-test)	Fold change
	Mean	SEM	Mean	SEM	Mean	SEM	Mean	SD		
hen-1										
daf-2(e1370)	14.72	3.18	23.26	2.91	32.22	7.47	23.40	8.75	control	control
daf-16(mu86);daf-2	1.06	0.22	0.43	0.06	2.22	0.46	1.24	0.91	0.0200	0.053
daf-16(mg54);daf-2	0.72	0.18	0.58	0.05	2.25	0.85	1.18	0.93	0.0092	0.051
daf-16(tm5030);daf-2	17.39	2.36	43.11	8.19	15.45	5.37	25.32	15.44	0.9712	1.082
daf-16(tm5032);daf-2	19.97	3.35	42.81	3.45	23.75	2.81	28.85	12.24	0.5286	1.233
daf-16(tm6659);daf-2	14.22	1.68	32.45	3.29	24.25	2.63	23.64	9.13	0.9818	1.010
N2 wild-type	1.00	0.15	1.00	0.18	1.00	0.34	1.00	0.00	0.0053	0.043
lea-1										
daf-2(e1370)	6.77	0.57	8.51	1.51	8.46	2.15	7.92	0.99	control	control
daf-16(mu86);daf-2	0.57	0.04	0.43	0.13	0.55	0.06	0.52	0.08	0.0029	0.066
daf-16(mg54);daf-2	0.54	0.04	0.54	0.12	0.56	0.10	0.54	0.02	0.0006	0.069
daf-16(tm5030);daf-2	6.50	0.42	10.34	2.70	6.02	0.40	7.62	2.37	0.7266	0.963
daf-16(tm5032);daf-2	7.01	0.66	8.88	1.91	6.96	0.77	7.62	1.09	0.6655	0.962
daf-16(tm6659);daf-2	0.68	0.05	0.70	0.22	0.87	0.19	0.75	0.11	0.0009	0.095
N2 wild-type	1.00	0.04	1.00	0.21	1.00	0.24	1.00	0.00	0.0013	0.126
lipl-2										
daf-2(e1370)	58.49	7.04	38.59	8.36	25.99	10.70	41.02	16.38	control	control
daf-16(mu86);daf-2	3.53	0.65	1.69	0.38	1.55	0.20	2.26	1.11	0.0013	0.055
daf-16(mg54);daf-2	2.57	0.32	1.12	0.27	1.83	0.53	1.84	0.72	0.0067	0.045
daf-16(tm5030);daf-2	17.75	1.14	15.89	3.01	13.27	1.71	15.64	2.25	0.0260	0.381
daf-16(tm5032);daf-2	18.38	1.74	16.11	2.40	10.85	3.10	15.11	3.86	0.0094	0.368
daf-16(tm6659);daf-2	50.21	6.19	41.50	10.08	27.67	7.90	39.79	11.37	0.9442	0.970
N2 wild-type	1.00	0.08	1.00	0.45	1.00	0.22	1.00	0.00	0.0041	0.024
lys-7										
daf-2(e1370)	30.70	14.42	3.27	0.78	11.63	1.06	15.20	14.06	control	control
daf-16(mu86);daf-2	2.25	1.32	0.76	0.07	1.09	0.13	1.37	0.78	0.0262	0.090
daf-16(mg54);daf-2	2.20	0.96	0.63	0.18	1.03	0.18	1.29	0.82	0.0213	0.085
daf-16(tm5030);daf-2	10.13	4.35	8.69	1.75	7.78	1.00	8.87	1.18	0.9199	0.583
daf-16(tm5032);daf-2	11.24	5.17	7.11	1.17	8.63	0.89	8.99	2.09	0.8731	0.592
daf-16(tm6659);daf-2	11.71	4.65	11.63	4.00	7.36	1.00	10.24	2.49	0.9438	0.673
N2 wild-type	1.00	0.56	1.00	0.12	1.00	0.13	1.00	0.00	0.0369	0.066
mtl-1										
daf-2(e1370)	23.59	6.28	28.25	0.01	28.64	1.59	26.83	2.81	control	control
daf-16(mu86);daf-2	0.35	0.10	0.31	0.02	0.09	0.01	0.25	0.14	0.0092	0.009
daf-16(mg54);daf-2	0.28	0.08	0.68	0.01	0.14	0.02	0.37	0.28	0.0104	0.014
daf-16(tm5030);daf-2	4.89	0.97	15.03	0.05	5.62	0.46	8.51	5.66	0.0587	0.317
daf-16(tm5032);daf-2	5.31	1.12	12.64	0.02	5.86	0.57	7.94	4.08	0.0344	0.296
daf-16(tm6659);daf-2	12.73	2.32	27.28	0.02	13.83	1.35	17.95	8.10	0.1658	0.669
N2 wild-type	1.00	0.30	1.00	0.05	1.00	0.08	1.00	0.00	0.0004	0.037

Table S14 (continued)

	Independent cohorts						Statistical Analysis			
	1		2		3				P value (ratio paired t-test)	Fold change
	Mean	SEM	Mean	SEM	Mean	SEM	Mean	SD		
sod-3										
daf-2(e1370)	22.94	4.39	14.52	2.91	24.08	2.51	20.52	5.22	control	control
daf-16(mu86);daf-2	0.47	0.09	0.55	0.06	0.65	0.07	0.56	0.09	0.0024	0.027
daf-16(mg54);daf-2	1.25	0.21	1.60	0.05	1.92	0.22	1.59	0.34	0.0064	0.077
daf-16(tm5030);daf-2	4.86	0.75	5.03	8.19	7.89	1.17	5.92	1.70	0.0153	0.289
daf-16(tm5032);daf-2	4.47	0.85	3.51	3.45	6.23	0.83	4.74	1.38	0.0034	0.231
daf-16(tm6659);daf-2	19.70	2.53	26.35	3.29	23.10	4.15	23.05	3.33	0.6236	1.124
N2 wild-type	1.00	0.20	1.00	0.18	1.00	0.13	1.00	0.00	0.0029	0.049
sams-5										
daf-2(e1370)	14.03	2.41	5.58	0.91	5.66	0.44	8.42	4.85	control	control
daf-16(mu86);daf-2	1.91	0.39	4.23	0.05	2.30	0.14	2.81	1.24	0.1698	0.334
daf-16(mg54);daf-2	2.62	0.50	2.38	0.04	2.27	0.17	2.42	0.18	0.0494	0.288
daf-16(tm5030);daf-2	6.28	0.96	3.36	0.09	7.84	0.47	5.83	2.27	0.4342	0.692
daf-16(tm5032);daf-2	5.90	1.23	1.64	0.09	6.06	0.47	4.53	2.51	0.2228	0.538
daf-16(tm6659);daf-2	2.14	0.31	2.55	0.54	1.38	0.27	2.02	0.60	0.0505	0.240
N2 wild-type	1.00	0.10	1.00	0.18	1.00	0.10	1.00	0.00	0.0218	0.119
scl-20										
daf-2(e1370)	512.00	97.88	229.13	0.01	198.09	23.47	313.07	172.97	control	control
daf-16(mu86);daf-2	0.85	0.13	0.17	0.02	0.28	0.01	0.43	0.36	0.0013	0.001
daf-16(mg54);daf-2	0.59	0.09	0.35	0.01	0.43	0.02	0.46	0.12	0.0008	0.001
daf-16(tm5030);daf-2	1.38	0.63	0.71	0.05	0.66	0.40	0.91	0.40	0.0001	0.003
daf-16(tm5032);daf-2	1.48	0.92	0.81	0.02	1.35	0.36	1.21	0.36	0.0022	0.004
daf-16(tm6659);daf-2	240.52	86.64	340.14	0.02	151.17	25.34	243.94	94.53	0.5928	0.779
N2 wild-type	1.00	0.09	1.00	0.05	1.00	0.02	1.00	0.00	0.0027	0.003
srr-4										
daf-2(e1370)	0.47	0.03	0.68	0.08	0.37	0.05	0.51	0.16	control	control
daf-16(mu86);daf-2	2.10	0.09	3.20	0.21	2.38	0.10	2.56	0.57	0.0047	5.041
daf-16(mg54);daf-2	1.75	0.04	2.57	0.13	2.53	0.08	2.28	0.46	0.0168	4.496
daf-16(tm5030);daf-2	1.87	0.08	2.31	0.20	2.33	0.09	2.17	0.26	0.0153	4.271
daf-16(tm5032);daf-2	1.73	0.07	1.88	0.17	1.67	0.11	1.76	0.11	0.0124	3.464
daf-16(tm6659);daf-2	0.50	0.06	0.69	0.07	0.31	0.03	0.50	0.19	0.6967	0.987
N2 wild-type	1.00	0.10	1.00	0.06	1.00	0.13	1.00	0.00	0.0573	1.969
ttr-23										
daf-2(e1370)	27.28	2.40	11.08	2.91	4.72	1.44	14.36	11.63	control	control
daf-16(mu86);daf-2	2.99	0.93	1.49	0.06	1.26	0.23	1.91	0.94	0.0204	0.133
daf-16(mg54);daf-2	3.10	0.22	1.09	0.05	1.72	0.30	1.97	1.02	0.0472	0.137
daf-16(tm5030);daf-2	9.99	1.10	5.94	8.19	4.20	0.67	6.71	2.97	0.1517	0.467
daf-16(tm5032);daf-2	9.65	0.75	8.11	3.45	3.78	0.35	7.18	3.04	0.1801	0.500
daf-16(tm6659);daf-2	12.21	1.33	16.22	3.29	2.41	0.40	10.28	7.10	0.4331	0.716
N2 wild-type	1.00	0.54	1.00	0.18	1.00	0.33	1.00	0.00	0.0410	0.070

Table S15 Output from LRpath and REVIGO used to generate plots in Fig. S14.

Available for download as an Excel file at www.genetics.org/lookup/suppl/doi:10.1534/genetics.115.177998/-/DC1

Table S16 Comparison of A- and F-indices calculated from qPCR and RNA-seq data. Indices are calculated from mean gene expression values (qPCR) or from FPKM gene expression values (RNA-seq) as described in Methods.

	A-Index		F-Index		
gene	**qPCR**	**RNA-seq**	**qPCR**	**RNA-seq**	**Class**
C08E8.10	0.93	0.88	-0.23	-0.21	A-specific
far-3	0.97	0.94	0.00	-0.14	A-specific
gst-20	0.83	0.85	-0.16	0.04	A-specific
scl-20	1.00	0.99	0.22	-0.10	A-specific
srr-4	0.82	0.88	0.00	-0.03	A-specific
lea-1	0.04	-0.18	0.97	1.00	F-specific
dod-17	0.09	0.13	0.03	0.05	Redundant
hen-1	-0.17	-0.21	-0.01	0.10	Redundant
lys-7	0.15	-0.03	0.00	-0.12	Redundant
mtl-1	0.70	0.61	0.34	0.23	Redundant
fat-7	0.37	0.36	-0.01	0.03	Shared A>F
lipl-2	0.65	0.58	0.03	-0.05	Shared A>F
sod-3	0.80	0.79	-0.13	-0.21	Shared A>F
sams-5	0.54	0.22	1.07	1.10	Shared F>A
ttr-23	0.60	0.49	0.33	0.36	Shared A=F

Table S17 List of DAF-16A-specific and redundant genes screened.

gene	allele	Isoform Class	Up/down class
acdh-2	*gk143151*	A-specific	2
C08E8.10	*gk356583*	A-specific	1
clec-190	*gk746445*	A-specific	2
cpg-7	*ok3141*	A-specific	1
F26A1.8	*gk639772*	A-specific	1
glt-5	*bz70*	A-specific	1
gst-20	*gk604858*	A-specific	1
K02E11.7	*ok3588*	A-specific	2
lipl-1	*gk832360*	A-specific	1
oac-5	*gk398429*	A-specific	2
pho-7	*gk658979*	A-specific	2
R06F6.7	*gk153756*	A-specific	2
sodh-1	*ok2799*	A-specific	1
sprr-2	*ok3290*	A-specific	2
srp-3	*ok1433*	A-specific	1
srr-4	*gk779731*	A-specific	2
ugt-11	*gk497718*	A-specific	1
ugt-32	*gk231667*	A-specific	2
ZC196.2	*gk242000*	A-specific	1
ctl-3	*ok2042*	F-specific	1
rgs-10	*ok1039*	F-specific	1
C07A4.2	*gk820370*	redundant	1
cth-1	*ok3319*	redundant	2
cyp-34A10	*gk761632*	redundant	1
F26C11.1	*gk635549*	redundant	2
hen-1	*tm501*	redundant	1
icl-1	*gk225172*	redundant	1
K08D10.14	*ok2976*	redundant	2
lips-5	*gk793539*	redundant	1
lys-7	*gk230857*	redundant	1

Table S18 Life span data and statistics for DAF-16A-specific and redundant target genes.

Available for download as an Excel file at www.genetics.org/lookup/suppl/doi:10.1534/genetics.115.177998/-/DC1

Table S19 Background mutations in whole-genome sequenced strains with life span phenotypes. Nonsense, splicing, indel, start ATG, and readthrough background mutations were identified using the Million Mutation Project website: (http://genome.sfu.ca/mmp/search.html).

Strain	VC40376		Prior evidence for life span effect	
sequence	gene	mutation type	GO term	Phenotype
Y48E1B.10	**gst-20**	**nonsense**	**no**	**no**
Y48E1B.10	**gst-20**	**nonsense**	**no**	**no**
C27A12.7a	C27A12.7	nonsense	no	no
F07G6.9	F07G6.9	nonsense	no	no
F37D6.3	F37D6.3	nonsense	no	no
W02D7.2	clec-218	nonsense	no	no
Y57A10B.3	btb-14	nonsense	no	no
Y41D4B.9	nhr-122	deletion, frame shift	no	no
R17.3	R17.3	readthrough	no	no
Strain	VC40724		Prior evidence for life span effect	
sequence	gene	mutation type	GO term	Phenotype
K11D12.3a	**srr-4**	**nonsense**	**no**	**no**
F07H5.8	F07H5.8	nonsense	no	no
F12E12.9	fbxb-92	nonsense	no	no
C11E4.6	C11E4.6	intron, splicing	no	no
F33H12.7	F33H12.7	intron, splicing	no	no
T07C12.12	T07C12.12	intron, splicing	no	no
Y75B8A.33	Y75B8A.33	intron, splicing	no	yes*
Y81B9A.2	Y81B9A.2	intron, splicing	no	no
Strain	VC20616		Prior evidence for life span effect	
sequence	gene	mutation type	GO term	Phenotype
C08E8.10	**C08E8.10**	**nonsense**	**no**	**no**
F13H8.8	F13H8.8	nonsense	no	no
W03D8.1	W03D8.1	nonsense	no	no
Y48G9A.10	cpt-3	nonsense	no	no
Y5H2A.4	Y5H2A.4	nonsense	no	yes
T20G5.13	T20G5.13	deletion, frame shift	no	yes
F26G1.6	nep-12	deletion, frame shift	no	no
F20D1.8	cutl-3	intron, splicing	no	no
F25B4.2	F25B4.2	intron, splicing	no	no
T01H8.1	rskn-1	intron, splicing	no	no

* Examination of Y75B8A.33 locus predicts this mutation is likely to preserve function. Other phenotypes caused by Y75B8A.33 inactivation (food avoidance, sterility, and slow growth) were not observed in this strain.

Table S20 Strains used and generated in this study. Double mutant strains and siblings were constructed using standard genetic techniques.

Strain	Genotype	Outcross	Reference
N2 Bristol	wild-type		
DR1572	*daf-2(e1368)* III	6X	Kimura 1997
CB1370	*daf-2(e1370)* III	6X	Kimura 1997
CB4037	*glp-1(e2141)* III	6X	Priess 1987
CF1038	*daf-16(mu86)* I	6X	Lin 1997
GR1308	*daf-16(mg54)* I	6X	Ogg 1997
BQ63	*daf-16(tm5030)* I	6X	This study
BQ64	*daf-16(tm5032)* I	6X	This study
BQ65	*daf-16(tm6659)* I	6X	This study
COP308	*knuSi263[Pdaf-16a::DAF-16A, cb-unc-119(+)]* II	6X	This study
COP339	*knuSi292[Pdaf-16f::DAF-16F, cb-unc-119(+)]* II	6X	This study

Table S21 Primers for RACE, qPCR, RNAi cloning, and construction of MosSCI transgenes (continued on next two pages).

RACE and cDNA sequencing primers			
Target	**Primer name**	**Primer sequence (5' to 3')**	**Reference**
daf-16a/d/f/h	A/F-RACE	TGGCGATTCGGACATTCTG	This study
daf-16a	A-RACE	AGGTCAGCATCTTCTTCAGGAA	This study
daf-16d/f/h	F-RACE	TGTTGATGGAGGTCGAGATTGA	This study
daf-16a, d/f/h	Abridged Anchor	GGCCACGCGTCGACTAGTACGGGIIGGGIIG GGIIG	Invitrogen cat. #18374-058
Pdaf-16f::daf-16a	AF-Junction-For	CCGCTACCATCTGACATCAC	This study
Pdaf-16f::daf-16a	AF-Junction-Rev	CCAGCATCTCCATCATAACGTC	This study
qPCR primers for *daf-16/FoxO* isoforms			
Target	**Primer name**	**Primer sequence (5' to 3')**	**Reference**
daf-16	pan-qPCR1_For	AAAGAGCTCGTGGTGGGTTA	This study
daf-16	pan-qPCR1_Rev	TTCGAGTTGAGCTTTGTAGTCG	This study
daf-16	pan-qPCR2_For	AAGCCGATTAAGACGGAACC	Bansal *et al* 2014
daf-16	pan-qPCR2_Rev	GTAGTGGCATTGGCTTGAAG	Bansal *et al* 2014
daf-16a	A30-qPCR_For	TGAAGAAGATGCTGACCTA	This study
daf-16a	A32-qPCR_For	TGAATGATGATATGGAACCG	This study
daf-16d/f/h	F-qPCR_For	TTGACAGCGGAAGAACTA	This study
daf-16a, *d/f/h*	AF-qPCR_Rev	ATCTGGAGTATGAAGCATTG	This study
daf-16b	B-qPCR_For	TCGGATATCATTGCCAAAGC	This study
daf-16b	B-qPCR_Rev	TGACGGATCGAGTTCTTCCAT	This study
qPCR primers for *daf-16/FoxO* target genes			
Target	**Primer name**	**Primer sequence (5' to 3')**	**Reference**
act-1	act-1_Rev	TGGAGAGGGAAGCGAGGATAGA	Alam *et al* 2010
act-1	act-1_For	CCAGGAATTGCTGATCGTATGCAGAA	Alam *et al* 2010
C08E8.10	C08E8.10_Rev	GTTTGGATTGGGCTCACTC	Gubelmann *et al* 2011
C08E8.10	C08E8.10_For	CATCAGCCTGTAATTCTGGAG	Gubelmann *et al* 2011
dod-17	dod-17_Rev	GTTAGCGACAGTGAGTGTG	Gubelmann *et al* 2011
dod-17	dod-17_For	CAGGAAATCTTATTCGGACTACTC	Gubelmann *et al* 2011
far-3	far-3_Rev	AGCAACTTGGGTTTCAATGAG	Gubelmann *et al* 2011
far-3	far-3_For	ACGTGGTCTTTATGCTCGT	Gubelmann *et al* 2011
fat-7	fat-7_Rev	GGGAAATAGTGCTTTCTCTGG	Gubelmann *et al* 2011
fat-7	fat-7_For	AGTTAAGGAGCATGGAGGC	Gubelmann *et al* 2011
gst-20	gst-20_Rev	TTTGGAGTCCCGAACTGAG	Gubelmann *et al* 2011
gst-20	gst-20_For	TTCTAGACAGCTCTTCGCC	Gubelmann *et al* 2011
hen-1	hen-1_Rev	AATCAGCCAGTTTGATACATGG	Gubelmann *et al* 2011
hen-1	hen-1_For	GTCATGGCAACAAGTACATACC	Gubelmann *et al* 2011
lea-1	lea-1_Rev	CCTTGTCCTTGGTCTTGTC	Gubelmann *et al* 2011
lea-1	lea-1_For	ATGTAGAGAACAAAGCAGCAG	Gubelmann *et al* 2011

lipl-2	lipl-2_Rev	AAACGAAAGCTGCACTCTG	Gubelmann *et al* 2011
lipl-2	lipl-2_For	GTTACATGGCCAAATGGGA	Gubelmann *et al* 2011
lys-7	lys-7_Rev	TTAATCCGGATTGTCTGGC	Gubelmann *et al* 2011
lys-7	lys-7_For	CAACTAACTGGCCAAATAACG	Gubelmann *et al* 2011
mtl-1	mtl-1_For	ATGGCTTGCAAGTGTGACTG	Alam *et al* 2010
mtl-1	mtl-1_Rev	CACATTTGTCTCCGCACTTG	Alam *et al* 2010
sams-5	sams-5_Rev	CTTATCCACATGAACTCCAGC	Gubelmann *et al* 2011
sams-5	sams-5_For	CTCGAAAGGATTTGACTACAAGAC	Gubelmann *et al* 2011
scl-20	scl-20_Rev	ACTCTTGGTTCTTCCATCCG	Gubelmann *et al* 2011
scl-20	scl-20_For	GTTCGCTGGATAAATATGCCC	Gubelmann *et al* 2011
sod-3	sod-3_Rev	CGTGCTCCCAAACGTCAATTCCAA	Alam *et al* 2010
sod-3	sod-3_For	TATTAAGCGCGACTTCGGTTCCCT	Alam *et al* 2010
srr-4	srr-4_Rev	TTTCTATGGTCCGCGAGAC	Gubelmann *et al* 2011
srr-4	srr-4_For	TTACAGTGGGATCCTTAAGCT	Gubelmann *et al* 2011
ttr-23	ttr-23_For	CTGCAATCATTACGGTATGTG	Gubelmann *et al* 2011
ttr-23	ttr-23_Rev	TCGTAGTTGTCTACTCCGA	Gubelmann *et al* 2011
RNAi cloning			
Target	**Primer name**	**Primer sequence (5' to 3')**	**Reference**
daf-16a	16C RNAi 5	AACTGAAGCTTCTGGACATCTAC	Kwon *et al* 2010
daf-16a	16C RNAi 3	TATAGGCTAGCATCTTCTTCAG	Kwon *et al* 2010
daf-16d/f/h	16D RNAi 5	AACTGAAGCTTGATTCGCCGCTACC	Kwon *et al* 2010
daf-16d/f/h	16D RNAi 3	CCCGTGCTAGCTAGTTCTTCCGC	Kwon *et al* 2010
daf-16	16ACD RNAi 5	ATCTGAAGCTTCATTCTCGTTTC	Kwon *et al* 2010
daf-16	16ACD RNAi 3	CTTGACTCGCTAGCTGTCTGATC	Kwon *et al* 2010
Construction of MosSCI single-copy *daf-16* transgenes			
***daf-16* element**	**Primer name**	**Primer sequence (5' to 3')**	**Notes**
daf-16a cDNA	daf-16a cDNA 5	ATGATGGAGATGCTGGTAGATC	Amplified from yk13f11/yk1006c10, then cloned into pCFJ151. Only exons common to *daf-16a* and *f* were later cloned into both pNU164 and 191
	daf-16a cDNA 3	GAAGAGAATTTACAAATCAAAATG	
daf-16 3'UTR	daf-16a 3UTR 5	CATTTTGATTTGTAAATTCTCTTC	Amplified from wild-type genomic DNA and cloned into pCFJ151
	daf-16a 3UTR 3	GCGCCCTGCAGGATTCAAATTTGATTTTTA TTAAATC	
daf-16a promoter	164-prom_For	CTTAAGGCCTTGACTAGAGGGTACCAGAG CTCACCTAGGTCTCGGGAGAGAGGGACA	Amplified from wild-type genomic DNA and cloned into pNU164
	164-prom_Rev	ATTGCACCGATCACGAGGA	
daf-16a 5' ORF	164-5ORF_For	CCGATTCCTCGTGATCGGTGCAATACGTG GCCAATGCGTAGGC	Amplified from wild-type genomic DNA and cloned into pNU164. Includes first three exons of *daf-16a.*
	164-5ORF_Rev	AGATTGTGACGGATCGAGTTCTTCCATCCA GCTGAACTGT	
daf-16a 3'cDNA + 3'UTR	164-hybrid_For	ACAGTTCAGCTGGATGGAAGAACTCGATC CGTCACAATCT	Amplified from pCFJ151-*daf-16a* and cloned into pNU164
	164-hybrid_Rev	TAATACGACTCACTAGTGGGCAGATCTATT CAAATTTGATTTTTATTAAATCATCATCAT	

daf-16d/f/h promoter	191-prom_For	GCCTTGACTAGAGGGTACCAGAGCTCACCTAGGGAGAGACGGCTCGAAAAGT	Amplified from wild-type genomic DNA and cloned into pNU191
	191-prom_Rev	AGATTGTGACGGATCGAGTTCTTCCATCCAGCTGAACTGT	
daf-16d/f/h 5' ORF	191-5ORF_For	ACAGTTCAGCTGGATGGAAGAACTCGATCCGTCACAATCT	Amplified from wild-type genomic DNA and cloned into pNU191. Includes first three exons of *daf-16d/f/h*
	191-5ORF_Rev	CACCAGGGGAAACAAAATGAAGAGAATGCTAGCTTACAAATCAAAATGAATATGCTGCC	
daf-16d/f/h 3'cDNA + 3'UTR	191-hybrid_For	GAGGGCAGCATATTCATTTTGATTTGTAAGCTAGCATTCTCTTCATTTTGTTTCCCCTG	Amplified from pNU164 and cloned into pNU191. Includes 4th and 5th exons of *daf-16d/f/h* (common to *daf-16a*)
	191-hybrid_Rev	TAATACGACTCACTAGTGGGCAGATCTATTCAAATTTGATTTTTATTAAATCATCATCAT	

Table S22 Number of 5′ RACE clones sequenced for each strain. For *daf-16(tm5032)*, a different primer A32-RACE was used, indicated by asterisks. See Figure S3 for details. All indicated RACE clones were consistent with sequences presented in Figures S2 and S4. Note that clones without SL1 trans-spliced leaders (w/o SL1) were partial fragments of the sequences.

	daf-16a RACE primer			*daf-16f* RACE primer		
	w/ SL1	w/o SL1	empty	w/ SL1	w/o SL1	empty
N2 wild-type	4	9	2	15	1	1
daf-16(tm5030)	10	3	6	7	0	0
daf-16(tm5032)	4*	5*	3*	7	3	0
daf-16(tm6659)	8	17	2	0	0	20

Table S23 Effect of more stringent cutoffs for selection of DAF-16A/F targets on downstream analysis of categories. We selected DAF-16A/F targets primarily on the basis of fold-change. Genes must meet the appropriate fold-change threshold for all three comparisons: (1) wild-type *vs. daf-2(e1370)*, *daf-2 vs. daf-16(mg54);daf-2,* and *daf-2 vs. daf-16(mu86);daf-2*. See Methods for all criteria.

	FDR < 0.05 for at least one comparison		FDR < 0.05 for at least two comparisons		FDR < 0.05 for all three comparisons	
	Number	Percent	Number	Percent	Number	Percent
A-specific	57	14	48	16	33	18
F-specific	8	2	6	2	4	2
Redundant	35	9	28	9	15	8
Shared A>F	219	55	173	56	102	56
Shared A=F	60	15	41	13	22	12
Shared F>A	20	5	13	4	6	3
Total	399	100	309	100	182	100